D6.4 - Validated numerical simulation of hydrodynamic interaction between devices for different compact array layouts

DATE: March 2018

PROJECT COORDINATOR:

WavEC Offshore Renewables

GRANT AGREEMENT NR: 641334

PROJECT: WETFEET

The WETFEET – Wave Energy Transition to Future by Evolution of Engineering and Technology project has received funding from the European Union's Horizon 2020 programme under grant agreement No 641334.

Validated numerical simulation of hydrodynamic interaction between devices for different compact array layouts			
Project	WETFEET – Wave Energy Transition to Future by Evolution of Engineering and Technology		
WP No.	6	WP Title	Array Breakthrough: Sharing Moorings (and Electrical Cables)
Deliverable No.		6.4	
Nature (R: *Report*, P: *Prototype*, O: *Other*)		R	
Dissemination level (PU, PP, RE, CO)		PU	
Lead beneficiary:		INNOSEA	
Contributing partners		WavEC Offshore Renewables, IST, UoP	
Authors List:		Violette HARNOIS (INNOSEA) Keri Collins (UoP) Deborah Greaves (UoP) Ben Howey (UoP) Rui P. F. Gomes (IST) Juan C. C. Portillo (IST) Pedro Vicente (WAVEC) Miguel Vicente (WAVEC)	
Quality reviewer		Peter Fraenkel	
Status (F: final; D: draught; RD: revised draught):		F	
Due Delivery Date:		31/12/2017	
Actual Delivery Date:		02/03/2018	

Version no.	Dates and comments
1	25/08/2017 Deliverable structure defined
2	24/11/2017 First draught for flexible device
3	09/02/2017 Final draught for internal review
4	02/03/2018 Final report

EXECUTIVE SUMMARY

This report presents Deliverable 6.4 of the WETFEET H2020 project – Validated numerical simulation of hydrodynamic interaction between devices for different compact array layouts.

This work is part of WETFEET work package 6. The purpose of this WP is to:

- Identify and quantify the potential of sharing mooring lines between nearby devices loosely connected to each other in terms of performance, survivability, cost reduction (to be addressed in WP7), environmental impacts (also in WP7) and sea space utilization (also in WP7). This is done with a 5-device array of oscillating water column (OWC) spar buoys referred in this report as "flexible array". A single OWC spar buoy was tested beforehand to provide useful data for calibration.
- As above for compact aggregates (rigidly connected nearby devices or nearby devices connected to a common structure moored to the seabed). An array of 5 devices is used in this study and referred to as "rigid array".

The topic of this report is the validation of the numerical simulation of hydrodynamic interaction.

For the flexible device (loosely connected),

- The single device model generally shows a good agreement with experiments. First order surge and pitch motions and heave motions are predicted well. Mooring loads are also predicted well.

  Inaccuracies are observed in surge and pitch caused by a slow drift motion which appears in the numerical model, and which is likely to be caused by inaccuracies in the experimental setup. A sensitivity analysis showed that this type of mooring is highly sensitive to the lengths or masses of the mooring system components.

  In addition, the heave motion is slightly overdamped. For example, the highest values of the heave displacement Response Amplitude Operators (RAOs) are equal to 1.6m/m for the model while they are equal to 2.4 m/m for the experiment.

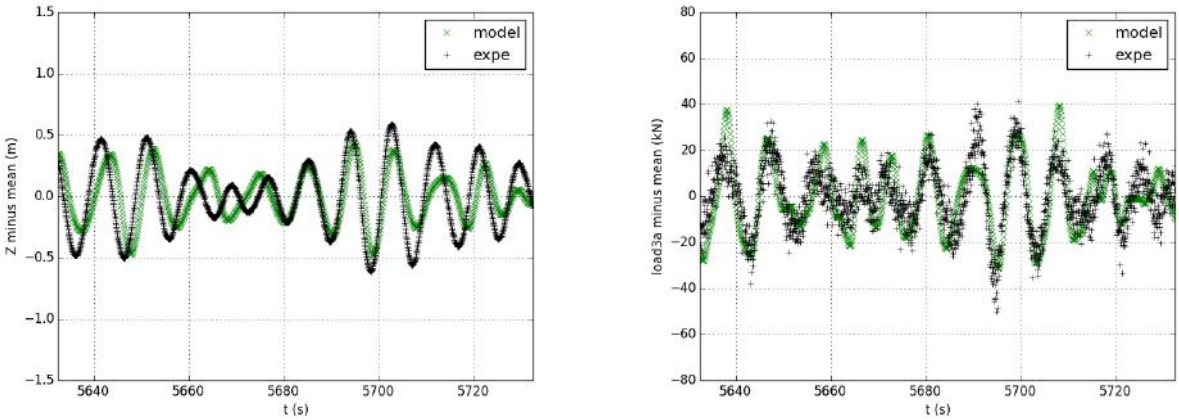

Z: Heave 3a

EXAMPLE OF TIME SERIES OF EXPERIMENTAL AND MODELLED DATA OF THE ISOLATED OWC SPAR BUOY FOR IRREGULAR WAVES FOR CASE C001 (H_S = 1.24 M AND T_P = 7.59 S). MEAN VALUES HAVE BEEN REMOVED FOR COMPARISONS OF AMPLITUDES AND PHASES

An improved heave damping could be estimated in a future model for example with sensitivity analysis. In addition, the OWC could be modelled. The model could also be built with the measured lengths and masses instead of target lengths and masses.

- The array Configuration D has been chosen for numerical modelling. This array used 5 devices similar to the single device previously considered. The devices are connected with few mooring lines: one external mooring line for each external buoy of the array, and one line connecting each external device to the internal device.

  The array Configuration D is more complex to model than the single device. First order motions and loads are modelled well with results similar as for the single device. The heave motions of the devices are replicated well in regular and irregular waves, but overdamped. This was also observed in the single device results. In irregular waves, a slow drift motion appears in the modelled data which makes the modelling of pitch and surge, and consequently of mooring line load inaccurate.

  The differences in slow drift motion may be due to the quadratic transfer function (QTFs) which are valid for the initial position at which they have been calculated, especially for a multibody model, to the lack of damping of second order motion, but also and similarly to the single device to inaccuracies in experimental layout.

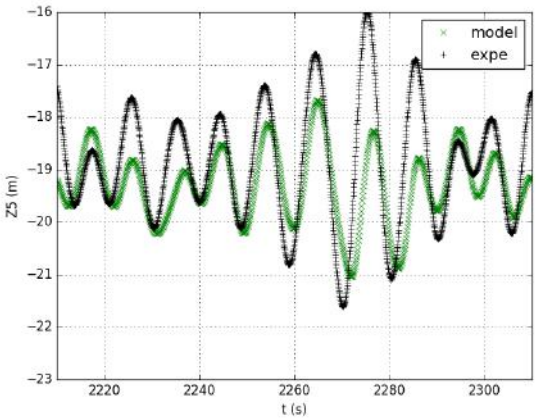

Z3: heave buoy 3

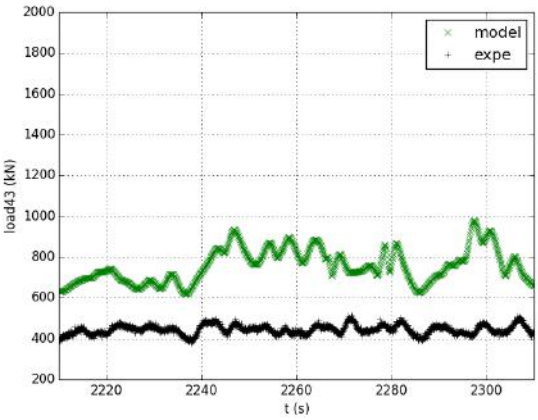

Load 43

EXAMPLE OF TIME SERIES OF EXPERIMENTAL AND MODELLED DATA FOR IRREGULAR WAVES FOR CASE DA038 (H_S = 2.9 M AND T = 9.9 S). OWC SPAR BUOY ARRAY, CONFIGURATION D

Similarly to the single device, in a future model, an improved heave damping could be estimated and the OWCs could be modelled. The model could also be built with the measured lengths and masses instead of target lengths and masses.

For the rigid device (compact aggregates),

- The numerical model was with low complexity, with standard catenary mooring lines, and limited motion amplitudes. The numerical model estimates fairly the motion of the rigid array and the load in the mooring lines in the experiments. The heave motion is predicted well.

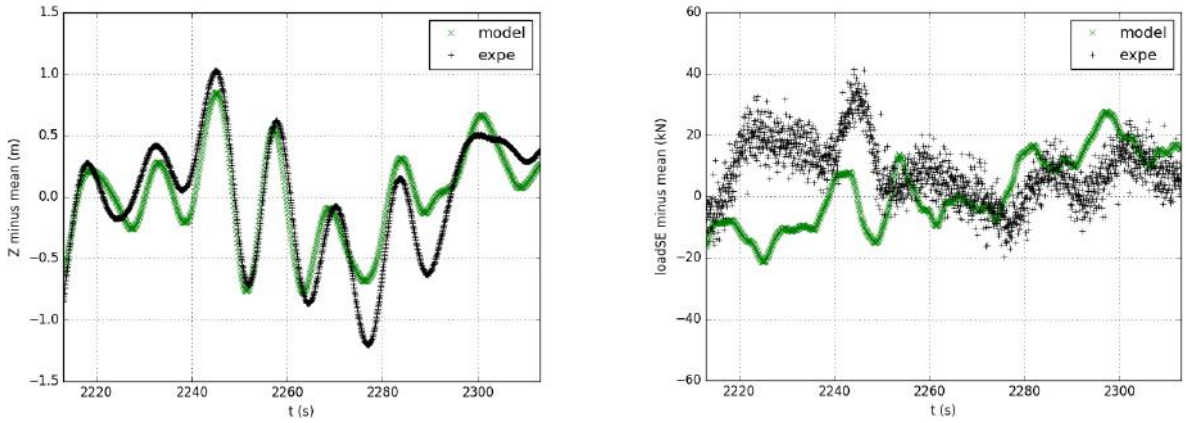

Z: Heave Load SE

EXAMPLE OF TIME SERIES OF EXPERIMENTAL AND MODELLED DATA OF THE RIGID ARRAY FOR IRREGULAR WAVES FOR CASE I004 (H_S = 2.24 M AND T_P = 14.55 S). MEAN VALUES HAVE BEEN REMOVED FOR COMPARISONS OF AMPLITUDES AND PHASES

The Power-Take off (PTO) and heave plates were not taken into account in the numerical model which may explain some differences between experimental and modelled results.

They could be added in a future model. Decay tests would be required to calibrate the damping generated by the heave plates.

All models generally show a good agreement with experiments and can be used to predict first order motions and mooring loads. These results can be used to predict a full size system with some adjustments [1] :

- The stiffness of the air spring is not scaled correctly.
- Viscosity does not scale appropriately and is likely to be overestimated during tank test.
- Friction does not scale appropriately.

In addition, there might be inaccuracies in sea trials in anchor position. Inaccuracies in line length and clump weight are also likely in sea trials. They have already been observed in tank tests. Their influence on results has been assessed with sensitivity analysis with the numerical model.
Due to the large size of the array, it would be complicated to conduct tank tests at a higher scale. Further scaled tests at a larger scale could be conducted in the sea, in sheltered locations.

These models could also be used in future developments of the devices.
The hydrodynamic databases do not need to be modified if the distance between devices is the same and if the hull of the devices is the same. For the flexible devices, all mooring configurations and other mooring configurations could be investigated, and for the rigid device the mooring configuration could be modified.
Otherwise, new hydrodynamic databases will need to be calculated. The methodology developed in this study can be used again, and the limitations of the numerical model are likely to be similar.

Some preliminary comments, based on the validated experimental work, of the benefits or influences of having shared mooring between devices of the array can be made below. These points will be discussed in more details in D6.5 [7].

- The flexible array is more complex to model than the related single device.

Large pitch motions are observed in the case of the array. This is likely to be detrimental to the power production and to increase mooring loads.

- The rigid array is less complex to model than the flexible array. This numerical model could be used for optimisation, for example on the mooring system.
  In addition, the rigid array is a large device which does not move much, and probably less than the related single device. This means that using an array is likely to be a benefit for power production.

Table of Contents

List of figures

List of tables

Lists of symbols

f	Frequency [Hz]
F_s	Sampling frequency [Hz]
H	Wave height [m]
H_s	Significant wave height [m]
T	Period [s]
T_p	Peak period [s]
(X, Y, Z)	Right-handed axes defining the basin
(X', Y', Z')	Right-handed axes defining the body/device

List of acronyms

CoB	Centre of buoyancy
CoM	Centre of mass
DOF	Degree of freedom
HDB	Hydrodynamic database
OWC	Oscillating Water Column
PM	Pierson Moskovitz (spectrum)
PSD	Power spectral density
PTO	Power Take-Off
QTF	Quadratic transfer function
RAO	Response amplitude operator *
MWL	Mean water line
UHMWPE	Ultra-high molecular weight polyethylene
UoP	University of Plymouth
WP	Work package

** RAOs are effectively transfer functions used to determine the effect that a sea state will have upon the motion/the loads of a floating structure or its mooring system. They are coming with phases showing the shift between a) the motion/loads of a floating structure or its mooring system and b) the waves.*

1 INTRODUCTION

1.1 Objectives

This report presents Deliverable 6.4 of the WETFEET H2020 project – Validated numerical simulation of hydrodynamic interaction between devices for different compact array layouts.

This work is part of WETFEET work package 6. The purpose of this WP is to:

- Identify and quantify the potential of sharing mooring lines between nearby devices loosely connected to each other in terms of performance, survivability, cost reduction (to be addressed in WP7), environmental impacts (also in WP7) and sea space utilization (also in WP7). This is done with a 5-device array of OWC spar buoys referred in this report as "flexible array". A single OWC spar buoy was tested beforehand to provide useful data for calibration.
- As above for compact aggregates (rigidly connected nearby devices or nearby devices connected to a common structure moored to the seabed). An array of 5 devices is used in this study and referred to as "rigid array".

The topic of this report is the numerical simulation of hydrodynamic interaction. For the single OWC spar buoy, and for each type of arrays (flexible and rigid), it is composed of three parts:

- Description of the experiment
- Description of the numerical model
- Presentation of results and comparison with experimental results

1.2 Methodology overview

One of the aims of the different tank tests conducted during the different campaign was to provide useful data for validation of the numerical models. These data allow a step-by-step validation of the different inputs of the numerical model:

- Static tests, with and without mooring system: validation of the mass and buoyancy of the buoy
- Pull-out tests with mooring system: validation of the mooring stiffness
- Decay tests with mooring system and Power Take-off (PTO): validation of the added mass and calibration of the linear and quadratic damping on the whole system
- Regular wave tests with PTO: validation of the motion Response Amplitude Operators (RAOs) and mean drift, observation of linear and non-linear behaviour
- Irregular wave tests with PTO: comparison of the behaviour of the system in a realistic sea state

A model created in OrcaFlex [1] was used with hydrodynamic database (HDB) calculated with WAMIT [3]. Comparisons were done with experimental results.

In addition, a configuration comparison based on model tests has been added to this report.

The surge, sway and heave directions are defined in Figure 2-3 (single OWC spar buoy), Figure 3-1 (flexible array) and Figure 4-1 (rigid array).

1.2.1 Static tests

The buoy position and mooring loads (when relevant) were measured (when possible) in still water.

1.2.2 Pull-out tests

The buoy was moved along a Degree of Freedom (DOF) (in this case surge and heave). The buoy is pull to various offsets by a rope. The motion was not constant but the buoy was held in different positions along a DOF. Each held position was used for further analysis.

1.2.3 Decay tests

The buoy was moved in still water from its equilibrium position in 1 DOF (or at least mainly in 1 DOF) and suddenly released. For each simulation, the time used for analysis was chosen as long as the motion in the investigated DOF was decreasing. This can lead to short experiment time if motions are strongly coupled or mooring line effects occur.

1.2.4 Regular wave test

The buoy motion and mooring loads were measured in several sets of regular waves (following Airy theory often referred to as linear wave theory). The waves are unidirectional and have only one frequency. Experiments were run for an approximate duration of 100 waves. The time series of position and mooring loads were used for further analysis. The RAOs, phases and mean of cycles of motions and mooring loads were extracted. Experimental data were analysed for t between 200 s and 750 s. Numerical model data were analysed for t between 0 s and 200 s (a 1000 s build-up preceded this period).

1.2.5 Irregular wave tests

The buoy motion and mooring were measured in several sets of irregular waves. The time series of position and mooring loads, as well as statistical and spectral analysis, were used for further analysis.

1.2.6 Hypotheses and limitations of the numerical model

The main hypotheses of the theories used in the calculation and the corresponding limitations are outlined in Table 1-1 (non-exhaustive list). Additional damping will be added to take the viscous effects into account.

Hydrodynamic interactions with other devices are taken into account.
The slack mooring system of the array is complex, therefore it may reach different equilibrium positions than the ones obtained in the experiment. The mooring system force is highly sensitive to the cable-segments length, chain mass, and clump weight and float mass.
The interaction between the internal water column of the OWC and the spar buoy are not modelled. This means that the water column is considered in phase with the spar buoy. In addition, the added mass and radiation damping associated with the water column are not modelled. This assumption can be done because this model does not aim the modelling of the air chamber dynamics. Its main limitation is disregarding the force (on the buoy and on the OWC) due to pressure variations inside the air chamber. However, since the opening of the OWC tube is at the bottom of the device (36 m below the free surface), where wave interactions are small, radiation damping and wave diffraction forces on the OWC are negligible when compared with the corresponding values of the buoy.

TABLE 1-1 HYPOTHESES AND LIMITATIONS OF THE NUMERICAL MODEL

	Theory	Hypothesis	Limitations
Ocean load model	Wave loads : Linear Potential Flow (1st order)	Non-rotational flow	
		Inviscid flow (viscous drag forces neglected)	Viscous effects on floater might be important on floater motion.
		Linear waves: wave amplitude small compared to wavelength	Large waves are out of linear wave scope.
		Wave amplitude small compared to body dimensions (Keulegan-Carpenter number below 4 or 5)	Might not be verified for extreme waves.
		Motion of the body are small relative to body dimensions	Large mean pitch angle will be a limitation. Parametric roll/pitch* cannot be modelled.
	Wave loads : Linear Potential Flow (2nd order)	Same hypothesis as 1st order. Quadratic transfer functions depend on 1st order motion.	First order motion depends on mooring system and cannot be estimated accurately before knowing it.
PTO	damping	The damping of the PTO is included in the overall damping.	The interaction between the internal water column of the OWC and the spar buoy are not modelled.

** Parametric roll/pitch is a parametric resonance effect that induces large roll/pitch amplitudes on the motion of a floating structure even in a moderate sea conditions. It is caused by time variations of the hydrostatic restoring moment, or by the nonlinear pressure variations induced by the wave passage on the structure wetted surface. For specific wave frequencies, the floating structure becomes dynamically unstable in roll/pitch, triggering the large motion amplitudes.*

1.3 Description of the software package, pre- and post-processing

1.3.1 Software package

OrcaFlex is a software package for the dynamic analysis of offshore marine systems. Mooring lines were modelled using a lumped mass element method. Motions of the floating structure were calculated by the software package from input wave conditions using the potential radiation-diffraction theory. Regular waves were generated by the software package using Airy theory. Time series of irregular waves were directly imported from the experimental data.

1.3.2 Inputs

HDB were imported and include:

- Added mass and radiation damping
- Load RAOs

- Displacement RAOs
- Quadratic transfer functions (QTFs)

This means that the potential linear theory is used.

Additional damping is added based on the experimental data results. This is explained in 1.3.6.3.

1.3.3 Outputs

Motions of the floating structure and tensions in the mooring lines were exported from the numerical model at the same position as used by Qualisys during the experiment to measure the motion. Qualisys measurement system (referred in this report as "Qualysis") is an optical motion capture system (cameras mounted on the side of the basin) which tracks the position of a floating structure during tank tests. For the OWC spar buoys, this point was located 0.5 m higher than the target Centre of Mass (CoM) of the buoy (full scale). This point was located theoretically 21.74 m below the mean water line (MWL) (full scale) in still water with a mooring system.

1.3.4 Statics tests

In order to determine the statics position and tension, a static test was used.

Statics simulations were run in OrcaFlex without environmental loads, with and without the mooring system. A static analysis determines the equilibrium configuration of the system under mean environmental loads, in this case no environmental loads. The statics position of the buoy and the tension in the mooring lines, where relevant, were output.

1.3.5 Pull-out tests

In order to determine the mooring stiffness, pull out tests were used.

Several static simulations were run in OrcaFlex without environmental loads and with the mooring system. In each simulation, the buoy was held in a position corresponding to a mean held position considered during the experimental pull out test. The angles were small so the buoy was not rotated in the model for simplification and was just held with a surge or a heave offset. The variation of the static mooring line tension was output at each variation of position.

1.3.6 Decay tests

In order to determine the natural period and damping, decay tests were used.

A dynamics simulation was run in OrcaFlex without environmental loads. The simulations used to validate the numerical model were the simulations with the mooring system and with the PTO. The buoy was released from a given position which corresponded to the first peak or trough after release during the experiment. The time series of the motion of the buoy at the measurement point were output.

1.3.6.1 Extraction of peaks and troughs

Peaks and troughs were extracted from the time series of experimental motion. Peaks and troughs were detected after the release. This was to avoid inaccuracies in the exact values of the release point, however, the first detected peak or trough started without initial speed in the numerical model which was not the case during the experiment. Peaks and troughs were no longer detected when the amplitude of oscillations was too small or increasing. This was detected visually.

1.3.6.2 Calculation of natural period

Natural periods were calculated from the experimental or model values as the double of the mean of the time difference between each peak/trough *n* and trough/peak *n+1*.

$$T_m = 2 \times mean(T_{n+1} - T_n) \quad (1\text{-}1)$$

In addition, natural periods for the uncoupled modes were calculated analytically. For the surge and sway motions, the natural period is equal to:

$$T_m = 2\pi \sqrt{\frac{M + M_a(\omega_0)}{K_m}} \quad (1\text{-}2)$$

Where:

- M is the mass of the OWC spar buoy (kg)
- M_a is is the added mass of the OWC spar buoy for this DOF and for the natural period of this DOF (kg). This parameter is chosen iteratively.
- ω_0 is the natural period of this DOF (rad/s)
- K_m is the mooring stiffness in surge or sway

For the heave motion, the natural period is equal to:

$$T_m = 2\pi \sqrt{\frac{M + M_a(\omega_0)}{K_m + K_h}} \quad (1\text{-}3)$$

Where:

- K_h is the hydrostatic stiffness in heave

For the roll and pitch motions, the natural period is equal to:

$$T_m = 2\pi \sqrt{\frac{Mr^2 + I_a(\omega_0)}{K_m + K_h}} \quad (1\text{-}4)$$

Where:

- r is the rotation (roll or pitch) radius of gyration
- I_a is the added inertia

1.3.6.3 Calculation of linear and quadratic damping

Using these peaks and troughs, linear and quadratic damping coefficients are evaluated. Based on Faltinsen [1], linear and quadratic damping coefficients, as expressed below were calculated by plotting $\frac{2}{T_m}\log\left(\frac{X_{n-1}}{X_{n+1}}\right)$ against $\frac{16}{3}\frac{X_n}{T_m}$. An example of fit is shown in Figure 1-1.

$$\ddot{x} + p_1\dot{x} + p_2|\dot{x}|\dot{x} + p_3 x = 0 \quad (1\text{-}5)$$

$$\frac{2}{T_m}\log\left(\frac{X_{n-1}}{X_{n+1}}\right) = p_1 + \frac{16}{3}\frac{X_n}{T_m}p_2 \quad (1\text{-}6)$$

Where:

- $X_n$is the amplitude of the n^{th} half-period oscillation (m or deg)
- T_m is the natural period (s)
- p_1 is linear damping coefficient (s^{-1})
- p_2 is quadratic damping coefficient (m^{-1} or deg^{-1})

X_n is the mean of the time difference between peak and trough.

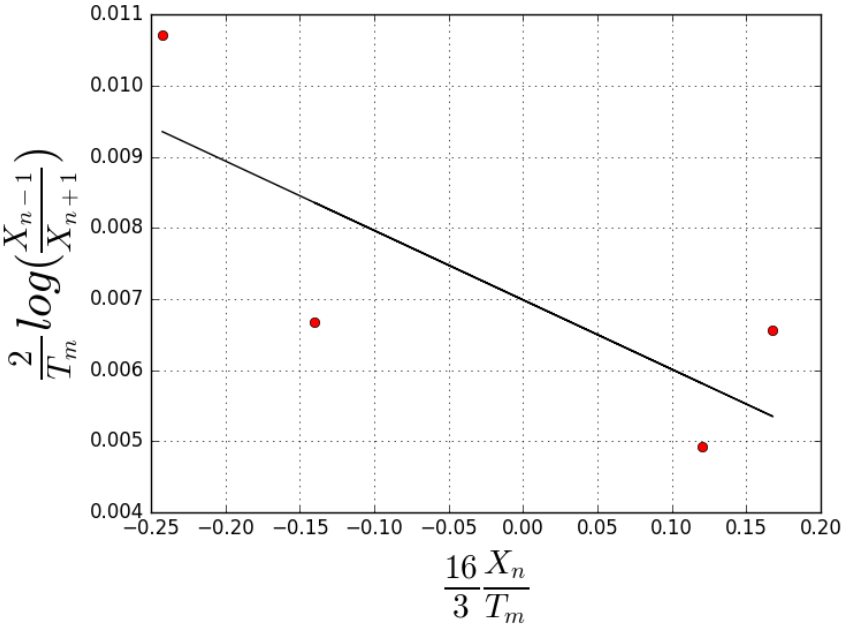

FIGURE 1-1 – EXAMPLE OF FIT TO ESTIMATE LINEAR AND QUADRATIC DAMPING COEFFICIENT, BASED ON EXPERIMENT G009 (SEE TABLE 2-12), WHICH IS A SURGE DECAY TEST

The mean of the signal was removed to X_n to obtain values around an equilibrium position. The coefficients were multiplied to fit the dimensions of linear B_1 and quadratic B_2 damping coefficients used by OrcaFlex. For translations, the linear and quadratic damping coefficients p_1 and p_2 were multiplied by the sum of the mass and added mass at the natural frequency in this DOF of the spar buoy. For rotations, the linear and quadratic damping coefficients p_1 and p_2 were multiplied by the sum of the inertia and added inertia at the natural frequency in this DOF of the OWC spar buoy. This is described in (1-7) to (1-10).

For translations:

$$B_1 = (M + M_a(\omega_0))p_1 \quad (1\text{-}7)$$

$$B_2 = (M + M_a(\omega_0))p_2 \quad (1\text{-}8)$$

For rotations:

$$B_1 = (I + I_a(\omega_0))p_1 \quad (1\text{-}9)$$

$$B_2 = (I + I_a(\omega_0))p_2 \quad (1\text{-}10)$$

Where:

- M is the mass of the OWC spar buoy (kg)
- M_a is the added mass of the OWC spar buoy for this DOF at the natural period of this DOF (kg)
- I is the moment of inertia of the buoy for this DOF (kg.m^2)
- I_a is the is the added moment of inertia of the OWC spar buoy for this DOF at the natural period of this DOF (kg.m^2)

- B_1 is the linear damping coefficient used as an input in the numerical model (translation $\frac{N}{m/s}$ or rotation $\frac{N.m}{rad/s}$)
- B_2 is the quadratic damping coefficient used as an input in the numerical model (translation $\frac{N}{(m/s)^2}$ or rotation $\frac{N.m}{(rad/s)^2}$)

1.3.7 Regular wave tests

In order to determine the RAOs and phases of motions and loads, regular wave tests were used.

A dynamics simulation was run in OrcaFlex with regular waves (Airy). The wave height and period used for the model were the target wave height and period used for experiment, instead of the measured wave height and wave period, or ideally the measured wave heights and wave periods in an empty basin. Empty basin tests were not available for all tested states. For simplification, target wave height and periods were used for all tests. Time series of motion and mooring loads were output. RAOs and phases were calculated using spectral analysis. In addition, mean drift and mean position were also calculated

1.3.8 Irregular wave tests

In order to determine the behaviour (motion and loads) in a realistic sea state, irregular wave tests were used.

A limited number of irregular wave tests was chosen for comparison with the numerical model. A dynamics simulation was run in OrcaFlex. Time series of surface elevation were input in OrcaFlex. Time series of motion and mooring loads were output.

2 FLEXIBLE ARRAY: SINGLE OWC SPAR BUOY

The aim of the numerical model with the single device is to calibrate the damping caused by the PTO in the numerical model. In addition, this model will highlight inaccuracies caused by the limitations of the potential theory and simplified modelling of the PTO as a damper.

2.1 Experimental set-up – single OWC spar buoy

The numerical model of the single OWC spar buoy device was used to calibrate the damping caused by the PTO in the numerical model. In addition, this model allowed inaccuracies caused by the potential theory and simplified modelling of the PTO as a damper to be investigated.

2.1.1 OWC spar buoy physical models

The OWC spar buoy models were created at a 1:40 scale from the full-scale designs provided by IST [5]. There were six models made in total: one to determine suitable manufacturing techniques and to allow preliminary results to be obtained (named TM0) and five further models (TM1 – TM5) to make up the array. The manufacturing process is described in detail in D6.3 [6].

A simple sketch of the OWC spar buoy is given in Figure 2-1 with an isometric view of the CAD model and a photograph of the TM0 model for comparison. The 1:40 physical models were made from an aluminium base cone and acrylic tube sections. Moveable masses in the upper chamber allowed the position of the CoM to be changed.

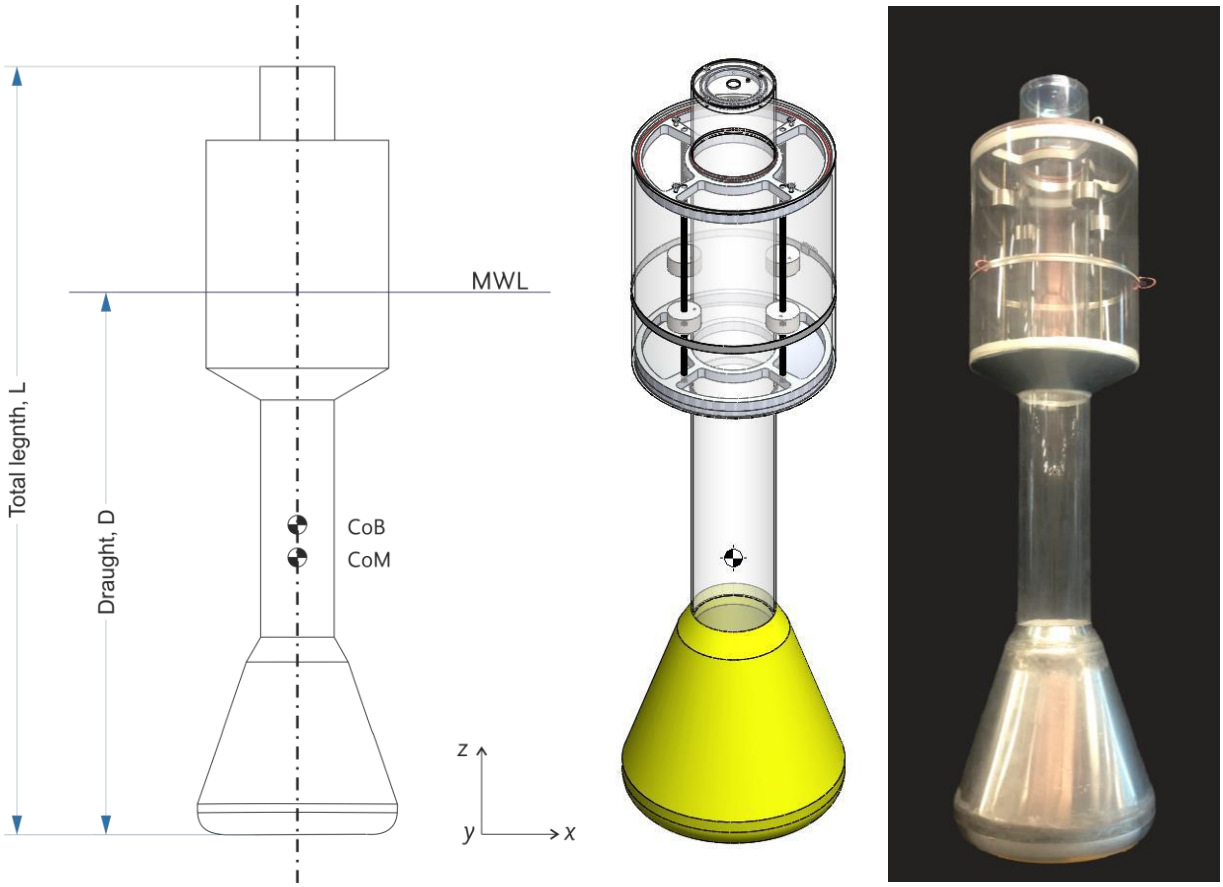

FIGURE 2-1 – SCHEMATIC OF THE OWC SPAR BUOY, ISOMETRIC VIEW OF THE OWC SPAR BUOY CAD MODEL (CENTRE) AND PHOTOGRAPH OF THE TM0 MODEL (RIGHT)

In the original specified full-scale design [5], the positions of the CoM and Centre of Buoyancy (CoB) were given relative to the mean water line (MWL) meaning that they were dependent on the draught of the model. The values of the principal physical properties for the idealised 1:40 scale, the CAD models of the designs and of the finished models are given in Table 2-1.

The fairleads were attached to the device with a large diameter hose clamp, as described in D6.3 [6]. The positions of the fairlead clamps were measured after experimentation for each of the OWC spar buoy devices and the mean position is given in Table 2-1.

TABLE 2-1 PHYSICAL PROPERTIES OF THE FULL-SCALE, IDEALISED 1:40 SCALE AND CONSTRUCTED MODELS OF THE OWC SPAR BUOY

Parameter	Idealised 1:40 scale	CAD model TM1-5	Physical test models				
			TM1	TM2	TM3	TM4	TM5
L [mm]	1275	1275 (1275)		1275	1276	1277	1274
D [mm]	900	894		890	888	890	887
Mass, M [kg]	19.022	18.87 (18.87)	18.92	18.73	18.77	18.92	18.83
I_{xx} (I_{yy}) [kg m^2]	3.17	3.84 (3.89)	n.d.	5.24	7.16	3.86	6.12
CoB to MWL [mm]	451	454	n.d.	n.d.	n.d.	n.d.	n.d.
CoM to MWL [mm]	482	476		481	475	470	476
Base to CoM [mm]	418	412 (418)		409	413	420	411

Draught measurements are considered to have an uncertainty of ±2 mm, other distance measurements are ±1 mm.
n.d. = no data
Distances relating to the MWL for the CAD models are relative to the calculated MWL position

For the isolated device experiments, TM3 was used. This model was placed at the centre of the basin in both the isolated case and for the arrays.

2.1.2 Mooring system physical model

The bottom mooring line design chosen was that of a "lazy-S" or hybrid mooring line consisting of a chain and synthetic rope design with floaters and clump weights on the line, as shown in Figure 2-2. Mooring lines were made from stainless steel and UHMWPE line (LIROS DC Dyneema SK78 Competition Kite Line). The Dyneema was chosen as it was possible to geometrically scale the thickness of the line while retaining a suitable safety factor for the breaking load. The buoyancy provided by the floats was split between six individual polystyrene floats to reduce the drag on the line. Clump weights were made from lead and tied to the lines in the appropriate places.

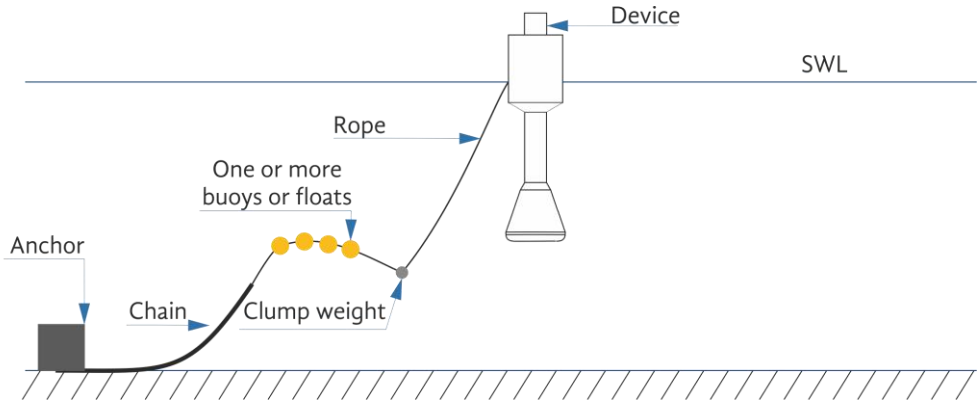

FIGURE 2-2 EXAMPLE OF THE HYBRID BOTTOM MOORING LINE DESIGN OF THE OWC SPAR BUOY

Mooring line lengths were scaled from the full size equivalent. The Dyneema section had a loop tied into its length for the attachment of the clump weight. One end of the line was tied to the chain and one end to the force sensor attached to the fairlead. Once assembled, the total line length depended on the tightness of the knots linking the line to the fairlead and as such each line had an uncertainty of ±10 mm. The values of the unassembled mooring lines are given in Table 2-2. Results indicate that the relative difference between the measured line length and the target line length is between -3% and +2%. The model is built with the target values and a sensitivity analysis is conducted in 2.3.6.

TABLE 2-2 MEASURED VALUES OF MOORING LINE COMPONENTS OF THE OWC SPAR BUOY (ISOLATED DEVICE) WITH TARGET VALUES GIVEN IN PARENTHESES

Line	Chain [m]	Fairlead to clump [m]	Total Dyneema [m]	Total line length [m]	Clump [kg]	Floats [g]
	(1.155)	*(1.289)*	*(5.012)*	*(6.167)*	*(1.807)*	*(6.5)*
3A	1.126	1.256	4.955	6.081	1.806	6.5
3B	1.173	1.285	4.965	6.138	1.808	6.5
3C	1.173	1.310	4.980	6.153	1.807	6.5
Largest deviation	2.5% (3A)	2.6% (3A)	1.1% (3A)	1.4% (3A)	0.1% (3A, B)	--

Line lengths given unassembled.
Floats were measured before assembly but their individual measurements were not recorded, once assembled measurement not feasible so target values are given.

Material properties were:

- Chain: 4 mm stainless steel (316) short link chain
- Dyneema: 1.6 mm, 2 kN breaking strength

More details on the chain are given in the D6.3 [6].

Mooring lines were tied to a load cell (described in Section 2.1.5) which was attached to a fairlead made from a Dyneema loop fixed to the model. The load cell serial numbers and offsets are given in Table 2-3.

TABLE 2-3 LOAD CELL DESIGNATIONS FOR THE ISOLATED OWC SPAR BUOY EXPERIMENTS

Line number	Load cell number	No load reading [N]	Still water reading [N]
3A	698 314	-0.641	~15.4
3B	698 315	+5.131	~15.4
3C	698 317	-1.851	~16.5

Sensor readings when moored in still water are approximate values taking into account the no load reading. For specific values, see the beginning of each file.

The moored draught measured for the TM3 device was 972 ±2 mm.

2.1.3 Experimental set-up

The device (TM3) was moored so that it was coincident with the centre of the University of Plymouth (UoP) Ocean Basin and details of this testing facility are given in D6.5 [3]. Figure 2-3 shows the set-up of the device in relation to the basin.

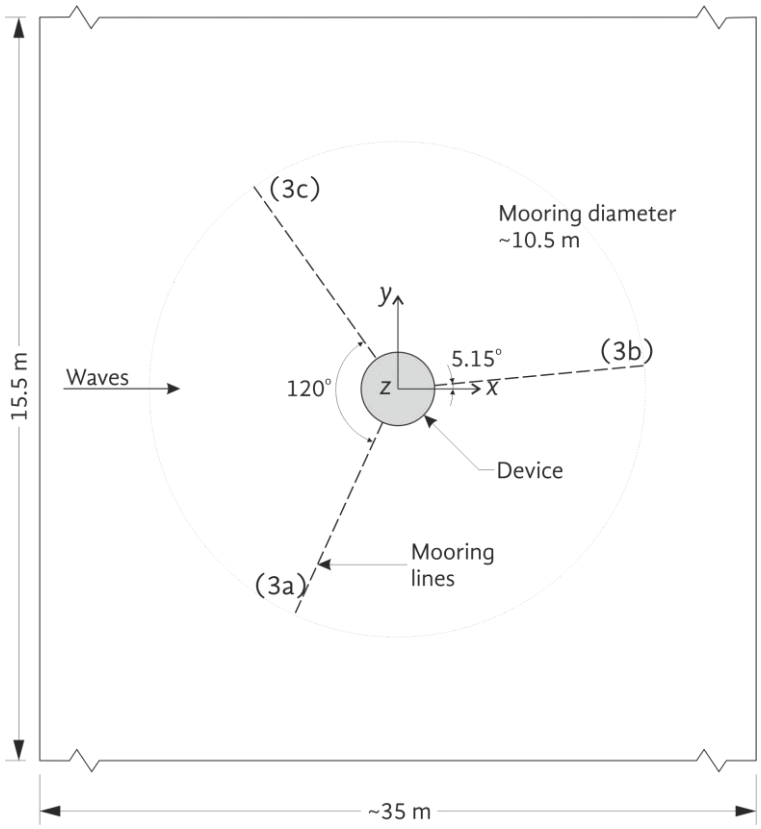

FIGURE 2-3 SCHEMATIC OF THE ISOLATED OWC SPAR BUOY MOORING LAYOUT (MODEL SCALE). X AXIS IS ALSO THE SURGE DIRECTION, Y THE SWAY DIRECTION. Z AXIS UPWARDS THE HEAVE DIRECTION

Three mooring lines were positioned at equal angles around the model such that there were two anchor points facing the waves. There was a slight rotation on the mooring lines relative to the longitudinal (*X*) axis of the basin and this was to permit the same mooring layout to be used in other configurations.

TABLE 2-4 POSITIONS OF THE ANCHORS WITH RESPECT TO THE CENTRE OF THE BASIN FOR THE ISOLATED OWC SPAR BUOY

Device	Line #	*X* [m]	*Y* [m]
TM3	3A	-1.688	-4.971
TM3	3B	5.149	1.024
TM3	3C	-3.462	3.947

2.1.4 Input wave conditions

Three types of waves were chosen for experimentation:

- regular waves to establish a capture width curve and motion and load RAOs
- irregular sea states based on a PM spectrum to examine performance in a real sea state
- survivability waves to examine the mooring loads in extreme conditions

Regular waves were run at two different wave heights: H = 0.05 m and H = 0.1 m, at frequencies between f = 0.3 Hz and f = 1.0 Hz.

The irregular sea states were based on the wave climate encountered at Leixões, Portugal. There were generated with the Njord Wave Synthesis program based on a Pierson Moskovitz spectrum. The survivability waves represented the 10-, 25-, 50- and 100-year return periods based on the same spectral shape. More details about the wave climate are given in D6.5 [7].

The irregular and survivability wave heights and periods were Froude scaled from full-scale equivalents. Irregular waves were run for 11 minutes (69m34s at full scale) with a repeat time of 10 minutes (63m14s full scale). Similarly, the survivability waves were run for 29m30s (186m34s) with a repeat time of 28m28s minutes (180m2s at full scale). This provided a section of the time series matching the repeat time to be chosen after which the basin could be said to be operating in a steady state.

2.1.5 Data acquisition

To measure the positions of the devices throughout the experiments, a 6 DOF tracking system was used (Qualisys) and the set-up and functioning of this system is described in D6.5 [7] in more detail.

Data were collected from four different instruments: wave gauges, pressure sensors, load cells and from the 6 DOF tracking system, along with four digital video cameras positioned both above and below the water. For most of the experimental campaign, data acquisition was synchronised between the various systems. Table 2-5 gives details of the data acquisition for the various systems. Examples of file headers are given in the Appendix. Pressure data are not used in this document.

TABLE 2-5 DETAILS OF INSTRUMENTATION AND DATA ACQUISITION FOR BOTH FLEXIBLE AND RIGID ARRAYS

	Waves	Pressure	Load	Motions
Software	Edinburgh Designs Ltd.	Labview (bespoke)	Labview (bespoke)	Qualisys QTM v2.7
Hardware	Twin wire resistance wave gauges, Edinburgh Designs Ltd DAQ	Honeywell HSCSAAN010NDA A5 NI compact DAQ9191 Chassis	Futek LSB120 miniature s-bean load cell NI compact DAQ9191 Chassis	Qualisys
Start	Triggered by wave makers	Triggered by wave makers	Triggered by wave makers	Triggered by wave makers
Stop	Triggered 30 s after wave makers end	Manual	Manual	Manual
F_s [Hz]	128	1667	1667	128
Files	.txt	.lvm	.qtm and .tsv	

The load cells were calibrated by the supply company (FUTEK) and each had a calibration certificate supplied. Details on linearity are given in the Appendix.

Uncertainties on the other instruments are as follows:

- Wave gauges: daily calibration of wave gauges gave error typically <0.0095%. This is negligible.
- Pressure sensor total error band: ±1% of full scale span (see data sheet for details)
- Qualisys positions: Residuals for markers are defined as the difference between the average error measured (mm) compared to the (initial) 6 DOF body definition and these are given in the output (.tsv) files

Wave gauges were positioned around the basin as shown in Figure 2-4, with the precise positions given in the Appendix. The position of the wave gauges has been decided for the flexible array, and were similar for the single device. Further explanations about the position of the wave gauges in the flexible array are given in 3.4.

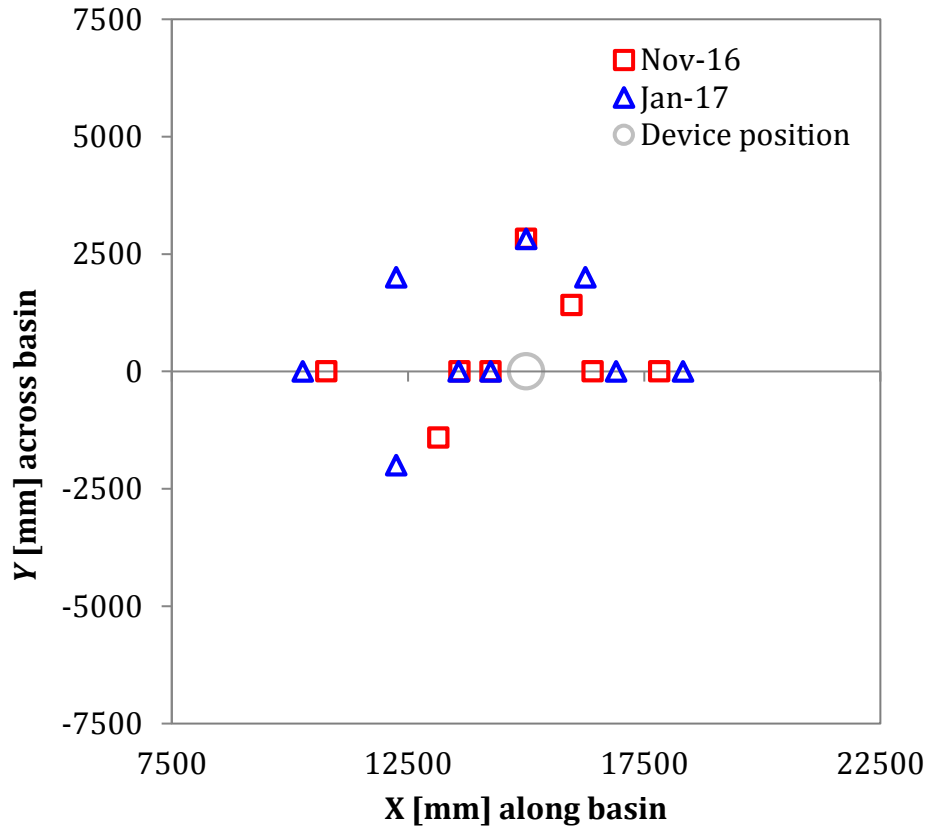

FIGURE 2-4 WAVE GAUGE POSITIONS FOR ALL OWC SPAR BUOY EXPERIMENTS WITH THE ORIGIN AT THE FACE OF THE PADDLES AT REST

2.2 Description of the numerical model

In order to run the simulations using the OrcaFlex software, a set of hydrodynamic coefficients were required as input. Under the assumption of linear water wave theory and potential flow, the commercial code WAMIT (version 7.0), which solves the radiation-diffraction problem based on the boundary element method, was applied. The frequency-domain coefficients of the added mass, the hydrodynamic damping and the excitation force were computed for the single buoy and for the selected array configuration. Hydrostatic coefficients and response amplitude operators (RAOs) were also computed.

The geometry of the buoy is described in section 2.1.1. The water depth is 80m. The total draught of the single buoy has been measured and was equal to 38.96 m. The six rigid degrees of freedom were considered for the buoy.

The motions of the internal free surfaces were not represented by any mode. The internal free surfaces were subject only to the atmospheric pressure. No external damping and no external stiffness were considered in these simulations. Hence, power take-off and mooring forces were not modelled.

The numerical model is built at full scale. However, for easier comparison with the tank test data, the density of water in the model is taken equal to 1000 kg/m^3, which is the density of water in the basin.

OrcaFlex model is shown in Figure 2-5.

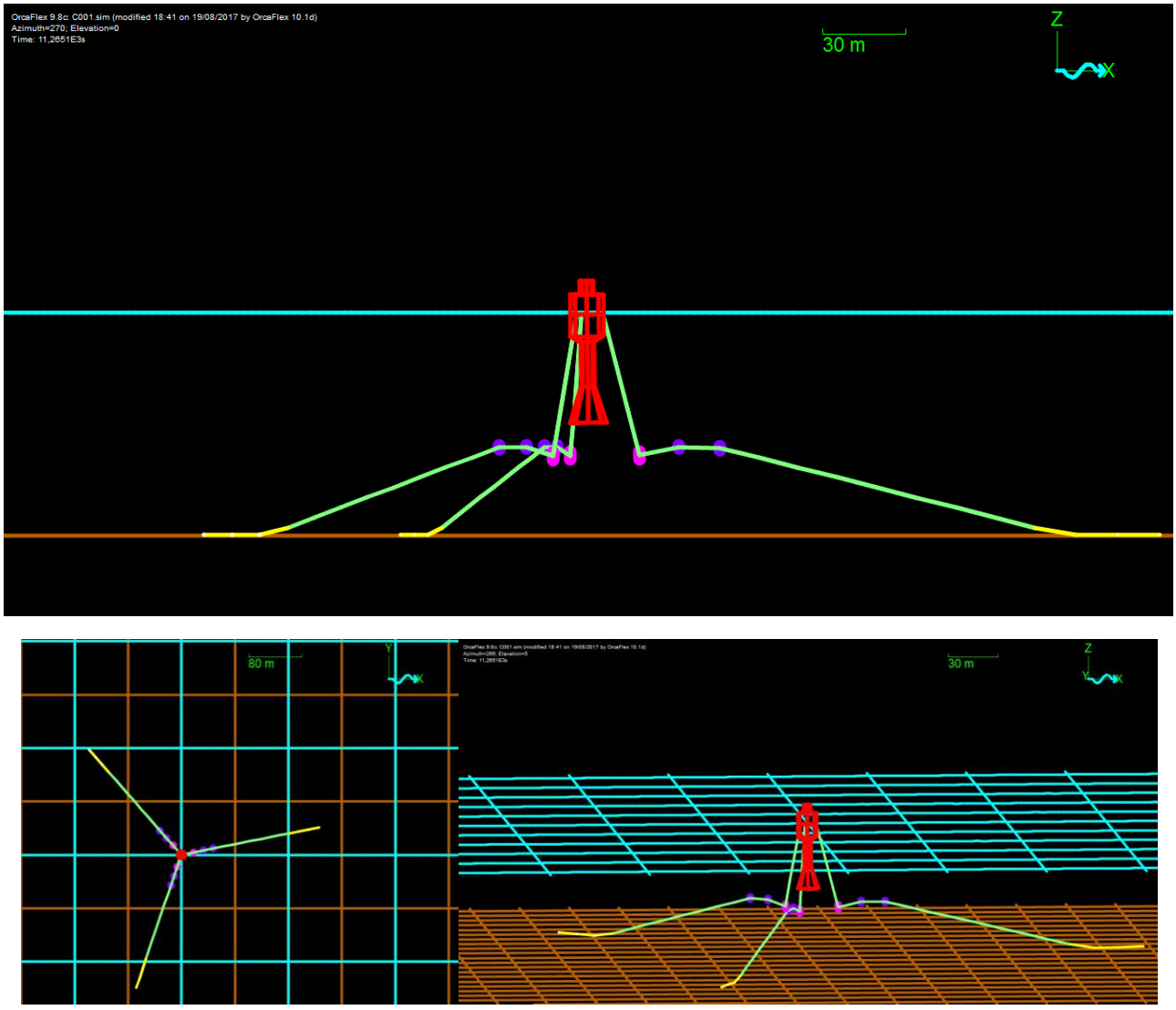

FIGURE 2-5 ORCAFLEX MODEL OF THE SINGLE SPAR BUOY

2.3 Results

All results are given at full scale. For simplicity, the ideal system was modelled, with the target values for masses or lengths for example.

2.3.1 Statics tests

Qualisys data were not available for a still case, so the mean values for the pitch decay cases with PTO were used instead.

The name of the simulations used for this analysis are summarised in Table 2-6.

TABLE 2-6 SUMMARY OF THE STATICS TESTS EXPERIMENT

Simulation name	Mooring	Comments
F008	without	Mean values used, these are pitch decay tests
F009	without	
F010	without	
F011	without	
G004	with	
G005	with	
G006	with	

2.3.1.1 Draught of the buoy

The draught of the OWC spar buoy was directly measured with a scale fixed to the device during the experiments. The measured values are summarised in Table 2-7 along with the numerical model results. The target draught without the mooring system was 36 m. The WAMIT file used for calculation was calculated with the measured draught with a mooring system.

A good agreement was found between the experimental and numerical model values, with less than 2% difference. This difference may be caused by small differences in mass of the buoy and lines, length of the lines or positions of the anchors and fairlead.

TABLE 2-7 EXPERIMENTAL AND NUMERICAL STATICS VALUES OF THE DRAUGHT OF THE ISOLATED OWC SPAR BUOY (M)

			Relative diff (m)	Relative diff %
	Tank test	Numerical model		
Without mooring	35.84	36.36	0.52	1.5%
With mooring	38.96	39.47	0.51	1.3%

2.3.1.2 Vertical position of the buoy (from Qualisys)

The next step was to compare the vertical position of the CoM. The experimental vertical position of the CoM was obtained from the draught (see Table 2-7) as well as from Qualisys data. This aims to cross-check Qualisys results. Results are presented in Table 2-8.

A good agreement was found between the experimental values measured with Qualisys and those deduced from the draught measurement with less than 1% differences between the values. Less than 3% difference is observed between the experimental and numerical values.

TABLE 2-8 EXPERIMENTAL AND MODELLED STATICS VALUES OF THE ISOLATED OWC SPAR BUOY FOR THE VERTICAL POSITION OF COM RELATIVELY TO THE MEAN WATER LEVEL (IN M)

	Experimental (Qualisys)	Experimental (deduced from draught measurement)	Numerical model
Without mooring	-19.03	-19.12	-19.64
With mooring	-22.08	-22.24	-22.75

2.3.1.3 Position of the buoy in the other DOFs

The final step with the statics results was to observe the experimental statics position of the buoy.

Similarly, Qualisys data were not available for a still case so the mean values for the heave decay cases with PTO (F004 to F007 without mooring and G001-G003 with mooring) were used instead.

In a still position, the buoy angles were below 2°; X and Y positions were in the order of 2 m and 1 m respectively, which was acceptable compared to the dimensions of the buoy.

The experimental heading values were not available because the mean yaw values provided by Qualisys were not centred around the origin.

TABLE 2-9 EXPERIMENTAL AND MODELLED VALUES OF THE ISOLATED OWC SPAR BUOY FOR THE STATICS VALUES OF X AND Y (IN M) AND HEEL AND TRIM ANGLES (IN DEG)

		Experimental (Qualisys)	Numerical model
Without mooring	**Heel**	0.97	0
	Trim	-0.43	0
With mooring	**X**	-2.19	0
	Y	-0.99	0
	Heel	1.18	0
	Trim	-0.99	0

2.3.1.4 Mooring line tensions

The mooring line tensions are now compared. This allows a first check on the correction of the load cells. Results are presented in Table 2-10. The flat water static value for each load cell and sensor dry offset were provided and were used for this comparison.

A good agreement was found between the experimental and the numerical values with less than 1% difference.

TABLE 2-10 EXPERIMENTAL AND MODELLED STATICS VALUES OF THE ISOLATED OWC SPAR BUOY FOR THE MOORING LINE TENSION (IN N)

Line	Experimental	Numerical model	Relative difference
3a	1.00E6	1.01E6	-1%
3b	1.02E6	1.01E6	1%
3c	1.02E6	1.01E6	1%

2.3.1.5 Summary

A good agreement was found for the statics position and mooring line tension. The most noticeable difference is that the buoy floated 0.5 m lower in the numerical model than in the experiment. This may be caused by small differences between the experiment layout and the target values.

2.3.2 Pull-out tests

Experimental results were found to be highly repeatable.

The name of the simulations used for this analysis are summarised in Table 2-11.

TABLE 2-11 SUMMARY OF THE PULL-OUT TESTS EXPERIMENT

Simulation name	DOF
I003	Surge
I004	Surge
I001	Heave
I002	Heave

2.3.2.1 Surge

Cases I003 and I004 were used to compare the mooring stiffness in surge. Both tests were similar (same surge direction and same amplitude of surge) but I004 was shorter. Motions in the pull-out direction are presented in Figure 2-6.

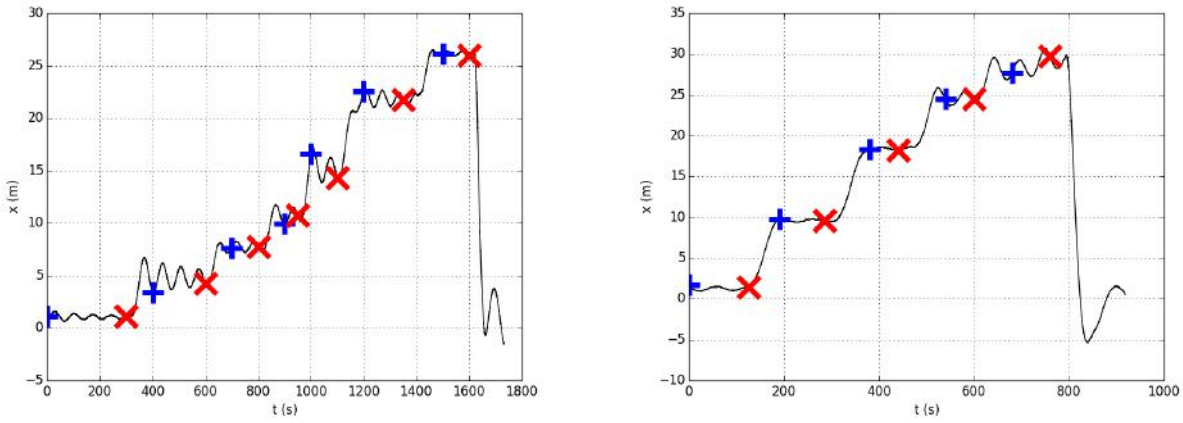

I003 I004

FIGURE 2-6 EXPERIMENTAL MOTIONS OF POINT O OF THE ISOLATED OWC SPAR BUOY IN THE SURGE DIRECTION DURING SURGE PULL-OUT TESTS

The buoy was not still at each step of the pull-out test and small oscillations were observed around each equilibrium position. In addition, the buoy was not perfectly pulled along the X axis. For example, in case I003, the position along the Y axis was modified by ± 1.5 m, and the pitch angle by ± 3°. Figure 2-7 shows the variation of the tension recorded in the experiments for each of the mooring lines (3a, 3b, 3c) and those modelled numerically for file I003 and Figure 2-8 shows those from file I004. The variation in tension for a given position is similar in the experiment and the numerical model and both cases (I003 and I004) are similar. This means that the mooring stiffness in surge in the numerical model replicated the mooring stiffness of the experiment correctly.

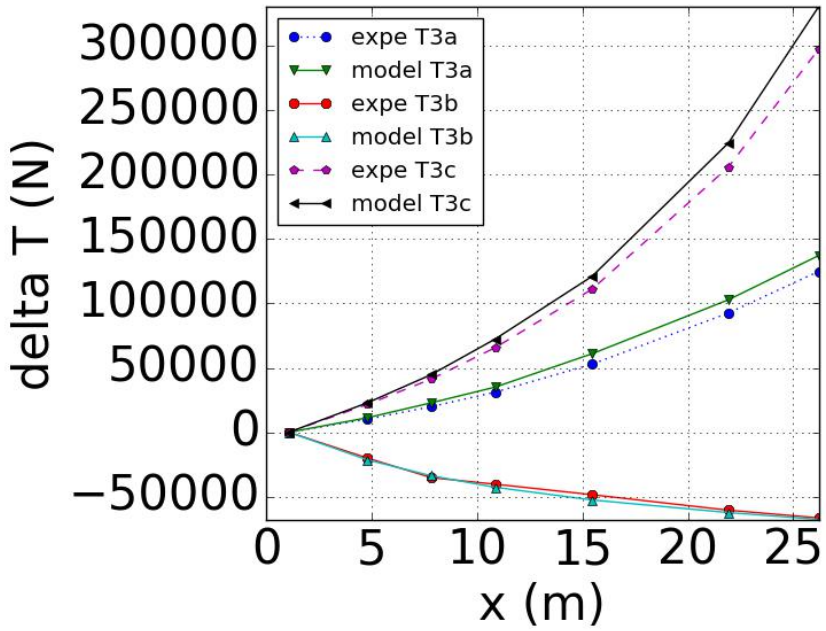

FIGURE 2-7 EXPERIMENTAL AND MODELLED VARIATIONS OF TENSIONS OF THE ISOLATED OWC SPAR BUOY FOR DIFFERENT SURGE POSITION DURING SURGE PULL-OUT TEST I003

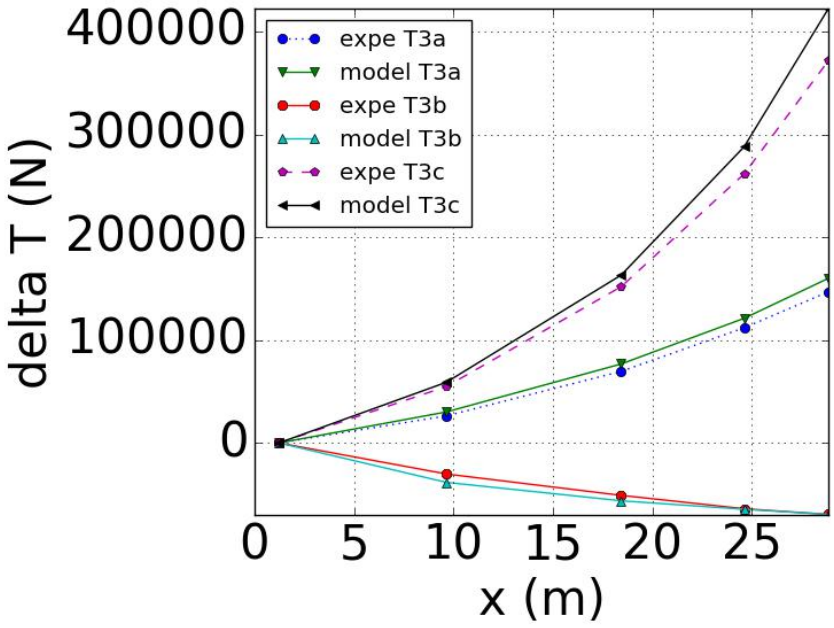

FIGURE 2-8 EXPERIMENTAL AND MODELLED VARIATIONS OF TENSIONS OF THE ISOLATED OWC SPAR BUOY FOR DIFFERENT SURGE POSITION DURING SURGE PULL-OUT TEST I004

2.3.2.2 Heave

Cases I001 and I002 were used to compare the mooring stiffness in heave. Both tests are similar (same heave direction and same amplitude of heave). Motions in the heave pull-out direction are presented in

Figure 2-9. The buoy was relatively still at each step of the pull-out test but it was not perfectly pulled along the Z axis. The last two steps of I001and the first step of I002 are very short and the experimental values may be inaccurate, especially in the X and Y directions. For I001, for the last two steps, the X mean position varies between -0.15 m and -1.22 m. For I002, for the first step, the X position varies between 0.48 m and -0.81 m.

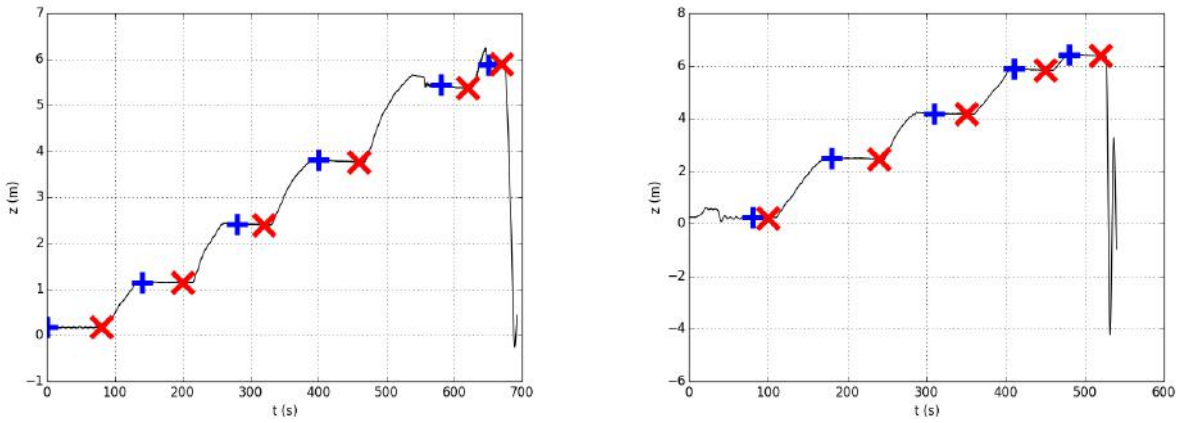

I001 I002

FIGURE 2-9 EXPERIMENTAL MOTIONS OF POINT O OF THE ISOLATED OWC SPAR BUOY IN THE HEAVE DIRECTION DURING HEAVE PULL-OUT TESTS

Experimental and numerical results for the change in line tension for each mooring line are presented in Figure 2-7 (I001) and Figure 2-11 (I002). Differences are observed for the last two steps of I001 and the first step of I002, which potentially have inaccurate X and Y mean positions as explained above. The variation in X and Y motions explains the decreases in model tensions. Apart from these points, the variation in tension for a given position is similar in the experiment and the numerical model. This means that the numerical model replicates correctly the mooring stiffness of the experiment.

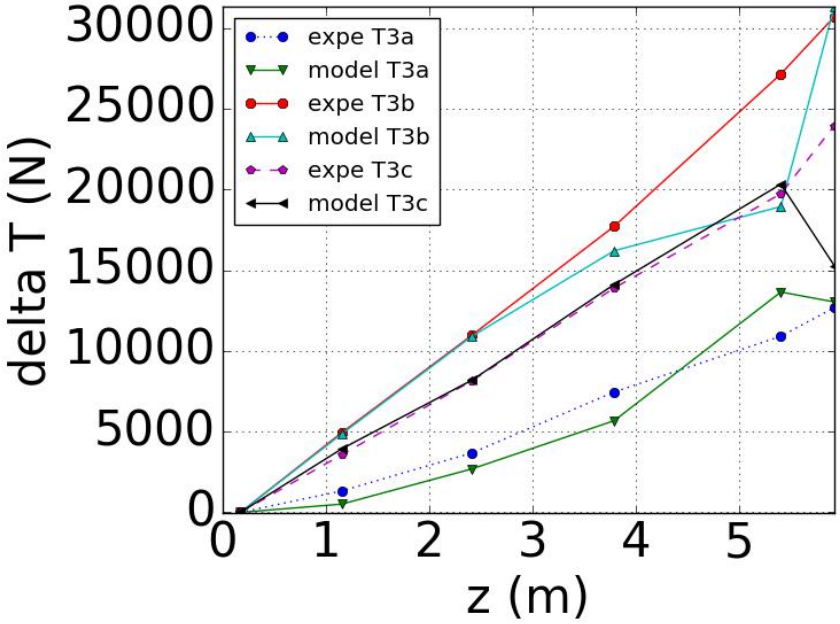

FIGURE 2-10 EXPERIMENTAL AND MODELLED VARIATIONS OF TENSIONS OF THE ISOLATED OWC SPAR BUOY FOR DIFFERENT HEAVE POSITION DURING HEAVE PULL-OUT TEST I001

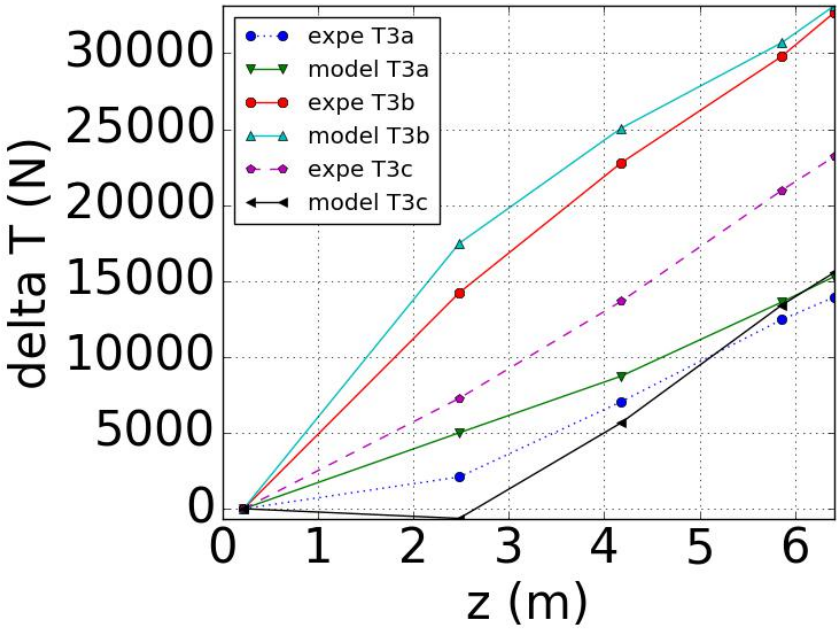

FIGURE 2-11 EXPERIMENTAL AND MODELLED VARIATIONS OF TENSIONS OF THE ISOLATED OWC SPAR BUOY FOR DIFFERENT HEAVE POSITION DURING HEAVE PULL-OUT TEST I002

2.3.2.3 Summary

Pull-out tests indicate that the mooring stiffness in heave was similar in the experiment and the numerical model.

2.3.3 Decay tests

Experimental decay tests were more or less repeatable. Experimental heave decay test results were the most repeatable. The less repeatable tests were the roll decay tests; this was due to difficulty restricting the motion to one degree of freedom.

The name of the simulations used for this analysis are summarised in Table 2-12.

TABLE 2-12 SUMMARY OF THE DECAY TESTS EXPERIMENT

Simulation name	DOF
G001	Heave
G002	Heave
G003	Heave
G004	Pitch
G005	Pitch
G006	Pitch
G007	Surge
G008	Surge
G009	Surge
G010	Roll
G011	Roll
G012	Roll
G013	Roll
G014	Sway
G015	Sway
G016	Sway

Experiments G001 to G016 were used to estimate the damping of the buoy and its mooring system. These are the experiments with the mooring system and the PTO. This damping was then implemented in the five buoy array.

The following steps were done for each DOF (except yaw):

- linear and quadratic damping coefficients are calculated based on the time series of the experiment
- initial position for each decay test is extracted from the experimental data
- values are implemented in OrcaFlex model and numerical and experimental results are compared

Yaw decay tests with the mooring system and the PTO were not conducted.

No damping was included on the mooring line as this damping is considered to be negligible.

Each decay test was repeated 3 or 4 times.

Experimental tests were not oscillating around zero, therefore means were removed from time series for comparison. Means were removed instead of the statics position because the buoy could achieve several statics equilibrium position.

2.3.3.1 Surge

Tests G007-9 are used for this study.

In each simulation 3 to 4 troughs and 2 to 4 peaks were detected (Figure 2-12). This means that the linear fit to obtain damping coefficients was done with between 3 and 5 points. This is a limited number of data points. The buoy oscillated around an equilibrium position with the surge amplitude X close to -2 m.

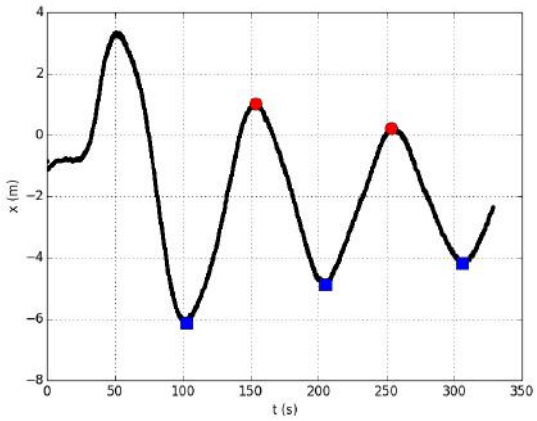

G007

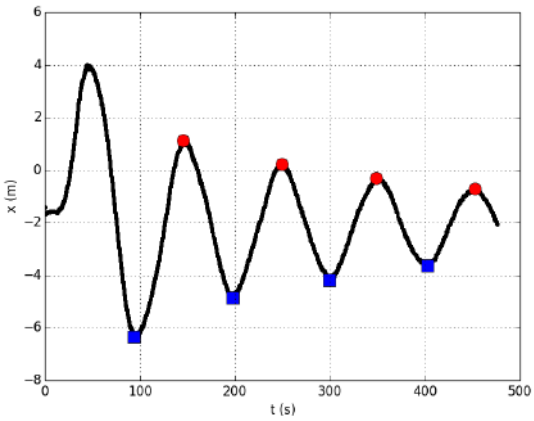

G008

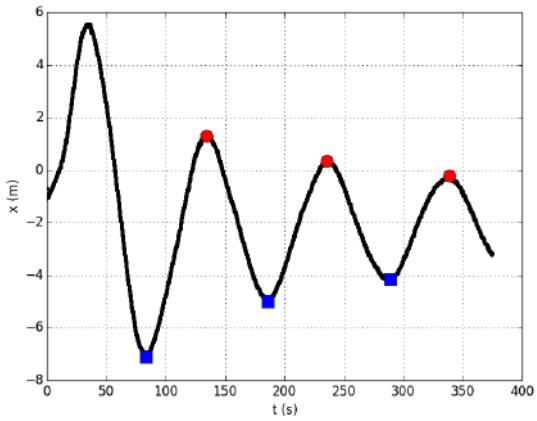

G009

FIGURE 2-12 SURGE DECAY TESTS OF THE ISOLATED OWC SPAR BUOY. EXPERIMENTAL MOTIONS IN SURGE AND PEAKS (RED DOTS) AND TROUGHS (BLUE DOTS) USED FOR DAMPING COEFFICIENTS CALIBRATION AND NATURAL PERIOD ESTIMATION

Natural periods and linear and quadratic damping coefficients for the different simulations and the mean values are summarised in Table 2-13.

TABLE 2-13 RESULTS FOR SURGE DECAY EXPERIMENT OF THE ISOLATED OWC SPAR BUOY: NATURAL PERIOD AND LINEAR AND QUADRATIC DAMPING

	T_m (s)	p_1 (s^{-1})	p_2(m^{-1})	Nb of points for linear fit
G007	101.81	6.22E-03	-5.63E-03	3
G008	102.63	5.93E-03	-5.73E-03	6
G009	102.26	6.99E-03	-9.77E-03	4
Mean	102.23	6.38E-03	-7.04E-03	

The values used as input in OrcaFlex are summarised in Table 2-14. Negative values do not have a physical meaning. They have been included in the single buoy model but a sensitivity analysis indicated that they do not have an influence on the results. They are zeroed for the flexible array.

TABLE 2-14 LINEAR AND QUADRATIC SURGE DAMPING OF THE OWC SPAR BUOY USED AS INPUT IN ORCAFLEX AND VALUES OF MASS/ADDED MASS USED FOR CALCULATION

M (kg)	Ma (kg) at Tm	B1 (kg/s)	B2 (kg/m)
1.22E+06	2.49E+06	2.36E+04	-2.61E+04

Experimental, numerical model and analytical natural periods for surge decay are compared in Table 2-15. Relatively large differences (-17%) were observed between the numerical model and experimental values, as well as between the analytical and experimental values (-30%). This can be explained in coupling appearing in the experiment, which was also present but to a lesser extent in the numerical model. The analytical value is for an uncoupled motion. This result does not have a large influence on the modelling. Since the period of the surge is much larger that the simulated wave periods (and the usual wave periods), the difference found between the numerical model and the experiment does not affect much the regular and irregular wave simulations results. Eventually, the model would not work so well for longer periods.

TABLE 2-15 COMPARISON OF NATURAL PERIOD OF THE ISOLATED OWC SPAR BUOY FOR SURGE DECAY EXPERIMENT AND NUMERICAL MODEL

T_m (s)	Experiment	Numerical model	Analytical value
G007	101.81	85.30	
G008	102.63	85.32	
G009	102.26	85.34	
Mean	102.23	85.32	71.69
Relative difference with experiment		-17%	-30%

Time series of the relative motion of surge during the decay tests is compared in Figure 2-13. The amplitude of the surge motion is higher in the numerical model compared to the experiment indicating that the damping was slightly underestimated.

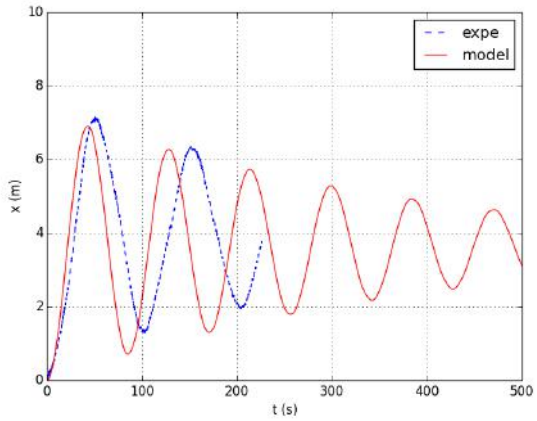

G007

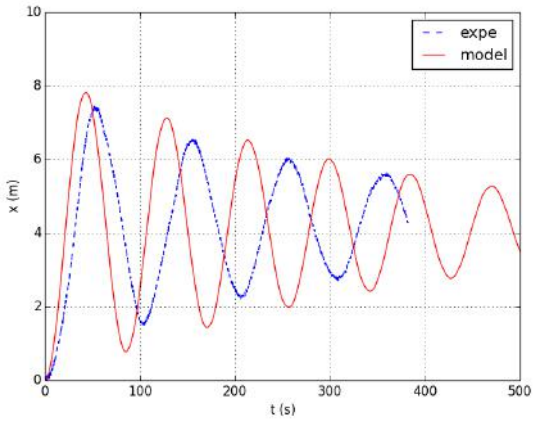

G008

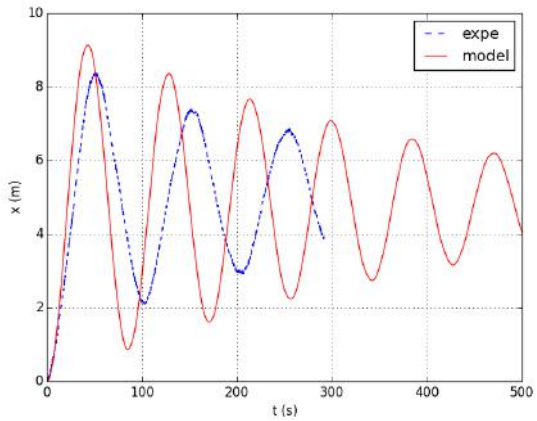

G009

FIGURE 2-13 SURGE DECAY TESTS OF THE ISOLATED OWC SPAR BUOY. EXPERIMENTAL AND MODEL RELATIVE MOTIONS

2.3.3.2 Sway

Tests G014-16 were used for this study. Experimental results are shown in Figure 2-14.

In each simulation two or three troughs and two peaks were detected (7.1.1 in the Appendix). This means that the linear fit to obtain damping coefficients was done with 2 to 3 points which is a limited number of data points.

Natural periods and linear and quadratic damping coefficients for the different simulations and the mean values are summarised in Table 2-16. The buoy oscillated around an equilibrium position with the sway amplitude y close to -1 m. The values for natural period, linear and quadratic damping in sway are similar to the values in surge.

Similarly than for the surge, differences in natural period between the numerical model and the experiment do not affect much the regular and irregular wave simulations results.

TABLE 2-16 RESULTS FOR SWAY DECAY EXPERIMENT OF THE ISOLATED OWC SPAR BUOY: NATURAL PERIOD AND LINEAR AND QUADRATIC DAMPING

	T_m (s)	p_1 (s^{-1})	p_2 (m^{-1})	Nb of points for linear fit
G014	102.81	6.67E-3	-6.87E-3	2
G015	102.18	4.98E-3	-3.76E-3	3
G016	100.53	6.63E-3	-3.96E-3	2
Mean	101.84	6.09E-3	-4.87E-3	

The values used as input in OrcaFlex are summarised in Table 2-17.

TABLE 2-17 LINEAR AND QUADRATIC SWAY DAMPING OF THE OWC SPAR BUOY USED AS INPUT IN ORCAFLEX AND VALUES OF MASS/ADDED MASS USED FOR CALCULATION

M (kg)	Ma (kg) at Tm	B1 (kg/s)	B2 (kg/m)
1.22E+6	2.49E+6	2.26E+4	-1.80E+4

Experimental, numerical model and analytical natural periods for surge decay are compared in Table 2-18. Large relative differences were observed between the numerical model and experimental values (-16%), as well as between the analytical and experimental values (-30%). This can be explained in coupling appearing in the experiment, which was also present but to a lesser extent in the numerical model. The analytical value is for an uncoupled motion.

TABLE 2-18 COMPARISON OF NATURAL PERIOD OF THE ISOLATED OWC SPAR BUOY FOR SWAY DECAY EXPERIMENT AND NUMERICAL MODEL

T_m (s)	Experiment	Numerical model	Analytical value
G014	102.81	85.27	
G015	102.18	85.26	
G016	100.53	85.27	
Mean	101.84	85.27	71.69
Relative difference with experiment		-16%	-30%

Time series of the relative motion of sway during the decay tests is compared Figure 2-14. The damping is slightly underestimated in the numerical model compared to the experiment.

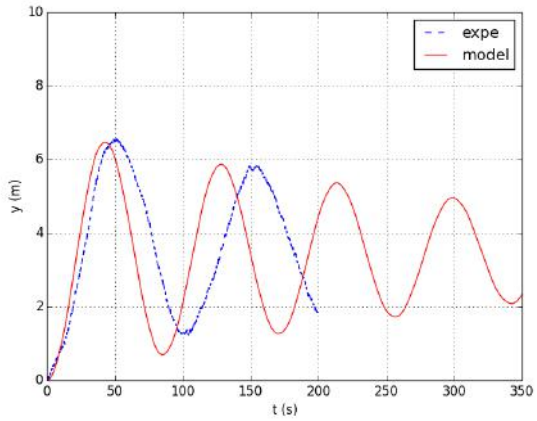

G014

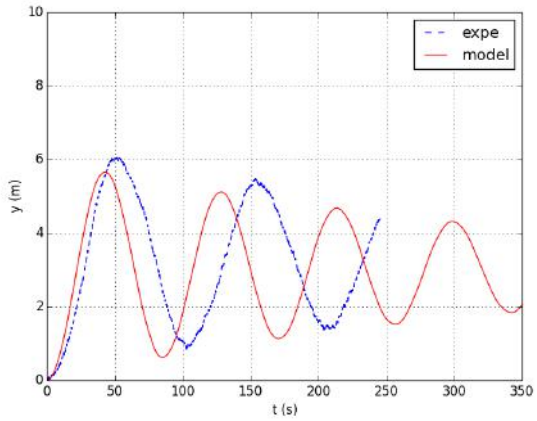

G015

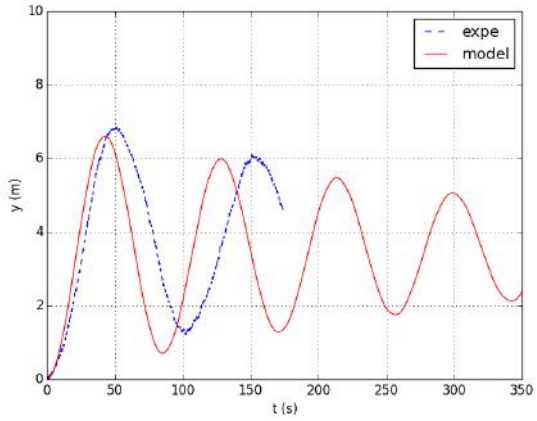

G016

FIGURE 2-14 SWAY DECAY TESTS OF THE ISOLATED OWC SPAR BUOY. EXPERIMENTAL AND MODEL RELATIVE MOTIONS

2.3.3.3 Heave

Tests G001-3 were used for this study. Experimental results are shown in Figure 2-15.

In each simulation four troughs and three peaks were detected (0 in Appendix). This means that the linear fit to obtain damping coefficients was done with five points. This is a relatively good number of data points. The buoy oscillated around an equilibrium position with the heave amplitude z equal to -21.6 m.

Natural periods and linear and quadratic damping coefficients for the different simulations and the mean values are summarised in Table 2-19.

TABLE 2-19 RESULTS FOR HEAVE DECAY EXPERIMENT: NATURAL PERIOD AND LINEAR AND QUADRATIC DAMPING

	T_m (s)	p_1 (s^{-1})	p_2 (m^{-1})	Nb of points for linear fit
G001	9.47	2.29E-1	2.14E-2	5
G002	9.34	2.15E-1	2.59E-2	5
G003	9.40	2.25E-1	1.97E-2	5
Mean	9.40	2.23E-1	2.23E-2	

The values used as input in OrcaFlex are summarised in Table 2-20.

TABLE 2-20 LINEAR AND QUADRATIC HEAVE DAMPING OF THE ISOLATED OWC SPAR BUOY USED AS INPUT IN ORCAFLEX AND VALUES OF MASS/ADDED MASS USED FOR CALCULATION

M (kg)	Ma (kg) at Tm	B1 (kg/s)	B2 (kg/m)
1.22E+6	7.81E+5	4.46E+5	4.46E+4

Experimental, numerical model and analytical natural periods for surge decay are compared in Table 2-21. Small relative differences were observed between the numerical model and experimental values (+10%), as well as between the analytical and experimental values (-3%).

TABLE 2-21 COMPARISON OF NATURAL PERIOD OF THE ISOLATED OWC SPAR BUOY FOR HEAVE DECAY EXPERIMENT AND NUMERICAL MODEL

T_m (s)	Experiment	Numerical model	Analytical value
G001	9.47	10.36	
G002	9.34	10.37	
G003	9.40	10.36	
Mean	9.40	10.36	9.10
Relative difference with experiment		+10%	-3%

Time series of the relative motion of heave during the decay tests are compared in Figure 2-15. The value of damping used in the numerical model, obtained from the decay test analysis seems to overestimate the damping of the experimental decay test, due to the faster decay of amplitude. However, since neither the method used to extract the heave damping value, nor the numerical model, considers the OWC interaction, it was not expected a great agreement in the heave decay tests.

Since the numerical model assumes that the buoy and OWC move together, this model is more reasonable for the simulation of the coupled motion between the buoy and the OWC. This justifies the higher natural period found by the numerical model.

A sensitivity analysis could be conducted in further work to calibrate the heave damping value.

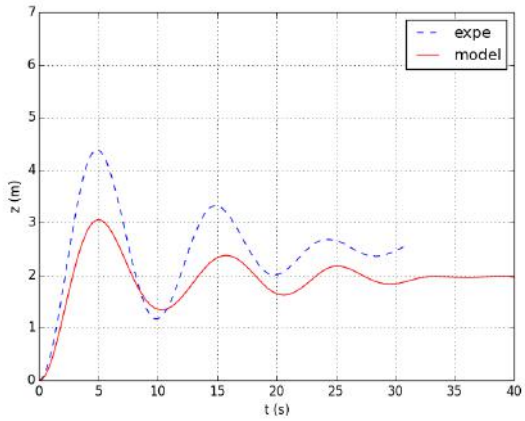

G001

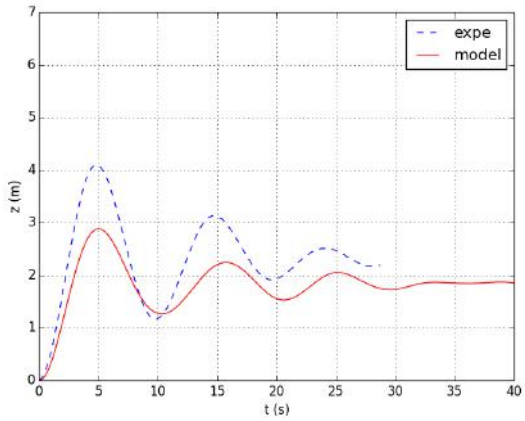

G002

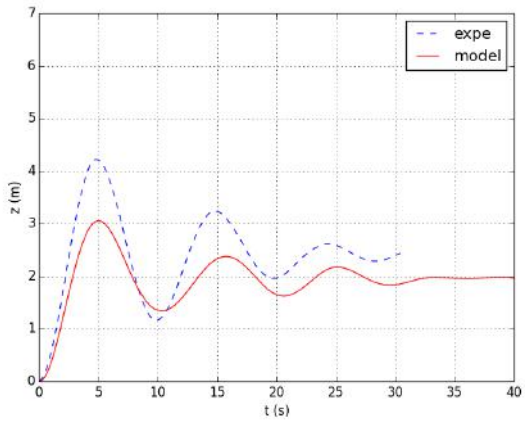

G003

FIGURE 2-15 HEAVE DECAY TESTS OF THE ISOLATED OWC SPAR BUOY. EXPERIMENTAL AND NUMERICAL MODEL RELATIVE MOTIONS

2.3.3.4 Roll

Tests G010-G013 are used for this study. Experimental results are shown in Figure 2-16.

In each simulation, only one or two troughs and two peaks were detected, (0 in the Appendix). This, means that the linear fit to obtain damping coefficients was done with only two points for simulation G010 and could not be done in the other cases.

Irregularities in the decay are likely to be caused by mooring line effects.

Natural periods and linear and quadratic damping coefficients for the different simulations and the mean values are summarised in Table 2-22.

TABLE 2-22 RESULTS FOR ROLL DECAY EXPERIMENT OF THE ISOLATED OWC SPAR BUOY: NATURAL PERIOD AND LINEAR AND QUADRATIC DAMPING

	T_m (s)	p_1 (s^{-1})	p_2(deg^{-1})	Nb of points for linear fit
G010	36.00	4.21E-2	1.98E-2	2
G011	33.45	N/A	N/A	1
G012	35.28	N/A	N/A	1
G013	36.61	N/A	N/A	1
Mean	35.34	4.21E-2	1.98E-2	

The values used as input in OrcaFlex are summarised in Table 2-23.

TABLE 2-23 LINEAR AND QUADRATIC ROLL DAMPING OF THE ISOLATED OWC SPAR BUOY USED AS INPUT IN ORCAFLEX AND VALUES OF INERTIA/ADDED INERTIA USED FOR CALCULATION

I ($kg.m^2$)	Ia ($kg.m^2$) at Tm	B1 (kg/(rad.s))	B2 $(N/(rad.m/s)^2)$
3.25E+08	1.33E+9	1.22E+6	5.71E+5

Experimental, numerical model and analytical natural periods for surge decay are compared in Table 2-24. Moderate relative differences were observed between the numerical model and experimental values (-23%), as well as between the analytical and experimental values (-16%).

TABLE 2-24 COMPARISON OF NATURAL PERIOD OF THE ISOLATED OWC SPAR BUOY FOR ROLL DECAY EXPERIMENT AND NUMERICAL MODEL

T_m (s)	Experiment	Numerical model	Analytical value
G010	36.00	27.06	
G011	33.45	27.01	
G012	35.28	27.06	
G013	36.61	27.02	
Mean	35.34	27.04	29.79
Relative difference with experiment		-23%	-16%

Time series of the relative motion of surge during the decay tests is compared in Figure 2-16. The damping was of the same order of magnitude in the numerical model compared to the experiment.

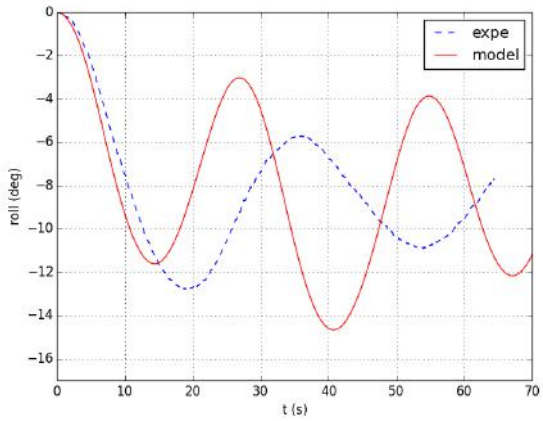

G010

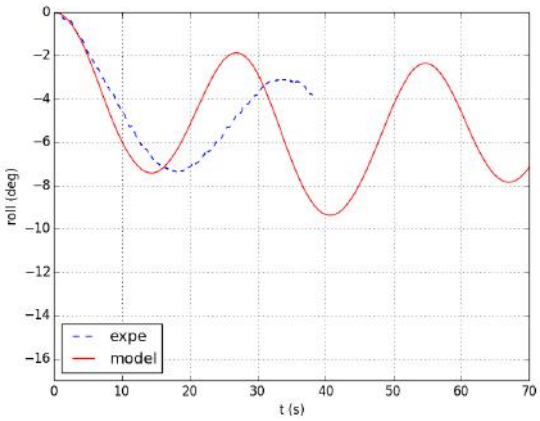

G011

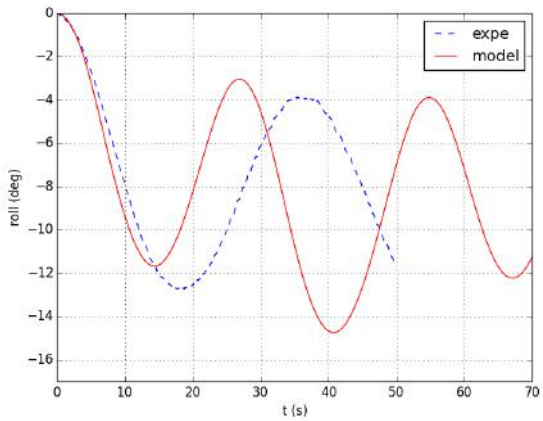

G012

FIGURE 2-16 ROLL DECAY TESTS OF THE ISOLATED OWC SPAR BUOY. EXPERIMENTAL AND MODEL RELATIVE MOTIONS

2.3.3.5 Pitch

Tests G004-6 were used for this study. Experimental results are shown in Figure 2-17.

In each simulation two troughs and one peak were detected (0 in the Appendix). This means that the linear fit to obtain damping coefficients could not be done. Irregularities in the decay are likely to be caused by mooring line effects.

The values of linear and quadratic damping for roll were used.

Natural periods for the different simulations and the mean values are summarised in Table 2-25.

TABLE 2-25 RESULTS FOR PITCH DECAY EXPERIMENT OF THE ISOLATED OWC SPAR BUOY: NATURAL PERIOD AND LINEAR AND QUADRATIC DAMPING

	T_m (s)	p_1 (s^{-1})	p_2(deg^{-1})	Nb of points for linear fit
G004	34.74	N/A	N/A	1
G005	35.82	N/A	N/A	1
G006	35.48	N/A	N/A	1
Mean	35.35	N/A	N/A	

The values used as input in OrcaFlex are summarised in Table 2-26.

TABLE 2-26 LINEAR AND QUADRATIC PITCH DAMPING OF THE ISOLATED OWC SPAR BUOY USED AS INPUT IN ORCAFLEX AND VALUES OF INERTIA/ADDED INERTIA USED FOR CALCULATION

I (kg.m²)	Ia (kg.m²) at Tm	B1 (kg/(rad.s))	B2 (N/(rad.m/s)^2)
3.25E+08	1.33E+09		

Experimental, numerical model and analytical natural periods for surge decay are compared in Table 2-27. Moderate relative differences were observed between the numerical model and experimental values (-23%), as well as between the analytical and experimental values (-16%).

TABLE 2-27 COMPARISON OF NATURAL PERIOD OF THE ISOLATED OWC SPAR BUOY FOR ROLL DECAY EXPERIMENT AND NUMERICAL MODEL

T_m (s)	Experiment	Numerical model	Analytical value
G004	34.74	27.16	
G005	35.82	27.14	
G006	35.48	27.17	
Mean	35.35	27.16	29.79
Relative difference with experiment		-23%	-16%

The time series of the relative surge motion during the decay tests is compared in Figure 2-17. The damping was of the same order of magnitude in the numerical model compared to the experiment.

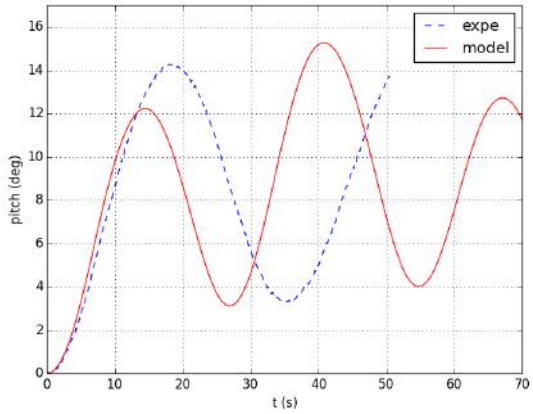

G004

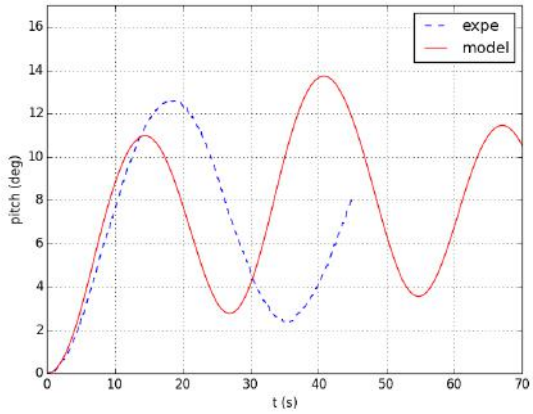

G005

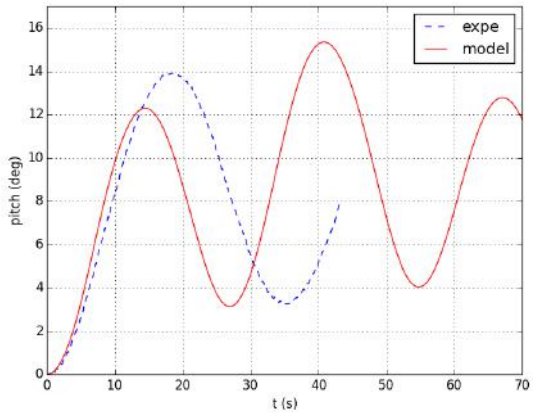

G006

FIGURE 2-17 PITCH DECAY TESTS OF THE ISOLATED OWC SPAR BUOY. EXPERIMENTAL AND MODEL RELATIVE MOTIONS

2.3.3.6 Negative damping values

A sensitivity analysis was conducted when negative quadratic damping values appear (for the surge and sway). Decay simulations were run without quadratic damping. The results indicate that the quadratic damping had no influence on the results. Further calculations for the single device were run with the calculated quadratic damping values. All calculations for the flexible array were run without quadratic damping.

2.3.3.7 Summary

Differences were found between the experiment and the numerical model for the natural period (Table 2-28), and damping (Table 2-29). The main difference is that the heave damping was underestimated in the numerical model.

TABLE 2-28 SUMMARY OF THE MEASURED AND MODELLED NATURAL PERIOD OF THE ISOLATED OWC SPAR BUOY IN ALL DOFS EXCEPT YAW

Mean natural period (Tm)	Experiment	Numerical model	Relative difference (%)
Surge	102.23	85.32	-17%
Sway	101.84	85.27	-16%
Heave	9.40	10.36	10%
Roll	35.34	27.04	-23%
Pitch	35.35	27.16	-23%

TABLE 2-29 SUMMARY OF THE MEASURED AND MODELLED DAMPING OF THE ISOLATED OWC SPAR BUOY IN ALL DOFS EXCEPT YAW. + MEANS THAT THE DAMPING IS OVERESTIMATED, - THAT IT IS UNDERESTIMATED, = THAT THE ESTIMATION IS CLOSE. IN ADDITION, THE LINEAR DAMPING VALUES IN THE NUMERICAL MODEL ARE SUMMARISED IN THIS TABLE

Damping	Numerical model	Linear damping values used in the numerical model (N/(m/s) or (N.m)/(rad/s)
Surge	-	23.60E3
Sway	-	22.60E3
Heave	- - -	446.0E3
Roll	=	1.220E6
Pitch	=	1.220E6

2.3.4 Regular wave tests

Regular wave fields have been tested with ten repeats of the same input wave, measuring the surface elevations and calculating the measured wave heights. The 95% confidence interval for the worst case showed results to be within ±4% of the mean wave height.

Experiments were conducted for two wave heights *H*: 1 m and 4 m and a wide range of periods, between 6 s and 22 s. In addition, several additional experiments were run for *T* equal to 10.04 s and *H* varying between 0.5 m and 4 m. This was close to the heave resonance, which was the only system resonance period inside the wave range. The aim of these additional experiments was to evaluate the system linear and non-linear behaviour close to one of its resonant periods. The experiment names, wave height and wave periods are summarised in Table 2-30 and Figure 2-18. Some waves (with *H* = 8 m and *T* below 7 s) were over the linear wave limit and close to the wave breaking limit. Some experiments were repeated. OrcaFlex simulations were unstable for periods over 10 s when the wave height was equal to 8 m (Table 2-30).

The set of regular waves covers periods that excite both the buoy heave and the OWC heave resonance conditions. This is the range of periods adequate for power extraction. The pitch and roll natural periods fall outside the range of wave periods. However, this device is prone to be excited by parametric resonance in pitch and roll, which is observed for periods around half the natural pitch/roll period, i.e. 17.7s. The range of periods with parametric resonance in pitch/roll is likely to increase as the wave height increases.

TABLE 2-30 SUMMARY OF THE REGULAR WAVE EXPERIMENT AND NUMERICAL MODEL STABILITY OF THE ISOLATED OWC SPAR BUOY

Simulation name	H (m)	T(s)	Comments
B062	2	6.66	
B061	2	7.03	
B060	2	7.44	
B059	2	7.91	
B058	2	8.43	
B053	2	8.72	
B036, B052	2	9.04	
B035, B051	2	9.37	
B034, B050	2	9.73	
B033, B049	2	9.88	
B066, B067, B068	2	10.04	
B032, B046	2	10.20	
B030, B045	2	10.54	
B044, B057	2	11.00	
B029, B043	2	11.50	
B064, B065	2	12.05	
B042, B056	2	12.65	unstable
B041, B055	2	14.05	unstable
B040	2	15.81	
B039	2	18.07	
B038, B054	2	21.08	
B025	8	6.32	
B024	8	6.66	
B023	8	7.03	
B022	8	7.44	unstable
B021	8	7.91	unstable
B020, B028	8	8.43	
B019	8	9.04	unstable
B018	8	9.73	unstable
B027	8	9.88	unstable
B071	8	10.04	unstable
B026	8	10.20	unstable
B015	8	10.54	unstable
B014, B070	8	11.50	unstable
B013, B069	8	12.65	unstable
B012	8	14.05	unstable
B011	8	15.81	unstable
B010	8	18.07	unstable
B009	8	21.08	unstable
B075	1.0	10.04	
B074	3.2	10.04	
B073	4.8	10.04	
B072	6.4	10.04	

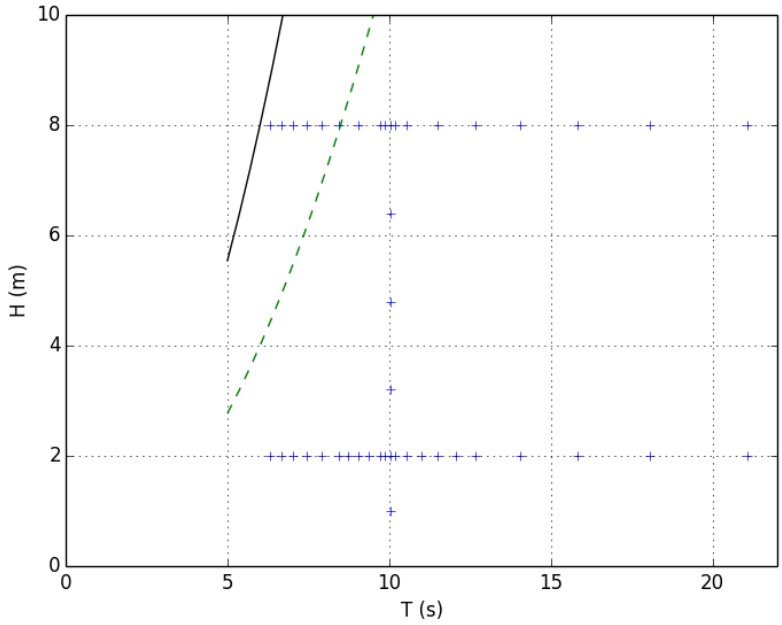

FIGURE 2-18 TESTED REGULAR WAVES (AIRY) FOR THE ISOLATED OWC SPAR BUOY. GREEN DOTTED LINE: LIMIT OF LINEAR WAVES; BLACK LINE: WAVE BREAKING LIMIT

The RAOs for the surge, heave and pitch are shown in Figure 2-19 (H = 2 m) and Figure 2-20 (H=8 m).

The surge RAOs increased with period with values up to 1.5 m/m. The experimental and modelled surge RAOS compared well for periods below 12 s. The numerical model underestimated the RAOs for periods over 12 s.

The heave RAOs increased for periods below 10 s with values up to 2.4 m/m (experiment, H = 2 m). This could be expected because the heave resonance period was close to 10 s. The experimental and model behaviour was similar, however the modelled RAOs were generally smaller than the experimental RAOs. This was expected because the heave damping was higher in the numerical model than in the experiment as observed during the decay tests. The RAOs were smaller for H = 8 m than for H = 2 m.

The pitch RAO was the highest for T = 14 s (experiment, the numerical model was not stable for this case). This could be expected because it is half the resonance period in pitch. The experimental and numerical model gave similar results for small and large periods but differed for periods between 9 s and 18 s. This can be explained by non-linearities (which can be observed in time series) in pitch motion; these non-linearities cannot be modelled with the linear theory. Another sign of non-linearities is that RAOs were generally smaller for H = 8 m than for H = 2 m.

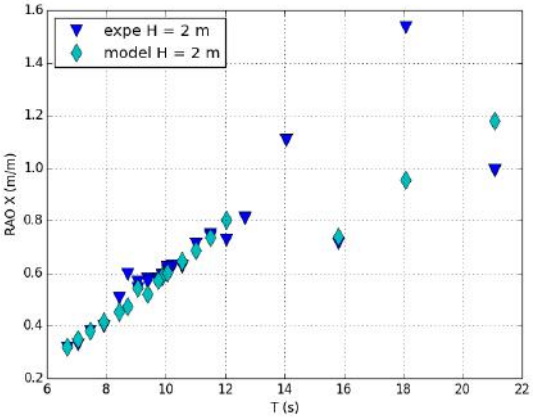

X: surge

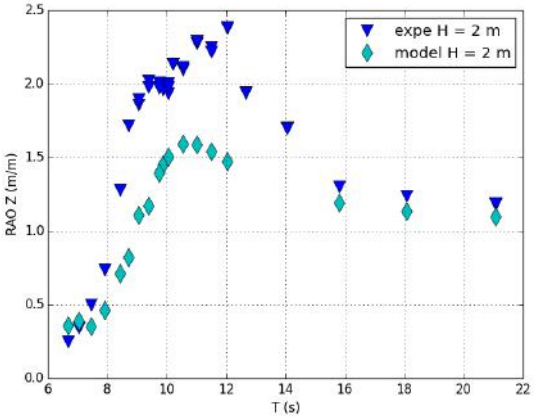

Z: heave

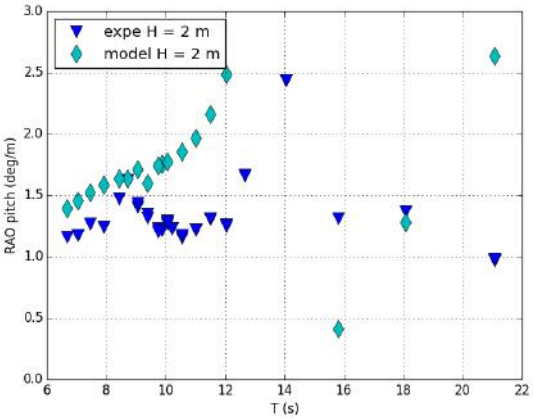

pitch

FIGURE 2-19 EXPERIMENTAL AND MODELLED DISPLACEMENT RAOS OF THE ISOLATED OWC SPAR BUOY IN THE 3 MAIN DOFS, H = 2 M

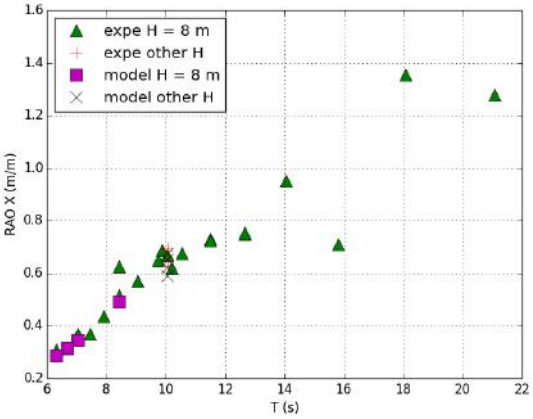

X: surge

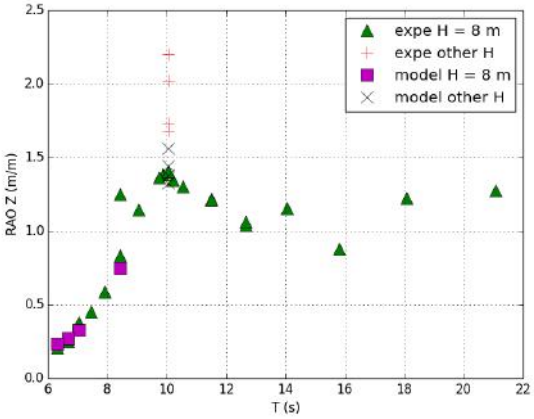

Z: heave

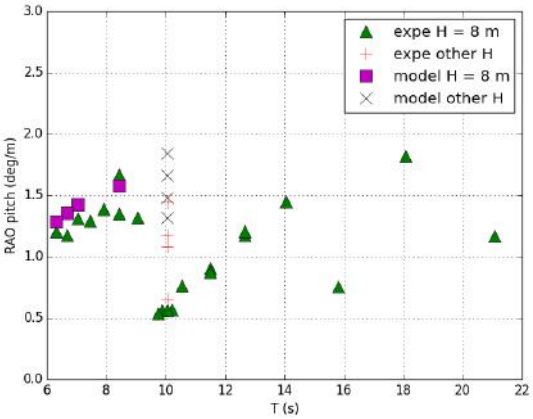

pitch

FIGURE 2-20 EXPERIMENTAL AND MODELLED DISPLACEMENT RAOS OF THE ISOLATED OWC SPAR BUOY IN THE 3 MAIN DOFS, *H* = 8 M AND OTHER VALUES OF H FOR T = 10.04 S

The displacement phases for surge, heave and pitch are shown in Figure 2-21 (H = 2 m) and Figure 2-22(H = 8 m).

The surge phase varied in the experiment but was more stable in the numerical model. A 90° lag was observed between the experimental and the numerical model values. The behaviour did not depend on wave height for periods over 14 s.

The heave phase increased steeply between 9 s and 12 s. This could be expected because the heave resonance period is close to 10 s. The experimental and model behaviour is similar, however the modelled phases are generally 40° to 90° smaller than the experimental phases. The phases were similar for *H* = 2 m and *H* = 8 m, except for the periods below 10 s where a 90° lag was observed.

The pitch phase is generally stable in the experiment and the numerical model, with values between 90 and 180°. The numerical model results are more stable than the experimental results. A lag of 90° can be observed between experimental values with H = 2 m and H = 8 m. The phase for the pitch is similar to the phase of the surge. This indicates that these motions are strongly coupled.

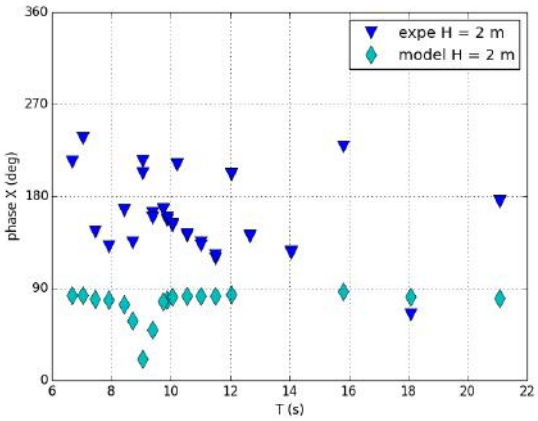

X: surge

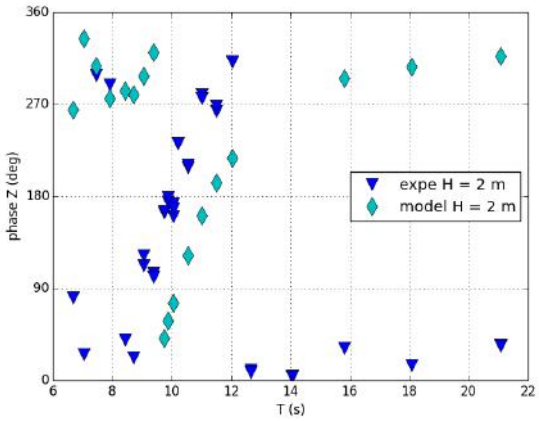

Z: heave

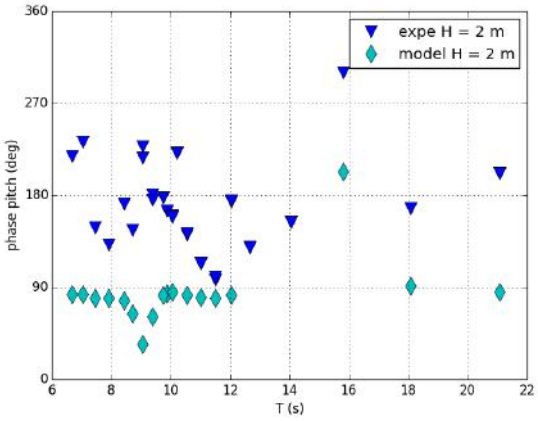

pitch

FIGURE 2-21 EXPERIMENTAL AND MODELLED DISPLACEMENT PHASES OF THE ISOLATED OWC SPAR BUOY IN THE THREE MAIN DOFS, H = 2 M

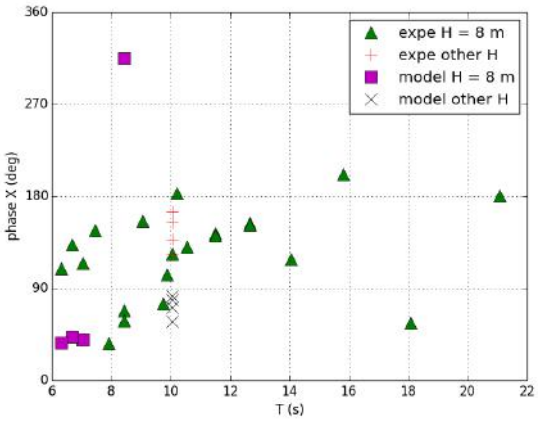

X:surge

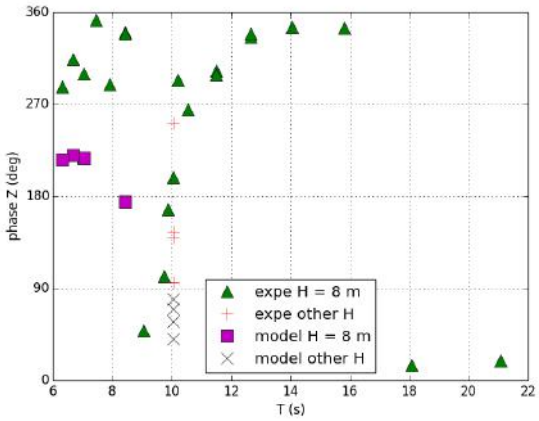

Z: heave

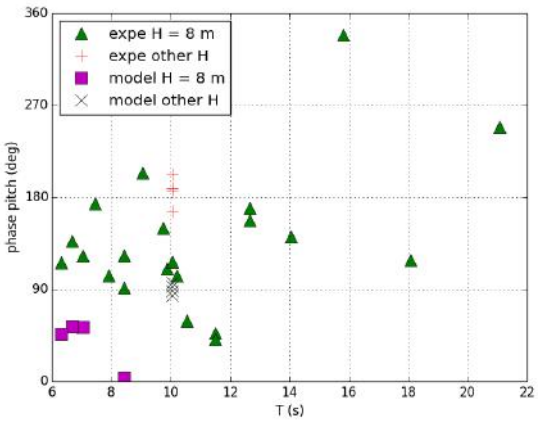

pitch

FIGURE 2-22 EXPERIMENTAL AND MODELLED DISPLACEMENT PHASES OF THE ISOLATED OWC SPAR BUOY IN THE THREE MAIN DOFS, H = 8 M AND OTHER VALUES OF H FOR T = 10.04 S

The mean drift, shown in Figure 2-23 (H = 2 m) and Figure 2-24 (H = 8 m) was stable with values around -2 m in the experiment with H = 2 m. The mean drift increased between 8 s and 9 s and decreased between 9 s and 10 s in the experiment with H = 8 m and in the numerical model with H = 2 m and H = 8 m. The experimental values with H = 2 m seem to be an experimental equilibrium position, and this explains why modelled results are different. The variation in drift corresponds to the heave resonance.

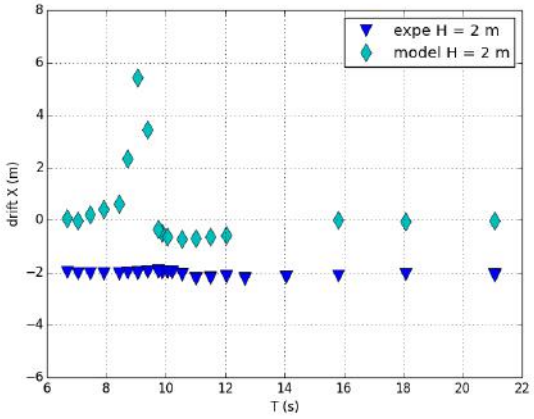

FIGURE 2-23 EXPERIMENTAL AND MODEL DRIFT OF THE ISOLATED OWC SPAR BUOY IN THE SURGE DIRECTION, H = 2 M

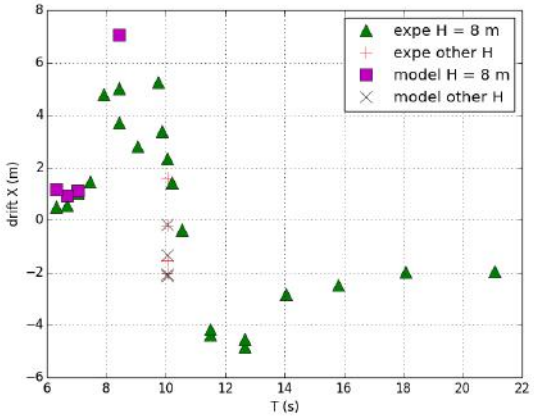

FIGURE 2-24 EXPERIMENTAL AND MODEL DRIFT OF THE ISOLATED OWC SPAR BUOY IN THE SURGE DIRECTION, H = 8 M AND OTHER VALUES OF H FOR T = 10.04 S

The experimental and modelled mooring load RAOs are given in Figure 2-25 for H = 2 m and in Figure 2-26 for H = 8 m. The results are similar in the three lines and do not differ strongly between the numerical model and the experiment. The RAOs increased between 6 s and 10 s and decreased for higher periods. This corresponded to the heave resonance. The experimental RAOs were slightly lower with H = 8 m than for H = 2 m.

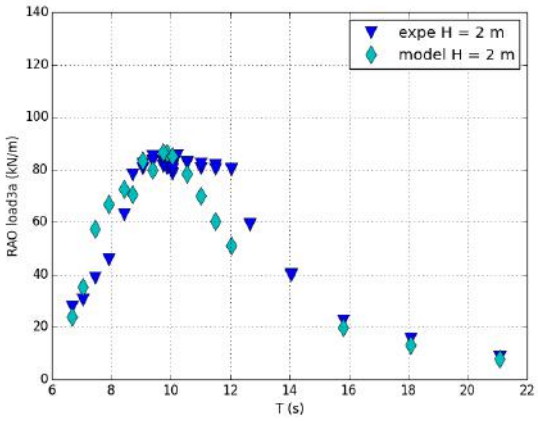

3a

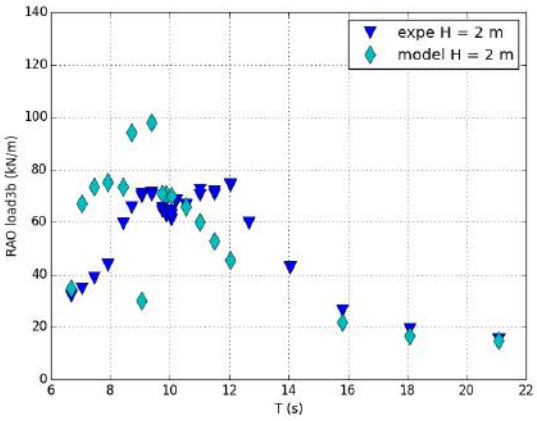

3b

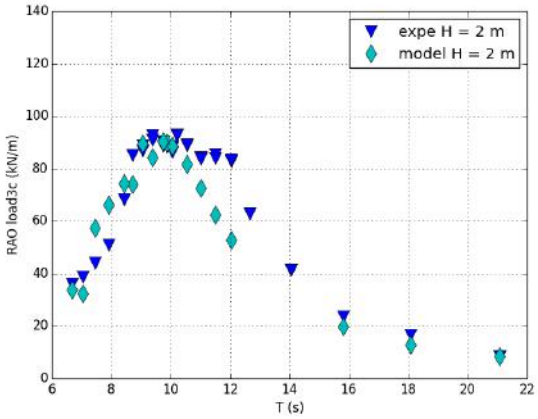

3c

FIGURE 2-25 EXPERIMENTAL AND MODELLED MOORING LINE RAOS OF THE ISOLATED OWC SPAR BUOY IN THE THREE LINES, H = 2 M

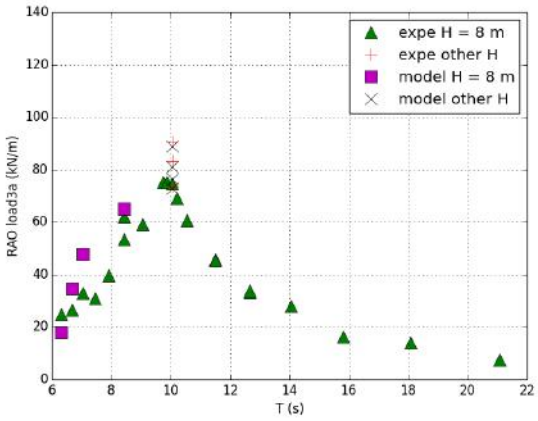

3a

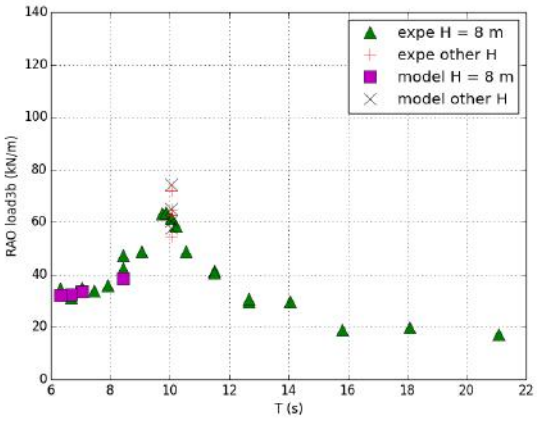

3b

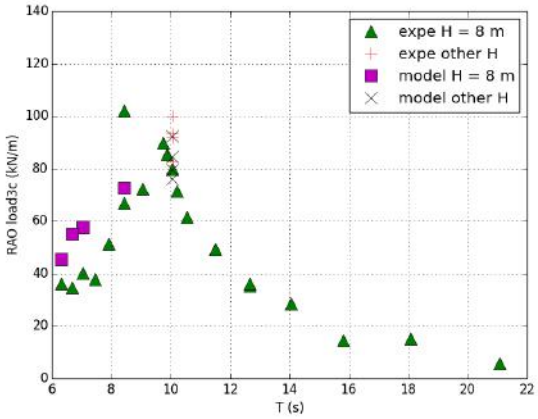

3c

FIGURE 2-26 EXPERIMENTAL AND MODELLED MOORING LINE RAOS OF THE ISOLATED OWC SPAR BUOY IN THE THREE LINES, H = 8 M AND OTHER VALUES OF H FOR T = 10.04 S

The experimental and modelled mooring line load phases are given in Figure 2-27 for H = 2 m and in Figure 2-28 for H = 8 m. As with the RAOs, the phases were similar in the three lines and did not differ strongly between the numerical model and the experiment. The phases increased steeply between 8 s and 12 s.

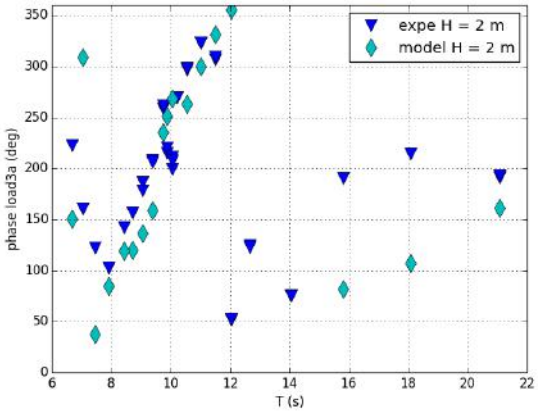

3a

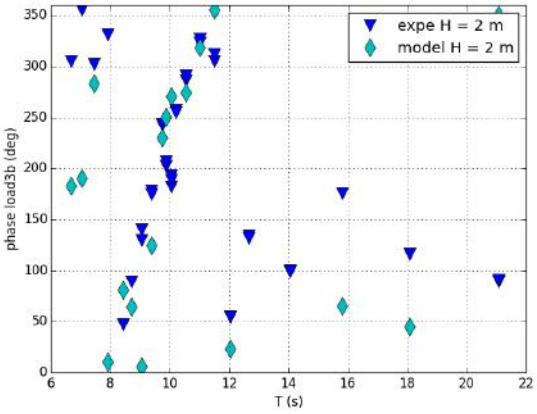

3b

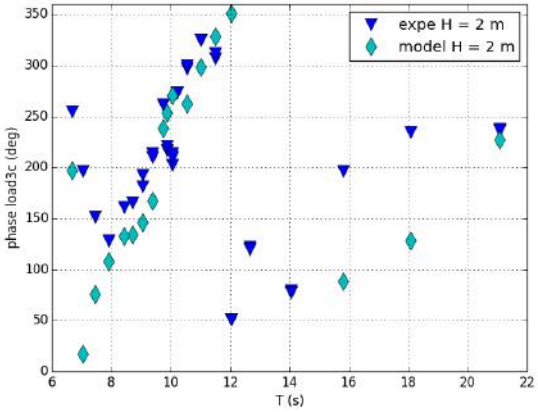

3c

FIGURE 2-27 EXPERIMENTAL AND MODELLED MOORING LINE PHASES OF THE ISOLATED OWC SPAR BUOY IN THE THREE LINES, H = 2 M

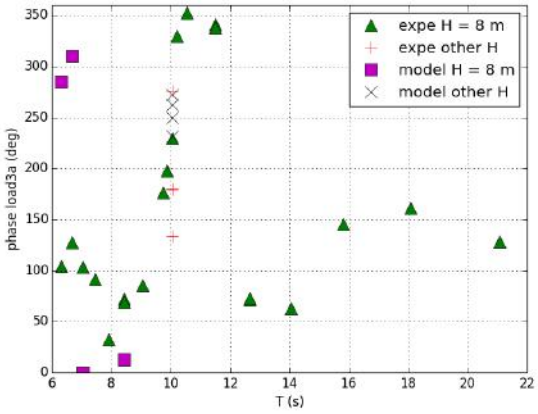

3a

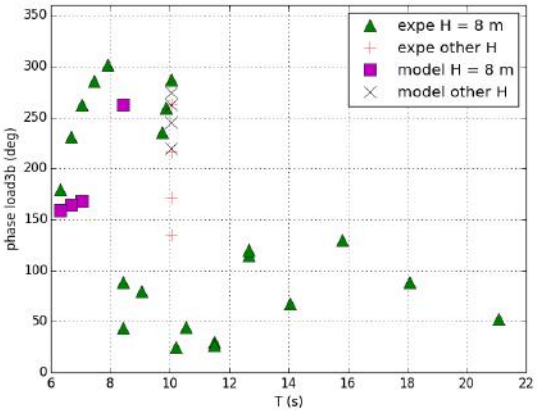

3b

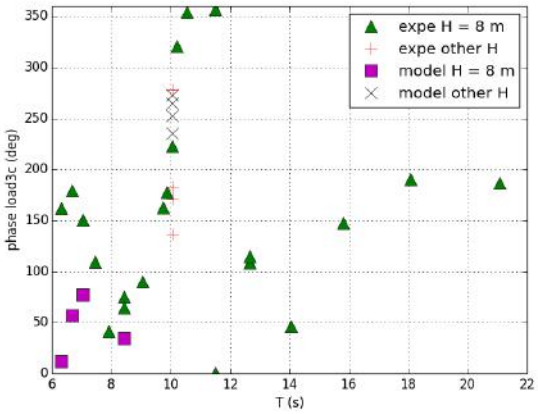

3c

FIGURE 2-28 EXPERIMENTAL AND MODELLED MOORING LINE PHASES OF THE ISOLATED OWC SPAR BUOY IN THE THREE LINES, H = 8 M AND OTHER VALUES H FOR T = 10.04 S

The time series describing the waves, motions and loads for H = 2 m and T = 6.66 s are given in Figure 2-29. The time series showed a nearly linear behaviour (sinusoids are observed) with a slow drift in pitch angle. Load measurements were noisy because the variation in load was small (70 kN peak to peak). Surge and pitch occur together, slightly after the wave and heave slightly later. Load in line 3a occurred slightly before the wave and load in line 3b occurred approximately at the same time as the wave.

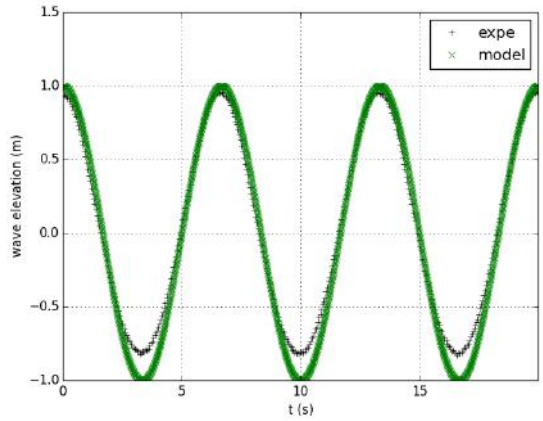

Waves

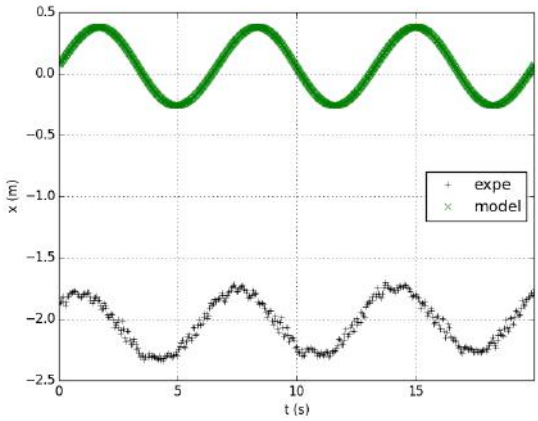

X: Surge

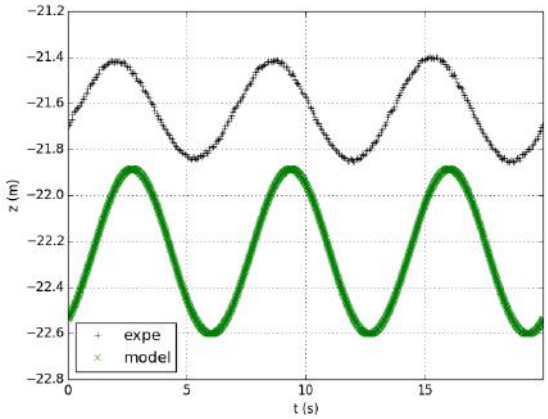

Z: Heave

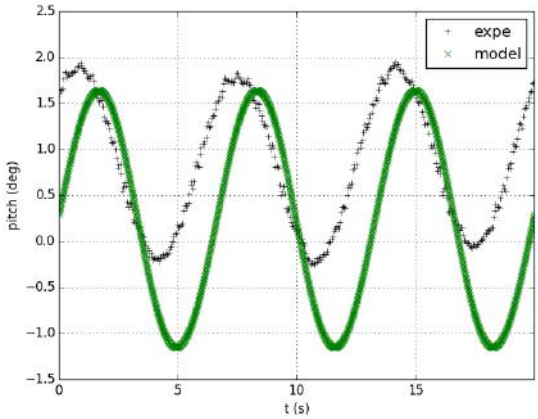

Pitch

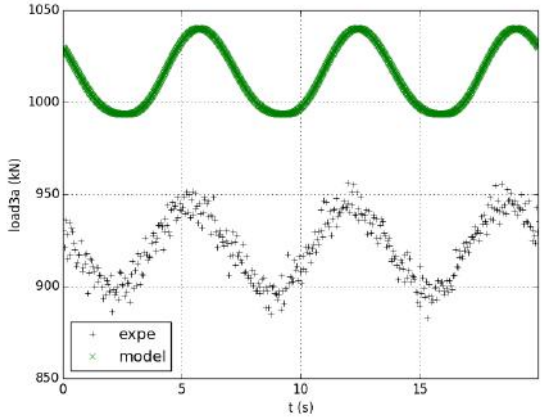

3a

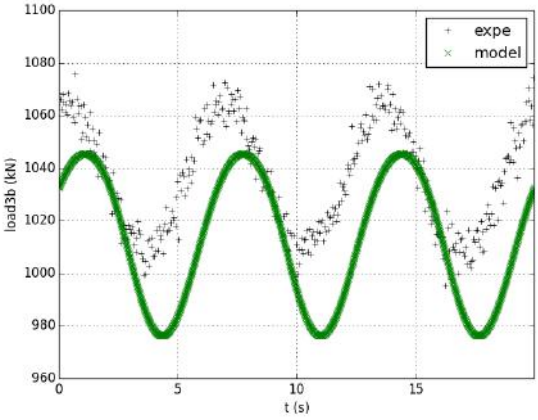

3b

FIGURE 2-29 EXAMPLE OF TIME SERIES OF REGULAR WAVES OF THE ISOLATED OWC SPAR BUOY FOR CASE B062 (*H* = 2 M AND *T* = 6.66 S)

The time series describing the waves, motions and loads for H = 8 m and T = 6.66 s are given in Figure 2-30. The results show a nearly linear behaviour except for the modelled load in line 3a. This behaviour cannot be clearly explained, and is not caused by the line becoming slack and then suddenly taut (snap

load). Surge and pitch occur together, slightly after the wave and heave slightly later. Load 3a occurs slightly before the wave and load 3b slightly after the wave.

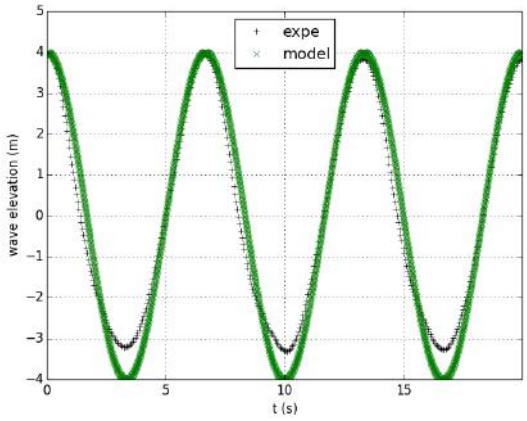

Waves

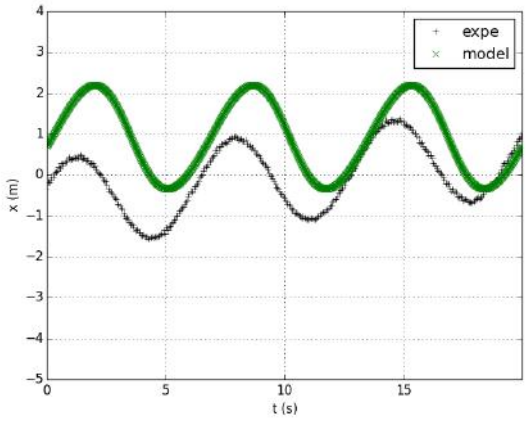

X: Surge

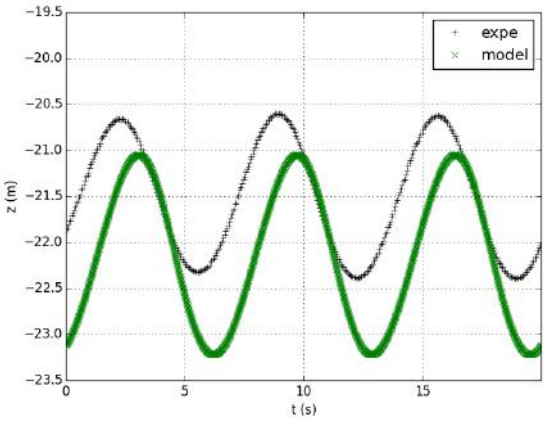

Z: Heave

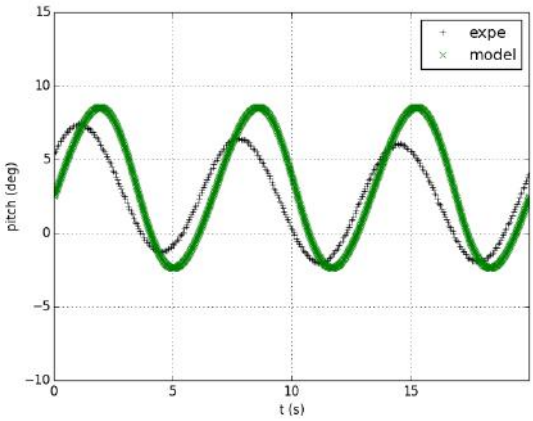

Pitch

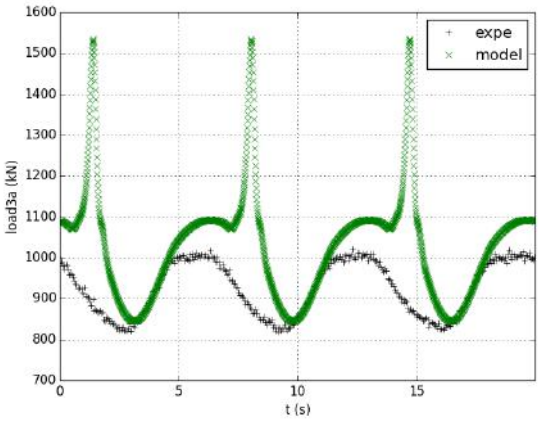

3a

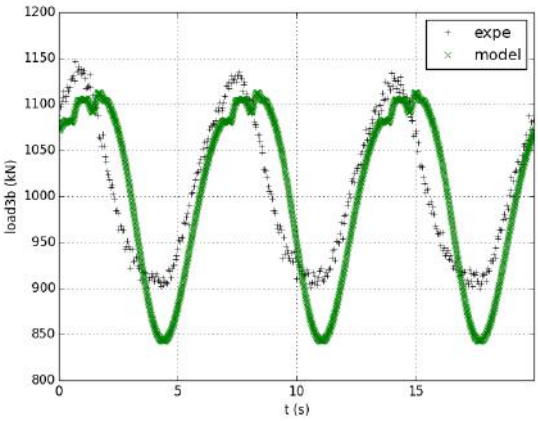

3b

FIGURE 2-30EXAMPLE OF TIME SERIES OF REGULAR WAVES OF THE ISOLATED OWC SPAR BUOY FOR CASE B024 (*H* = 8 M AND *T* = 6.66 S)

Examples of the times series of waves, motions and loads for $H = 2$ m and average wave period T = 10.04 s are given in Figure 2-31. The results show a nearly linear behaviour with a slow drift in pitch angle. Surge, pitch and heave occur together, slightly after the wave. Load 3a and load 3b both occurred slightly before the wave with load in line 3a preceding the load in line 3b.

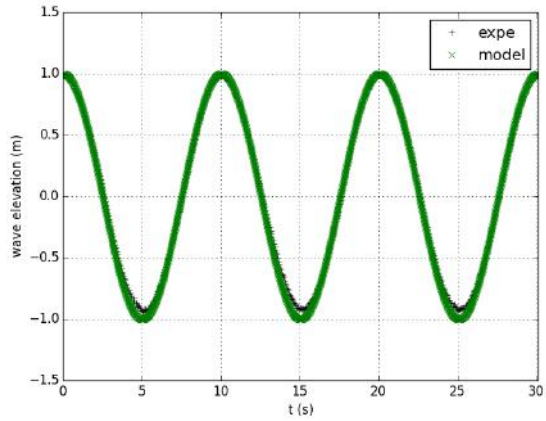

Waves

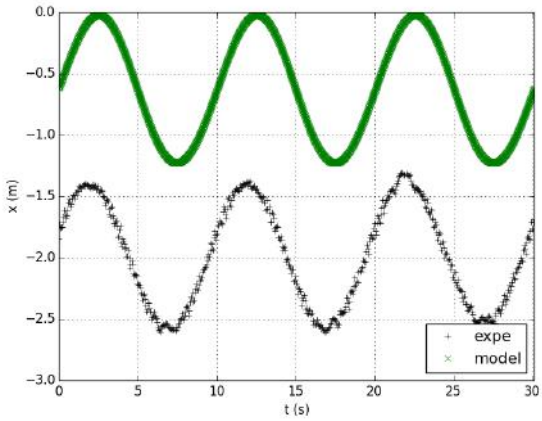

X: Surge

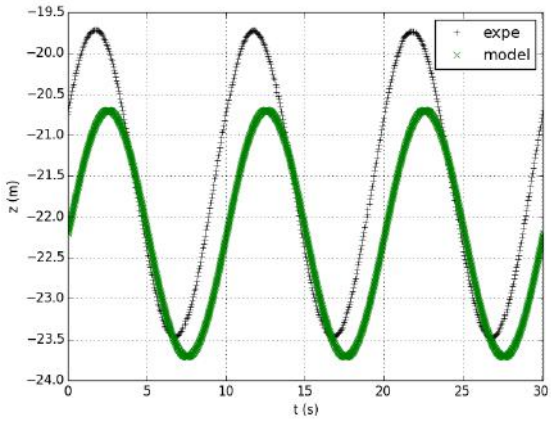

Z: Heave

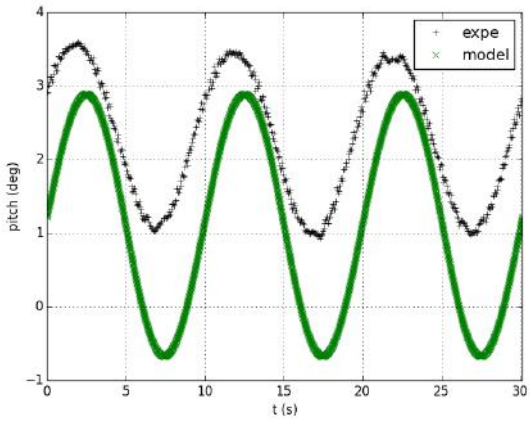

Pitch

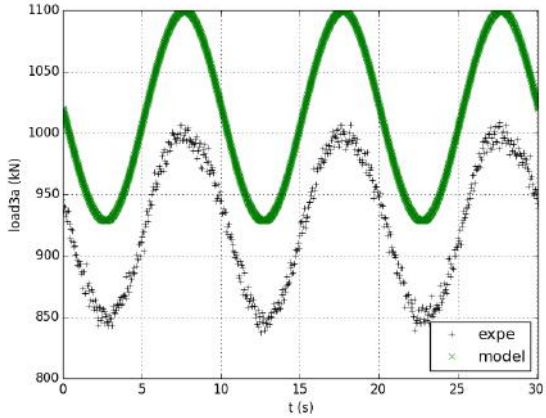

3a

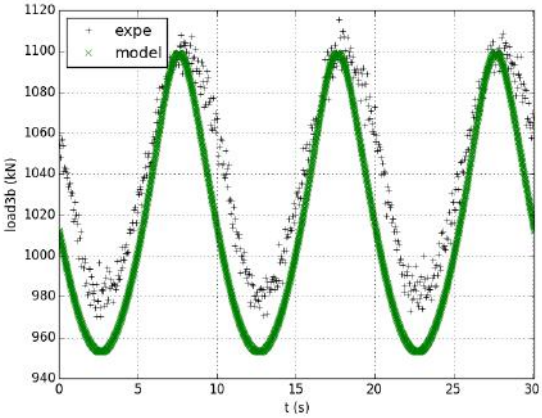

3b

FIGURE 2-31 EXAMPLE OF TIME SERIES OF REGULAR WAVES OF THE ISOLATED OWC SPAR BUOY FOR CASE B066 (H = 2 M AND T = 10.04 S)

The experimental wave, motion and load time series for the high amplitude waves (H = 8 m) with an average wave period (T = 10.04 s) are shown in Figure 2-32. The results show a nearly linear behaviour in heave. A slow drift is observed in surge and non-periodic behaviours are clearly observed in pitch motion and load 3a. In addition, measurement noise was observed in load 3a. Surge, heave pitch occur together, slightly after the wave. Load 3a and 3b occurs slightly before the wave. No convergence was achieved for a numerical model for this load case.

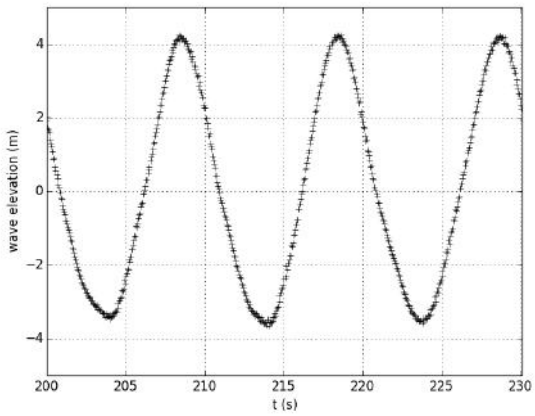

Waves

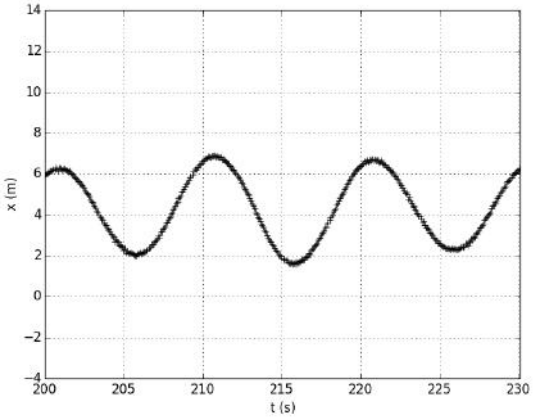

X: Surge

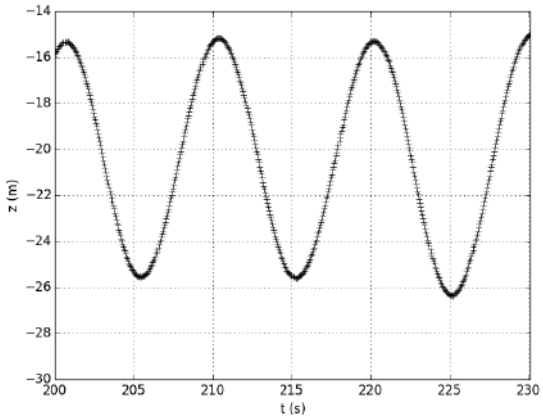

Z: Heave

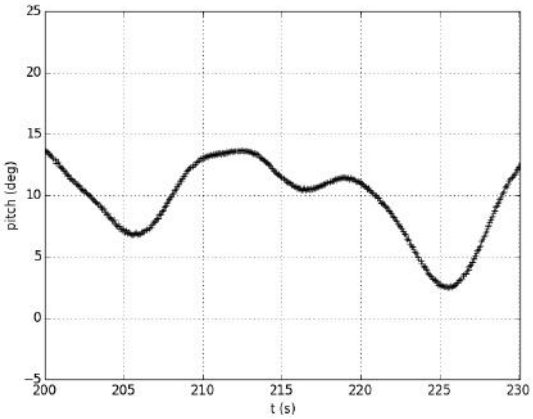

Pitch

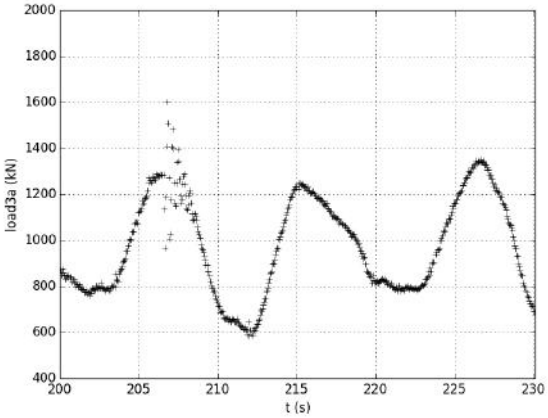

3a

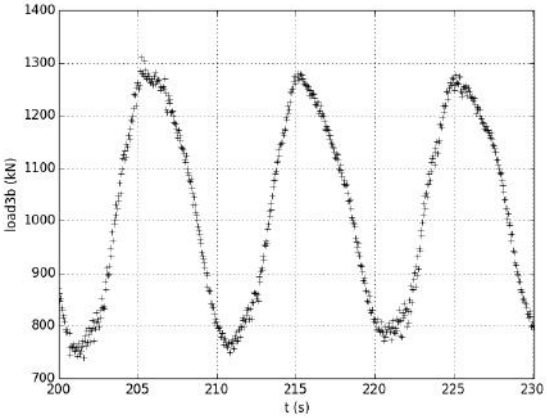

3b

FIGURE 2-32 EXAMPLE OF TIME SERIES OF REGULAR WAVES OF THE ISOLATED OWC SPAR BUOY FOR CASE B071 (*H* = 8 M AND *T* = 6.66 S)

Experimental and numerical time series for H = 2 m and high wave period, T = 21.08 s are shown in Figure 2-29. There was a nearly linear behaviour in heave, a slow drift was observed in surge and non-linearities were clearly observed in pitch. Load measurements were very noisy because the variation in load was small (50 kN peak to peak). Surge and pitch occur together, slightly after the wave and heave

at the same time as the waves. Load 3a and load 3b occur in opposition with the waves. Modelled load 3a and 3b are clearly non-linear.

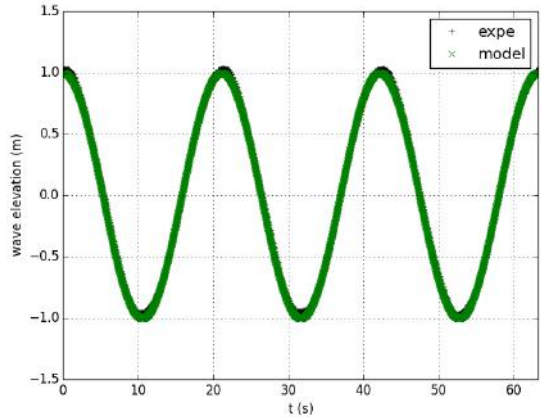

Waves

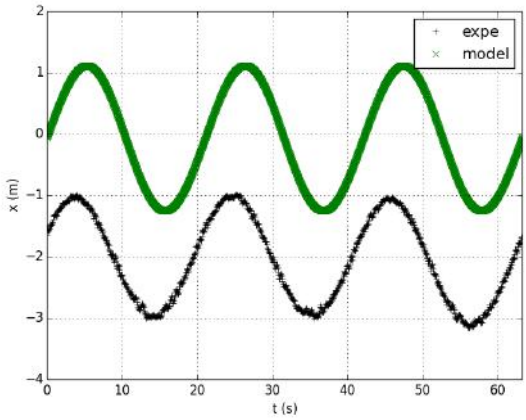

X: Surge

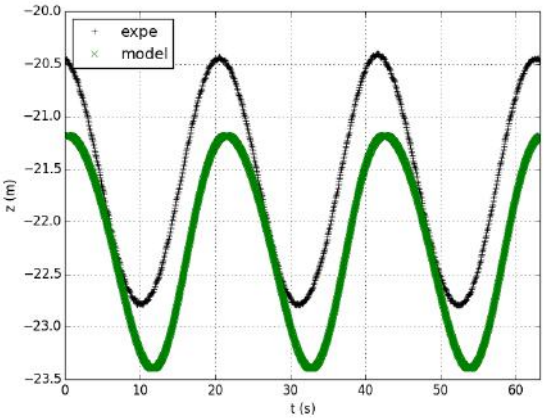

Z: Heave

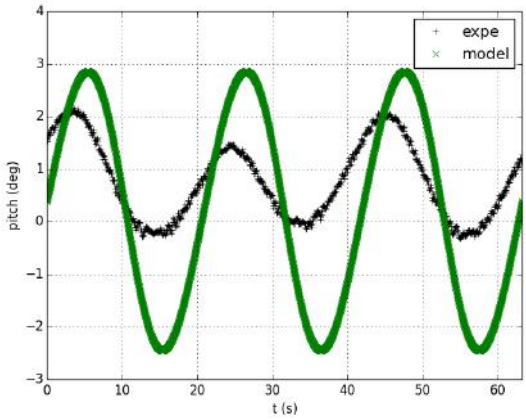

Pitch

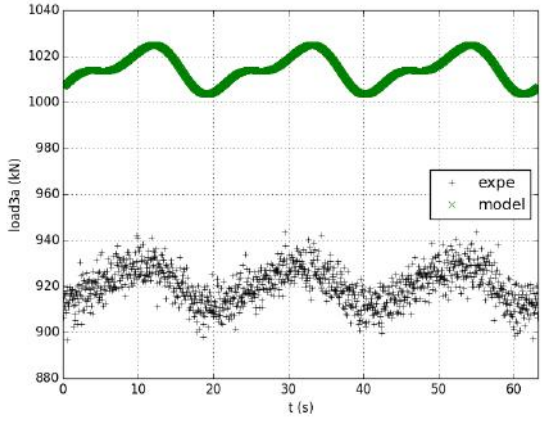

3a

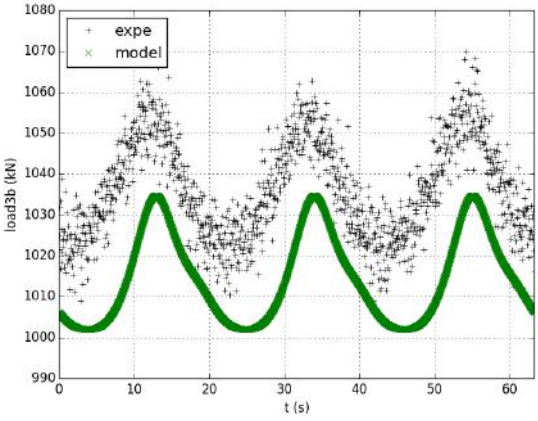

3b

FIGURE 2-33 EXAMPLE OF TIME SERIES OF REGULAR WAVES OF THE ISOLATED OWC SPAR BUOY FOR CASE B038 (*H* = 2 M AND *T* = 21.08 S)

Experimental time series for high amplitude (H = 8 m) and high wave period (T = 21.08 s) waves are given in Figure 2-34. There was a nearly linear behaviour in heave and a slow drift was observed in surge. Non-linearities were clearly observed in pitch motion and load 3a and 3b. Surge and pitch occur together, slightly after the wave and heave at the same time as the waves. Load 3a and load 3b are in opposition with the waves. No convergence was achieved for a numerical model for this load case.

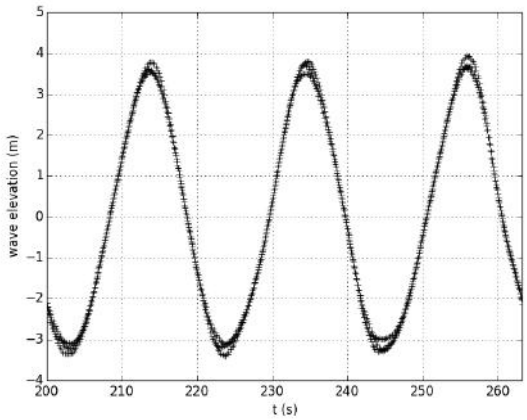

Waves

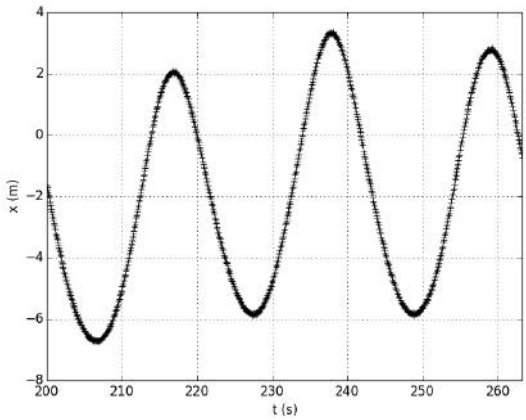

X: Surge

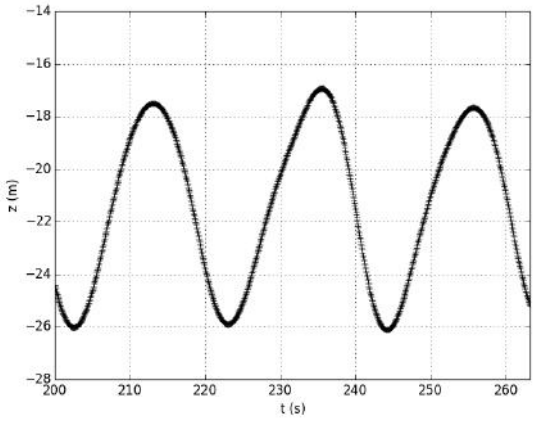

Z: Heave

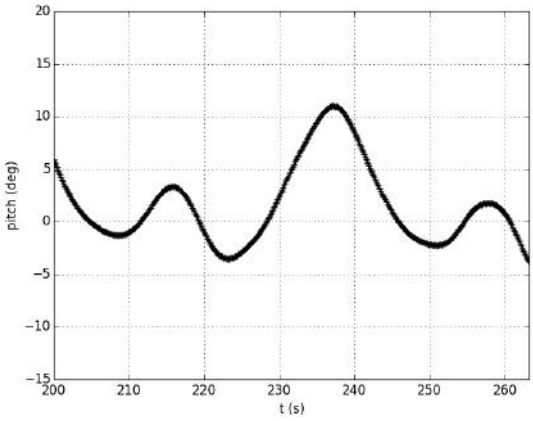

Pitch

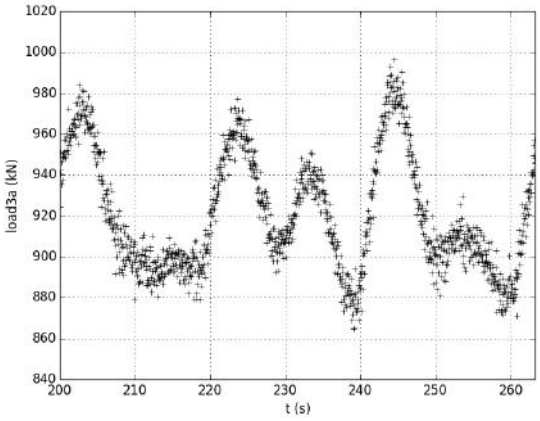

3a

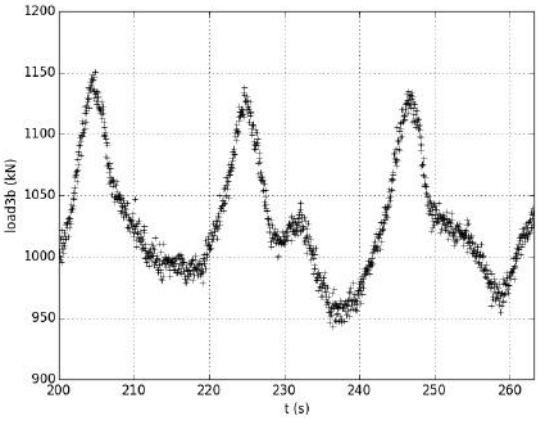

3b

FIGURE 2-34 EXAMPLE OF TIME SERIES OF EXPERIMENTAL DATA FOR REGULAR WAVES OF THE ISOLATED OWC SPAR BUOY FOR CASE B009 (H = 8 M AND T = 21.08 S)

2.3.5 Irregular wave tests

The experiment names, significant wave height, peak periods and case (operational or survival) are summarised in Table 2-31. Irregular wave tests were conducted for approximately 10 or 30 minutes, which corresponds to 1 h and 3 h full scale. Experiments starting with letters C and D lasted the equivalent of 3 h full scale while the ones starting with letter E lasted the equivalent of 1h.

All irregular wave tests were conducted with the PTO.

TABLE 2-31 SUMMARY OF THE IRREGULAR WAVE EXPERIMENT OF THE ISOLATED OWC SPAR BUOY

Simulation name	Hs (m)	Tp(s)	Case
C001, E001	1.24	7.59	Operational
C002, E002, E020	2.24	7.59	Operational
C003, E003	3.24	7.59	Operational
C004, E004	1.24	9.93	Operational
C005, E005, E021	2.24	9.93	Operational
C006, E006	3.24	9.93	Operational
C007, E007	4.24	9.93	Operational
C008, E008	1.24	12.21	Operational
C009, E009, E022	2.24	12.21	Operational
D001	12.00	17.20	Survival
D002	13.00	18.40	Survival
D003	14.00	19.35	Survival
D004	14.80	20.30	Survival
E010	3.24	12.21	Operational
E011	4.24	12.21	Operational
E012	5.52	12.21	Operational
E013	7.52	12.21	Operational
E014, E023, E024	2.24	14.55	Operational
E015	3.24	14.55	Operational
E016	4.24	14.55	Operational
E017	5.52	14.55	Operational
E018	7.52	14.55	Operational
E019	9.52	14.55	Operational

Experimental and numerical time series of motion and mooring loads in moderate sea conditions were compared. For comparisons of amplitudes and phases, data are plotted with their mean removed (Figure 2-35). Results indicate a fair modelling of motion and mooring loads.

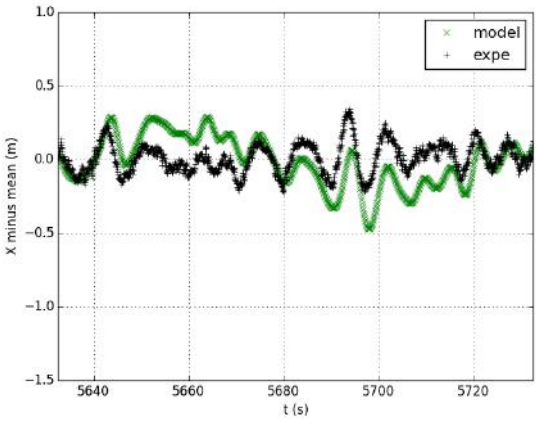

X: Surge

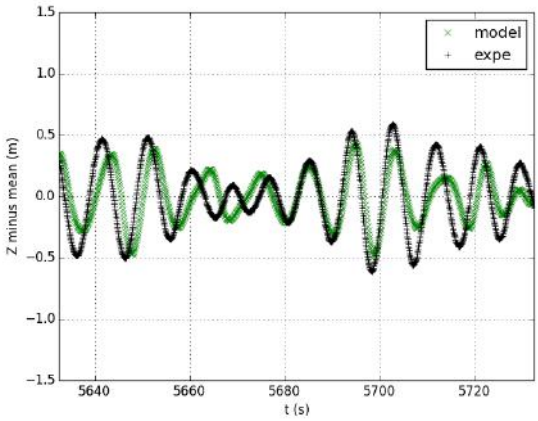

Z: Heave

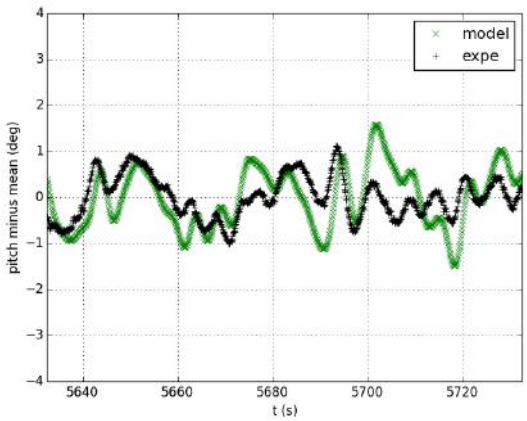

Pitch

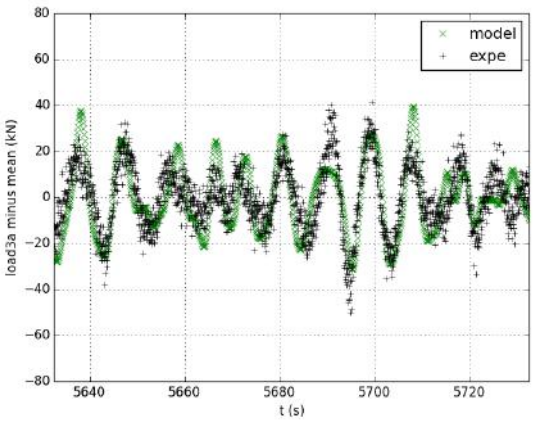

3a

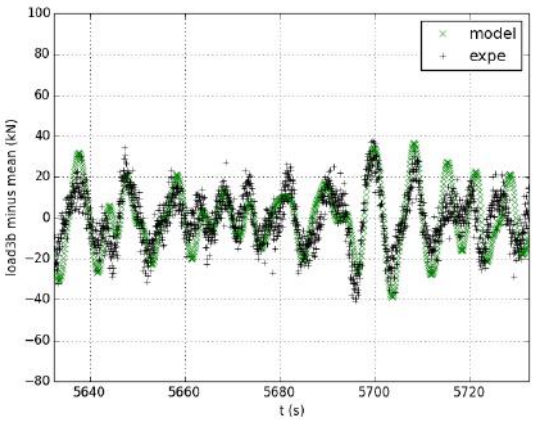

3b

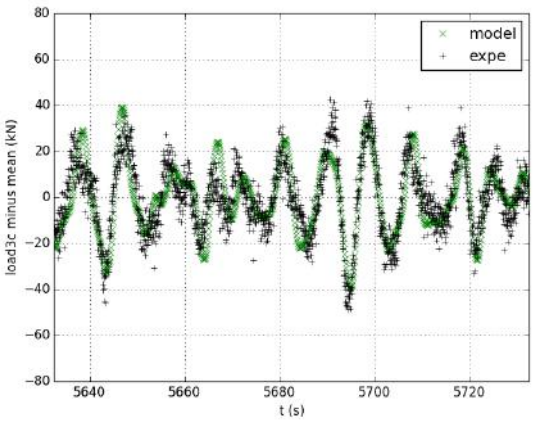

3c

FIGURE 2-35 EXAMPLE OF TIME SERIES OF EXPERIMENTAL AND MODELLED DATA OF THE ISOLATED OWC SPAR BUOY FOR IRREGULAR WAVES FOR CASE C001 (H_S = 1.24 M AND T_P = 7.59 S). MEAN VALUES HAVE BEEN REMOVED FOR COMPARISONS OF AMPLITUDES AND PHASES

Wave frequency surge motions are well represented, however the model adds a low frequency surge motion which did not occur during the experiment. Heave motions are well represented. Pitch motions are fairly represented, with some noticeable differences in behaviour. This was somehow expected due to the differences in the pitch natural period. A very good correlation is found for mooring loads. In this

example, mooring loads seem driven by heave motion. Mooring load is similar in lines 1 and 3 which are facing the waves (but the waves are not coming exactly between the 2 lines, see Figure 2-3).

Experimental and modelled power spectral densities (PSDs) are compared (Figure 2-36). Peaks occur at the same frequency for heave and load 3a and 3c but the amplitude of the peak was different for Z and spreading around the peak for load 3a.

For the surge PSD, a narrow peak occurred at 0.072 rad/s in the numerical model. This corresponds to the natural periods observed during the decay tests.

For the pitch PSD, two peaks occur in the model, one near the surge peak frequency and one at 0.23 rad/s while only one peak occurs in the experiment at 0.17 rad/s. The difference of frequency for this last peak corresponds to the difference observed in natural periods. The amplitude of this peak is much lower than the amplitude of the peak at a similar frequency in the numerical model.

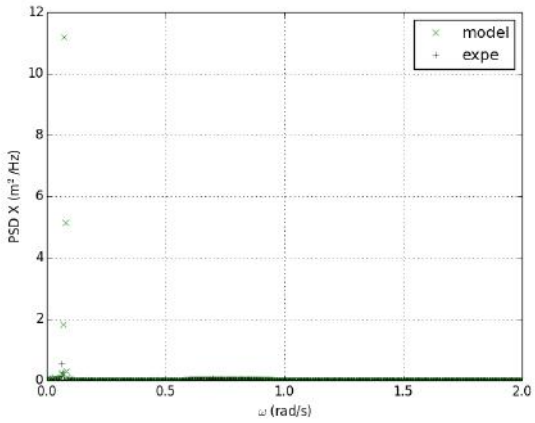

X: Surge

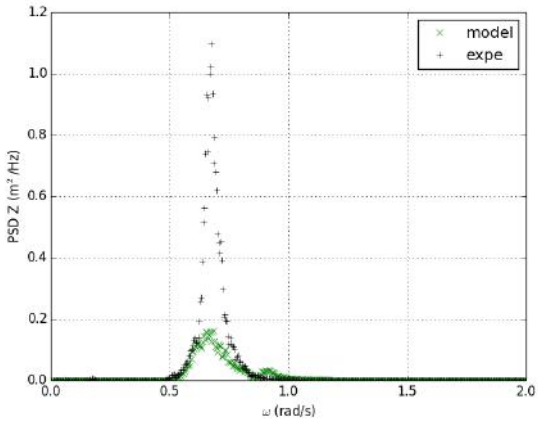

Z: Heave

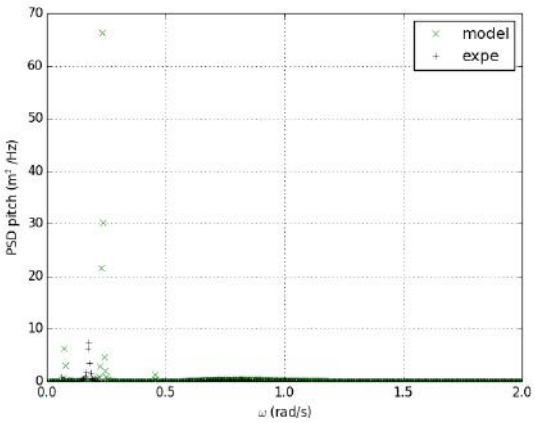

Pitch

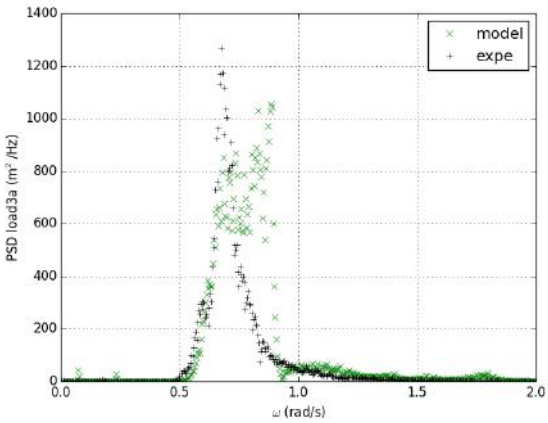

3a

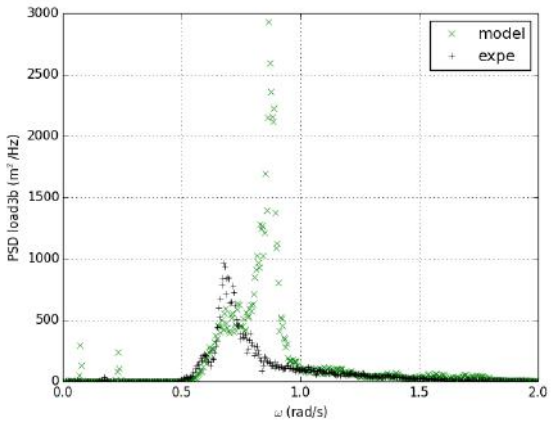

3b

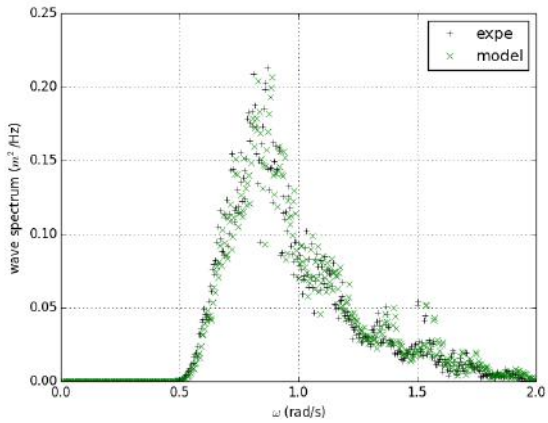

wave

FIGURE 2-36 EXAMPLE OF PSD OF THE ISOLATED OWC SPAR BUOY OF EXPERIMENTAL AND MODELLED DATA FOR IRREGULAR WAVES FOR CASE C001 (H_S = 1.24 M AND T_P = 7.59 S)

Statistical results for this example are given in Table 2-32 and indicate that the mean surge position during the experiment was negative. This was also the static position of the buoy before waves started (Table 2-9). This may be caused by small inaccuracies in the building of the physical model which lead to a slightly different equilibrium position.

As observed in the static equilibrium simulation, the mean Z position was shifted by 0.6 m in the numerical model. The extrema and standard deviation are modelled fairly with less than 42% relative difference between the experiment and the numerical model.

Similarly, for the surge, the pitch values are small in this example therefore relative differences are high.

As observed previously, the mean experimental value for load in line 3c seems suspicious and may result from an error in calibration. The load cell offset may have changed since the beginning of the tests, for example because of water ingress. However, the variations are similar in the experiments and numerical model. Otherwise, the tensions are modelled fairly, with less than 10% for the mean values in line 1 and 2, and less than 42% relative difference for the extrema and standard deviation.

TABLE 2-32 COMPARISON OF STATISTICAL VALUES OF THE ISOLATED OWC SPAR BUOY FOR CASE C001 (H_S 1.24 M AND T_P = 7.59 S): EXPERIMENTAL VALUE / MODEL VALUES. GREEN IS FOR RELATIVE DIFFERENCE BELOW 10 %, ORANGE BETWEEN 10 AND 100%, RED OVER 100%

	Mean	Min-mean	Max-mean	Std
Surge X (m)	-2/0.1	-0.5/-1.1	0.5/1	0.1/0.3
Heave Z (m)	-21.6/-22.2	-1/-0.7	1.1/0.7	0.3/0.2
Pitch (deg)	0.8/0.1	-1.7/-3	2.2/3.1	0.5/0.9
Load 3a (kN)	919/1013	-61/-54	63/68	14/15
Load 3b (kN)	1033/1012	-59/-67	64/91	14/18
Load 3c (kN)	479/1014	-66/-55	68/71	15/16

To conclude, the numerical model seems to estimate fairly the motion of the single buoy, especially the heave and pitch, and the load in the mooring lines for the single device. However, the numerical model can only replicate simulations with moderate sea states. In higher sea states, parametric roll/pitch occurs, which is outside of the capability of a linear theory model.

2.3.6 Irregular wave tests: sensitivity analysis on line length

The repeatability of the irregular wave fields in an empty basin results in Hs values within 1% of one another.

The model has been run with line 3a shortened or lengthened by ±10%. All sections of the lines were scaled. The aim of this analysis is to get an insight into the sensitivity of the numerical model to variations in line length. Results are presented in Figure 2-37 and Table 2-33.

Time series indicate that the surge and, to a lesser extent the pitch low frequency motions are modified if the line length varies. This low frequency motions were not well replicated by the numerical model compared to the experiment. The inaccuracies in length of lines could be an explanation of differences between the numerical model and the experiment.

Statistical values indicate that the mean surge position of the buoy is modified. This was expected that the buoy reaches a new equilibrium position. The difference in extrema and standard deviation is small or moderate. This means that the inaccuracies in line length have a limited influence on these results.

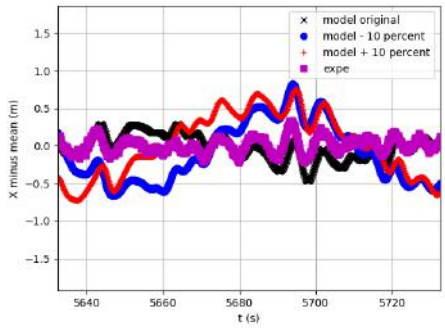

X: Surge

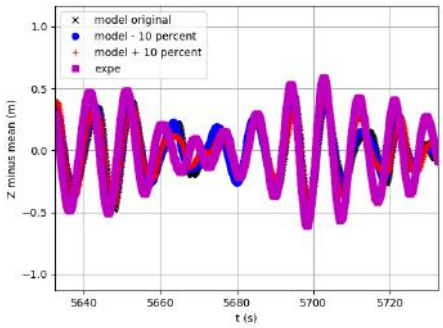

Z: Heave

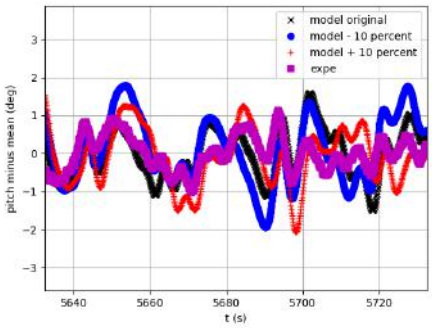

Pitch

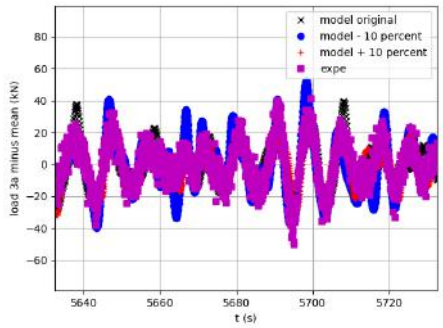

3a

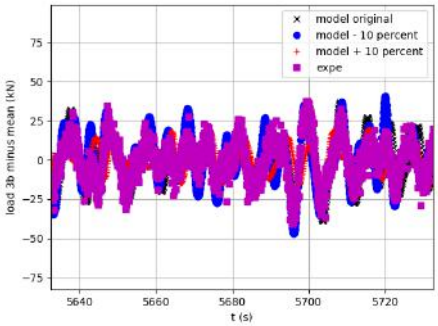

3b

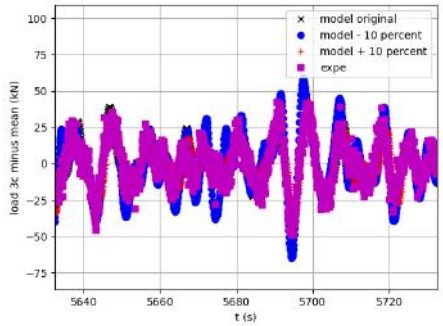

3c

FIGURE 2-37 EXAMPLE OF TIME SERIES OF EXPERIMENTAL AND MODELLED DATA OF THE ISOLATED OWC SPAR BUOY FOR IRREGULAR WAVES FOR CASE C001 (H_S = 1.24 M AND T_P = 7.59 S), AND WITH LINE 3A BEING SHORTEN OR LENGTHENED BY ±10%. MEAN VALUES HAVE BEEN REMOVED FOR COMPARISONS OF AMPLITUDES AND PHASES. IN BLACK THE ORIGINAL NUMERICAL MODEL, IN BLUE THE MODEL WITH LINE 3A SHORTER BY 10%, IN RED THE MODEL WITH LINE 3A LONGER BY 10%, IN MAGENTA THE EXPERIMENTAL DATA

TABLE 2-33 COMPARISON OF STATISTICAL VALUES OF THE ISOLATED OWC SPAR BUOY FOR CASE C001 (H_S 1.24 M AND T_P = 7.59 S): MODEL VALUES WITH ORIGINAL MODEL, SHORTER OR LONGER LINE 3A. GREEN IS FOR RELATIVE DIFFERENCE BELOW 10 %, ORANGE BETWEEN 10 AND 100%, RED OVER 100%

	Line length	Mean	Min-mean	Max-mean	Std
Surge X (m)	original	0,1	-1,1	1,0	0,3
	-10%	-4,5	-1,1	1,2	0,3
	+10%	4,6	-1,8	1,7	0,5
Heave Z (m)	original	-22,2	-0,7	0,7	0,2
	-10%	-22,4	-0,6	0,6	0,2
	+10%	-22,2	-0,6	0,7	0,2
Pitch (deg)	original	0,1	-3,0	3,1	0,9
	-10%	0,0	-3,3	3,5	0,9
	+10%	0,1	-3,0	3,1	0,9
Load 3a (kN)	original	1013	-54	68	15
	-10%	1144	-71	91	21
	+10%	958	-50	48	12
Load 3b (kN)	original	1012	-67	91	18
	-10%	1094	-74	77	18
	+10%	976	-47	44	12
Load 3c (kN)	original	1014	-55	71	16
	-10%	1096	-78	100	22
	+10%	977	-58	62	15

2.3.7 Irregular wave tests: sensitivity analysis on clump weight

The model has been run with line 3a having a clump 10% heavier or lighter than the target value. The aim of this analysis is to get an insight into the sensitivity of the numerical model to variations in clump weight. Results are presented in Figure 2-38 and Table 2-34.

Time series indicate that the surge low frequency motions are modified if the clump weight varies. This low frequency motions were not well replicated by the numerical model compared to the experiment. The inaccuracies in clump weight could be an explanation of differences between the numerical model and the experiment.

The difference in extrema and standard deviation is small or moderate. This means that the inaccuracies in clump weight have a limited influence on these results.

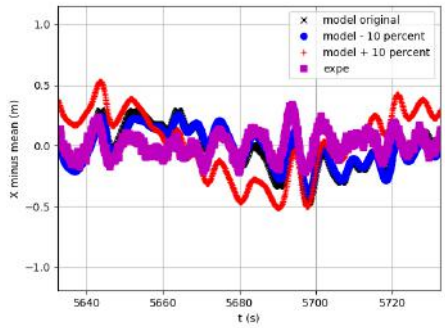

X: Surge

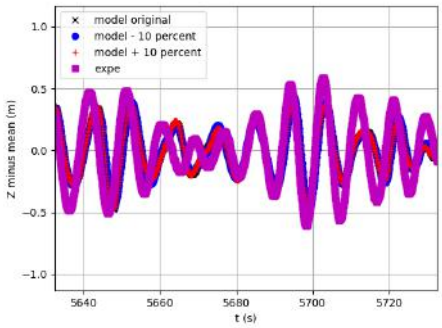

Z: Heave

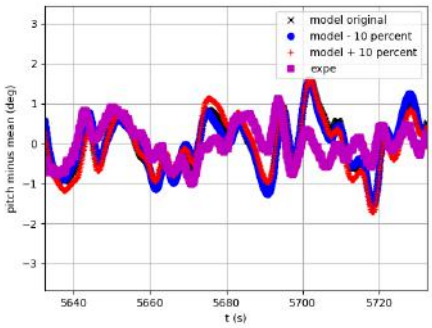

Pitch

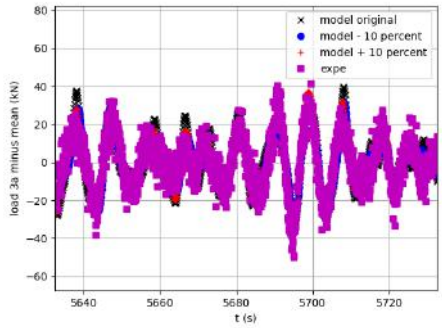

3a

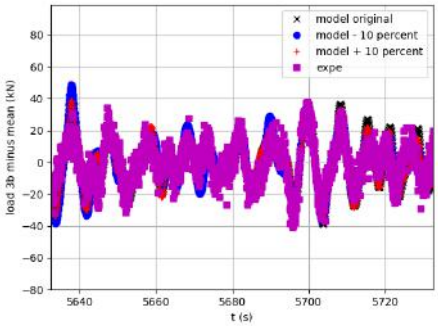

3b

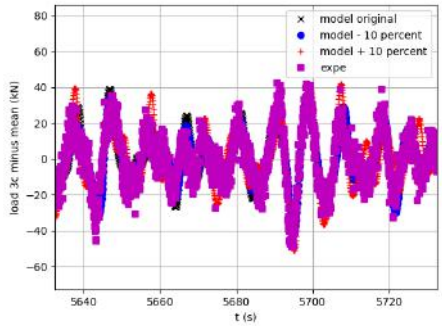

3c

FIGURE 2-38 EXAMPLE OF TIME SERIES OF EXPERIMENTAL AND MODELLED DATA OF THE ISOLATED OWC SPAR BUOY FOR IRREGULAR WAVES FOR CASE C001 (H_S = 1.24 M AND T_P = 7.59 S), AND WITH CLUMP OF LINE 3A BEING LIGHTENED OR MADE HEAVIER BY ±10%. MEAN VALUES HAVE BEEN REMOVED FOR COMPARISONS OF AMPLITUDES AND PHASES. IN BLACK THE ORIGINAL NUMERICAL MODEL, IN BLUE THE MODEL WITH LINE 3A WITH A CLUMP WEIGHT LIGHTER BY 10%, IN RED THE MODEL WITH LINE 3A WITH A CLUMP WEIGHT HEAVIER BY 10%, IN MAGENTA THE EXPERIMENTAL DATA

TABLE 2-34 COMPARISON OF STATISTICAL VALUES OF THE ISOLATED OWC SPAR BUOY FOR CASE C001 (H_S 1.24 M AND T_P = 7.59 S): MODEL VALUES WITH ORIGINAL MODEL, LINE 3A WITH LIGHTER OR HEAVIER CLUMP WEIGHT. GREEN IS FOR RELATIVE DIFFERENCE BELOW 10 %, ORANGE BETWEEN 10 AND 100%, RED OVER 100%

	Clump mass	Mean	Min-mean	Max-mean	Std
Surge X (m)	original	0,1	-1,1	1,0	0,3
	-10%	0,2	-1,0	1,0	0,3
	+10%	0,0	-1,0	1,0	0,3
Heave Z (m)	original	-22,2	-0,7	0,7	0,2
	-10%	-22,1	-0,7	0,7	0,2
	+10%	-22,4	-0,6	0,7	0,2
Pitch (deg)	original	0,1	-3,0	3,1	0,9
	-10%	0,4	-3,4	3,1	0,9
	+10%	-0,3	-2,8	2,9	0,9
Load 3a (kN)	original	1013	-54	68	15
	-10%	901	-52	75	15
	+10%	1126	-58	66	16
Load 3b (kN)	original	1012	-67	91	18
	-10%	1009	-68	85	18
	+10%	1015	-72	79	17
Load 3c (kN)	original	1014	-55	71	16
	-10%	1010	-53	61	15
	+10%	1016	-62	79	17

3 FLEXIBLE ARRAY: 5 DEVICES, CONFIGURATION D

The aim of the numerical model with the single device is to calibrate the damping caused by the PTO in the numerical model. In addition, the motion of a single buoy was analysed, and the capabilities of the numerical model to replicate the behaviour of a single buoy was assessed. In addition, this model will highlight inaccuracies caused by the potential theory and simplified modelling of the PTO as a damper.

3.1 Description of the experiment

During the course of WP6, a set of arrays were chosen to be investigated using the OWC spar buoy. The physical properties of all the OWC spar buoy models were given in Table 2-1 on page 9. For more details of the design and construction of the models, please refer to D6.3 [6]. The configurations used the same buoy position but different mooring arrangements. One configuration was chosen for analysis with the numerical model because of time limitations. Configuration D was chosen. This configuration was chosen after preliminary analysis of the experimental results, showing that configuration D was expected to be the configuration with the best power production. Final analysis and results on production are presented in D6.5 [7].

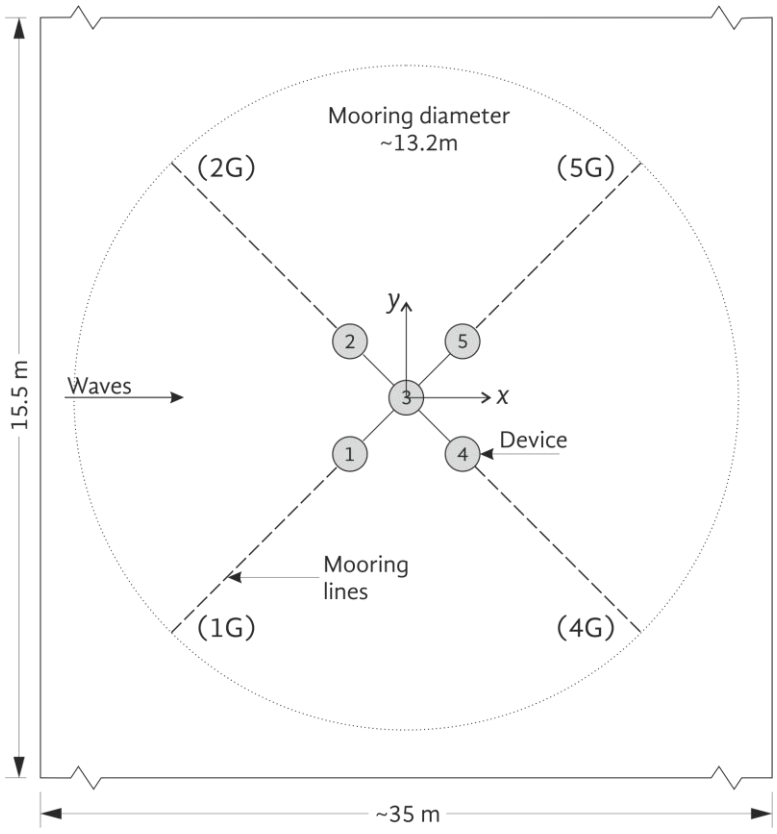

FIGURE 3-1 NUMBERING OF THE DEVICES AND OF THE EXTERNAL MOORING LINES WITHIN THE FLEXIBLE ARRAYS. (MODEL SCALE) X AXIS IS ALSO THE SURGE DIRECTION, Y THE SWAY DIRECTION. Z AXIS UPWARDS THE HEAVE DIRECTION

3.1.1 Mooring properties

The bottom lines followed the same construction process as described in Section 2.1.2 although the lengths of each section and the masses of the floats and clumps were different. The reason is to keep the same surge stiffness of the outer devices. It was not always possible to verify the same surge stiffness

for the middle device. The diagonal lines were made from Dyneema with a clump weight at the centre. The target and measured values of the unassembled mooring lines are given in Table 3-1.

TABLE 3-1 MOORING LINE PROPERTIES FOR CONFIGURATION D

	Bottom lines					
	Chain [m]	**Fairlead to clump [m]**	**Total Dyneema [m]**	**Total line length [m]**	**Clump [kg]**	**Floats [g]**
Target values	***3.399***	***2.127***	***3.589***	***6.988***	***0.533***	***53.1***
1G	3.406	2.130	3.570	6.976	0.533	53.1
2G	3.408	2.136	3.578	6.986	0.528	53.1
4G	3.408	2.122	3.532	6.940	0.532	53.1
5G	3.400	2.128	3.560	6.960	0.534	53.1
Largest deviation [%]	0.3% (4G)	0.4% (2G)	1.6% (4G)	0.7% (4G)	0.9% (2G)	--
	Diagonal lines					
Target values			2.668		0.797	
3—1	--	--	2.699	--	0.796	--
3—2	--	--	2.615	--	0.796	--
3—4	--	--	2.689	--	0.795	--
3—5	--	--	2.650	--	0.794	--
Largest deviation [%]			2% (3––2)		0.4% (3––5)	

Line lengths given unattached to the model
Floats were measured before assembly but their individual measurements were not recorded, once assembled measurement not feasible so target values are given.

Material properties were:

- Chain: 6 mm stainless steel (316) short link chain
- Dyneema: 1.6 mm

3.2 Experimental set-up

The devices were moored in each configuration so that the central device (TM3) was coincident with the centre of the UoP Ocean Basin. Table 3-2 lists the bottom line anchor positions with respect to the centre of the basin.

TABLE 3-2 POSITIONS OF THE ANCHORS AND LINE DESIGNATION WITH RESPECT TO THE CENTRE OF THE BASIN FOR THE OWC SPAR BUOY ARRAY

Device	Line designation	*X* [m]	*Y* [m]
TM1	1G	-6.590	-6.590
TM2	2G	-6.590	6.590
TM4	4G	6.590	-6.590
TM5	5G	6.590	6.590

3.3 Input wave conditions

Input wave conditions are as per the isolated OWC spar buoy experiments.

3.4 Data acquisition

The wave gauges were placed as close to the positions of the wave gauges for the single device experiments as practicable and the positions are given in the Appendix. The following process was followed to decide:

- Ideally:
  - Wave gauges should appear upwave of each device when in the array;
  - Some wave gauges should be along the centre line (in a group of three) so that reflections could be calculated if necessary;
  - It was aimed to keep the positions as similar as possible between experiments (whether there was one or 5 devices in the water);
  - One gauge was required out to the side in line with the central device;
  - One gauge was within the array.

- Limitations:

  - A maximum of 16 gauges was available in the laboratory;
  - Placement of the gauges was limited by the scaffolding/gantry placements.

- The final choice was:
  - one gauge up wave of 4 of the devices,
  - 2 additional gauges along the centre line in front of the devices
  - 2 behind the devices
  - 1 within the array perimeter (for the November tests, see 7.2)
- Some positions changed during array testing as the devices moved significantly in surge and impacted the gauges
- Empty basin tests tried to place gauges where the devices would be.

Load cells were placed at the fairleads of devices 1, 2 and 4 and on the inter-body mooring line fairleads, as described in Table 3-3.

TABLE 3-3 LOAD CELL DESIGNATIONS FOR THE OWC SPAR BUOY ARRAY EXPERIMENTS FOR CONFIGURATION D

Line number	Load cell number	No load reading [N]	Still water reading [N]
1G	698 315		7.784
2G	698 312		1.887
4G	546 534		8.852
3—5	698 313		9.060
3—2	698 317		15.658
2—3	698 314		4.415
4—3	546 532		13.283
disconnected	546 533	-0.773	-0.773
broken	698 316	-215.249	-215.249

Sensor readings when moored in still water are approximate values taking into account the no load reading. For specific values, see the beginning of each file
Still water readings are the mean of 110100 samples in file FlatWaterRun.lvm
3—5 indicates a load cell placed on the diagonal between TM3 and TM5 but on the TM3 fairlead
546 533 and 698 316 appear in the data files but are to be dismissed

Owing to the complexity of measuring the draughts of the devices in the arrays, only the moored draughts of the central and one corner device were measured. The moored draught measured for the TM3 device was 918±5 mm and the draught for the corner device (TM5) was 899±5 mm.

3.5 Description of the numerical model

This numerical model is similar to the model presented in 2.2. The layout of the array is illustrated in Figure 3-1. There are five buoys: one interior buoy, whose vertical axis of symmetry coincides with the origin of the array's coordinate system, and the other four are located on the coordinates (79.76m, 79.76m) of each quadrant. The draught of the buoys in their configuration has been measured and used as an input for the numerical model. The total draught of the outer buoys is 35.96 m, and for the inner buoy is 36.72m (values for still water).

The six rigid degrees of freedom were considered for each buoy.

Figure 3-2 shows the RAOs for the modes surge, heave and pitch, obtained for the central OWC spar buoy of the array.

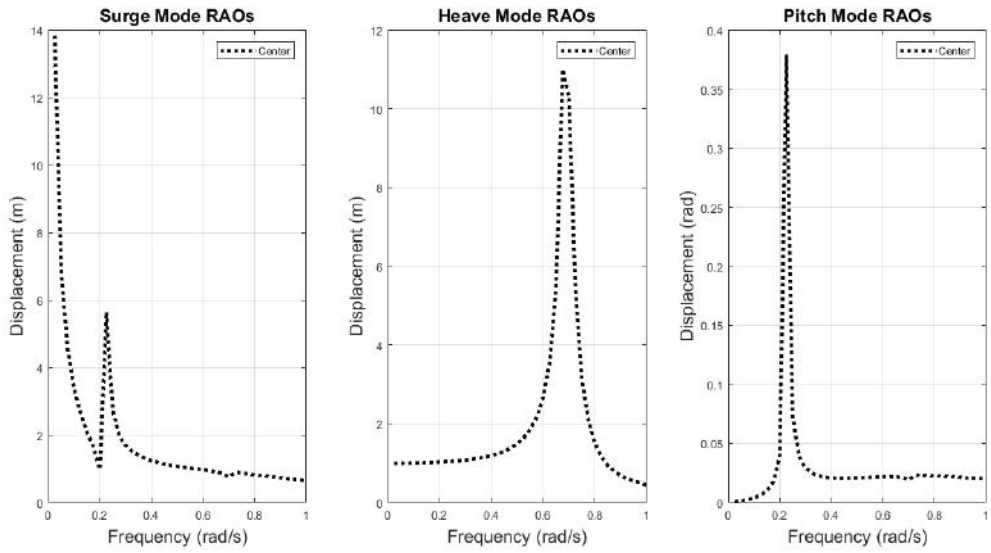

FIGURE 3-2 RAOS FOR THE CENTRAL OWC SPAR BUOY OF THE FLEXIBLE ARRAY FOR SURGE, HEAVE AND PITCH

OrcaFlex model is shown in Figure 3-3.

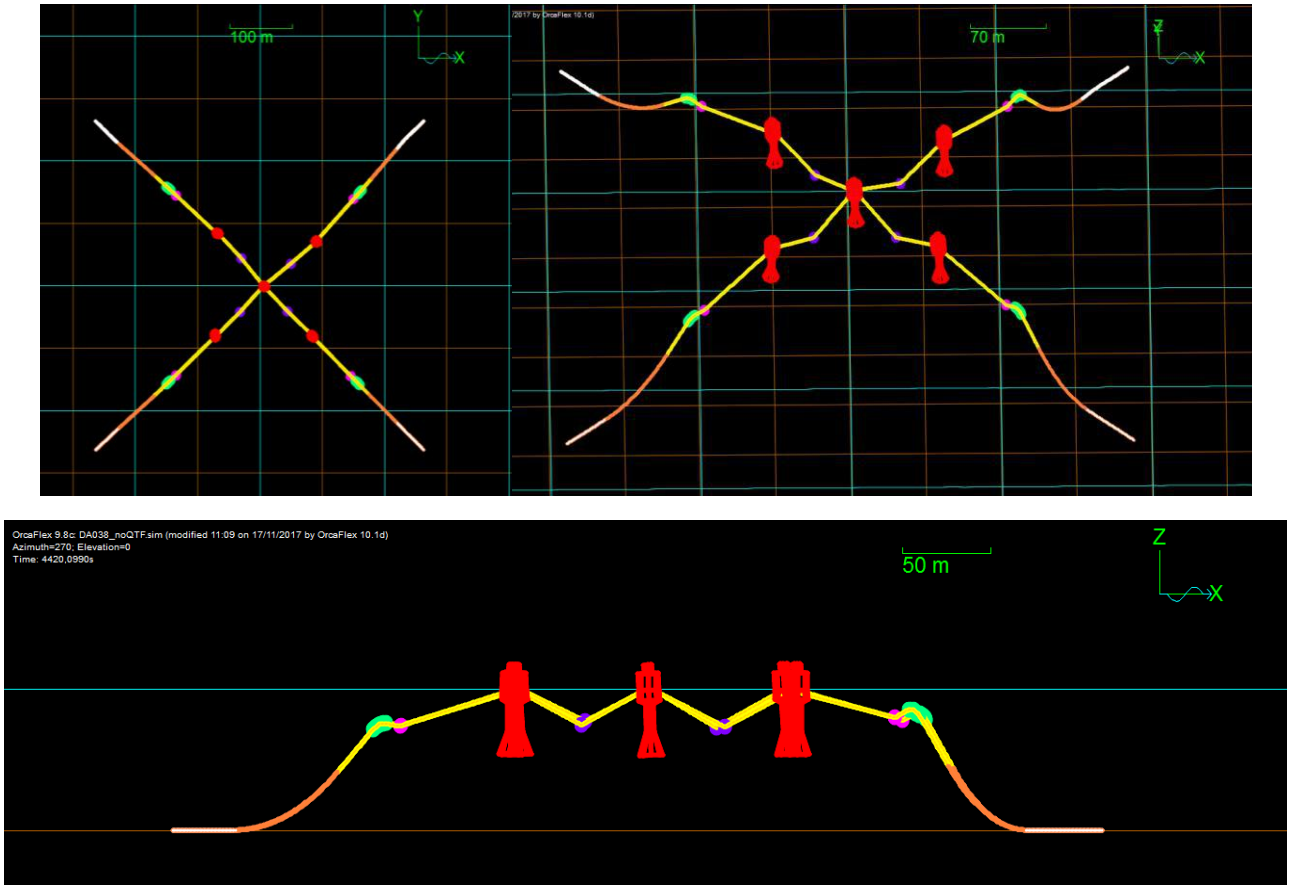

FIGURE 3-3 ORCAFLEX MODEL OF THE FLEXIBLE ARRAY, CONFIGURATION D.

3.6 Results

All results are at full scale. For simplicity, the ideal system was modelled, with the target values for masses, volumes and lengths.

Results indicate that Qualisys was not able to track the motion of buoy 1. Buoy 1 markers were probably hidden behind another buoy. Experimental buoy 1 results are not used in this report for this reason.

3.6.1 Statics

No independent tank tests were conducted to measure the static position of the buoys of the array. The static position is evaluated using the end of heave decay test DB001, as presented in Table 3-4.

TABLE 3-4 SUMMARY OF THE STATICS TESTS EXPERIMENT, FLEXIBLE ARRAY

Simulation name	
DB001	Heave decay test

3.6.1.1 Draught of the buoy

The draught of the OWC spar buoy was directly measured with a scale taped on the device during the experiment. The measured values are summarised in Table 3-5 as well as the numerical model results. The WAMIT file used for calculation has been calculated with the measured draughts with a mooring system.

Good agreement was found with the numerical model values, with less than 2.3% between the experimental and numerical values. This difference may be caused by small differences in mass of the buoy and lines, length of the lines or positions of the anchors and fairlead. The difference does not originate from the accuracy of the measurement (±0.5 mm, which is 0.02 m full scale).

The same difference was found for the single buoy (Table 2-7), with the draught being higher in the numerical model than in the experiment.

TABLE 3-5 EXPERIMENTAL AND NUMERICAL STATICS VALUES FOR THE DRAUGHT OF THE OWC SPAR BUOY (M), CONFIGURATION D

With mooring Buoy	Tank test	Numerical model	Difference (m)	Relative diff %
3	36.72	37.33	0.61	1.6%
5	35.96	36.80	0.84	2.3%

3.6.1.2 Vertical position of the buoy (from Qualisys)

The next step was to compare the vertical position of the CoM. The experimental vertical position of the CoM was obtained from the draught (see Table 3-5) as well as from Qualisys data as a check on the Qualisys results. Results are presented in Table 3-6.

Qualisys data were not available for a stationary case, so the mean values for the beginning of the heave decay cases (DB001) were used instead. A good agreement was found between the experimental values measured with Qualisys and deduced from the draught measurement with less than 2% differences

between the values. Less than 3% difference was observed between the experimental and numerical values.

TABLE 3-6 EXPERIMENTAL AND MODELLED STATICS VALUES FOR THE VERTICAL POSITION OF MEASUREMENT POINT RELATIVELY TO THE MEAN WATER LEVEL (IN M). WITH MOORING SYSTEM. OWC SPAR BUOY ARRAY, CONFIGURATION D

Buoy	Experimental (Qualisys)	Experimental (deduced from draught measurement)	Numerical model
1	error	/	-20.10
2	-19.56	/	-20.10
3	-20.50	-20.01	-20.62
4	-19.91	/	-20.10
5	-19.42	-19.25	-20.10

3.6.1.3 Position of the buoy in the other DOFs

The final step with the statics results was to observe the experimental statics position of the buoys.

As above, Qualisys data were not available for a stationary case so the mean values for the heave decay and pull-out cases with PTO (DB001 with mooring, OWC 3 was moved) were used instead. In stationary position, the experimental angles of heel and trim were below 3° and the modelled values below 1°. X and Y position were close to their target position (square of 80 m side): the experimental values were less than 4 m from their planned position, and the model values less than 1 m.

TABLE 3-7 EXPERIMENTAL AND MODELLED VALUES FOR THE STATICS VALUES OF X AND Y (IN M) AND HEEL AND TRIM ANGLES (IN DEG). WITH MOORING SYSTEM. OWC SPAR BUOY ARRAY, CONFIGURATION D. EXPE STANDS FOR EXPERIMENTAL MODEL (QUALISYS), NUM STANDS FOR NUMERICAL MODEL (ORCAFLEX), REL DIR STANDS FOR RELATIVE DIFFERENCE (REFERENCE: EXPERIMENT)

	OWC 1		OWC 2			OWC 3			OWC 4			OWC 5		
	Expe	Num	Expe	Num	Rel Dir	Expe	Num	Rel Dir	Expe	Num	Rel Dir	Expe	Num	Rel Dir
X	error	-79,77	-82,75	-79,93	-3%	0,63	0	-100%	80,9	79,93	-1%	82,23	79,77	-3%
Y	error	-79,93	83,76	79,77	-5%	-0,87	0	-100%	-84,11	-79,77	-5%	82,82	79,93	-3%
Heel	error	-0,61	2,23	0,61	-73%	-0,76	0	-100%	-2,02	-0,61	-70%	2,37	0,61	-74%
Trim	error	0,61	3,18	0,61	-81%	-0,48	0	-100%	-1,6	-0,61	-62%	-1,31	-0,61	-53%

3.6.1.4 Mooring line tensions

The mooring line tensions were compared. Mooring line numbering is summarised in Figure 3-1. This allowed a first check on the correction of the load cells. Results are presented in Table 3-8. For each load cell, the sensor dry offsets were provided and were used for this comparison. These values were removed from the static values obtained for the end of a decay test (DB001).

A fair agreement was found between the experimental and the numerical values with less than 30% difference. The numerical model generally overestimated the mooring load, except for line 4g for which it was very close (2% difference).

Static tension should be the same in lines

- 1g, 2g and 4g
- 3-2 and 3-5
- 2-3 and 4-3

Difference from experimental values was observed between

- 4g, with a static value of 6.8E+5 N
- 1g and 2g.with a static value of 5.3E+5 N.

This difference may be caused by an imbalance in the mooring system (one line being shorter, one clump weight heavier…) or by an inaccuracy in the calibration of the load cells.

TABLE 3-8 EXPERIMENTAL AND MODELLED STATICS VALUES FOR THE MOORING LINE TENSION (IN N). OWC SPAR BUOY ARRAY, CONFIGURATION D

Line	Experimental	Numerical model	Relative difference
1g	5.29E+05	6.68E+05	-26%
2g	5.25E+05	6.68E+05	-27%
4g	6.81E+05	6.68E+05	2%
3—2	5.88E+05	6.88E+05	-17%
3—5	5.78E+05	6.88E+05	-19%
2—3	5.46E+05	7.00E+05	-28%
4—3	5.79E+05	7.00E+05	-21%

3.6.1.5 Summary

A good agreement was found for the statics position and a fair agreement for the mooring line tension.

3.6.2 Pull-out tests

Due to difficulty restricting the motion specifically to one degree of freedom the repeatability of the experimental surge response is not as good as for the single device. The repeatability of the experimental heave pull out tests remains very good.

The name of the simulations used for this analysis are summarised in Table 3-9.

TABLE 3-9 SUMMARY OF THE PULL-OUT TESTS EXPERIMENT

Simulation name	DOF
DB001	Heave buoy 3
DB002	Heave buoy 3
DB003	Heave buoy 3
DB004	Surge buoy 3
DB006	Surge buoy 3
DB007	Surge buoy 3

3.6.2.1 Surge pull-out

Experimental data from surge pull-out tests have been inspected but clear steps cannot be observed and therefore these data cannot be used for pull-out checks. For example, the surge motion of buoy 3 during the surge pull-out test is shown in Figure 3-4.

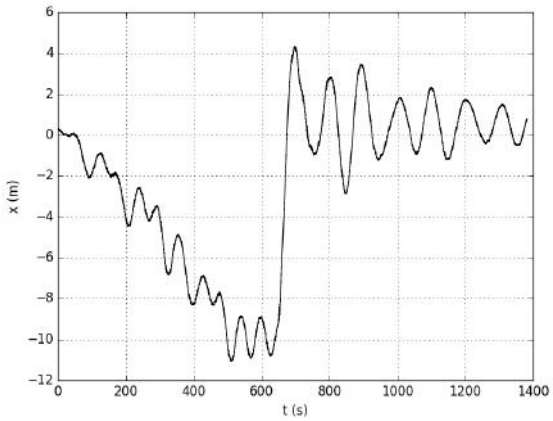

FIGURE 3-4 SURGE MOTION OF BUOY 3 DURING PULL-OUT OF BUOY 3. OWC SPAR BUOY ARRAY, CONFIGURATION D; TEST DB004

3.6.2.2 Heave buoy 3 pull-out

Cases DB001, DB002 and DB003 were used to compare the mooring stiffness when buoy 3 was lifted. The three tests were similar (same heave direction and same amplitude of heave). Motions in the pull-out direction are presented in Figure 3-5. The buoy was relatively still at each step of the pull-out test. The buoy was not perfectly pulled along the Z axis. The first two steps of DB001 were not still and experimental values are not used.

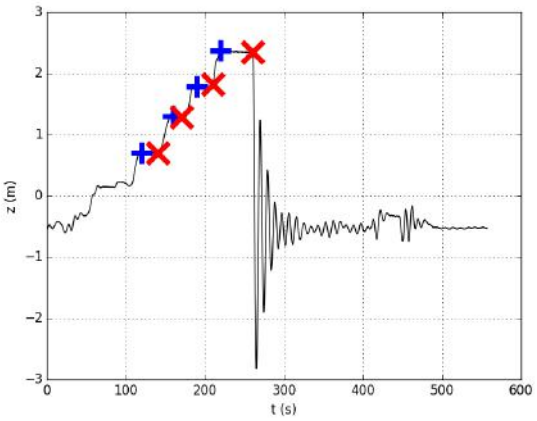

DB001

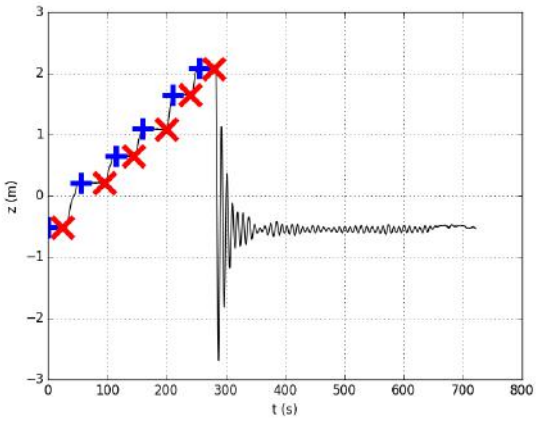

DB002

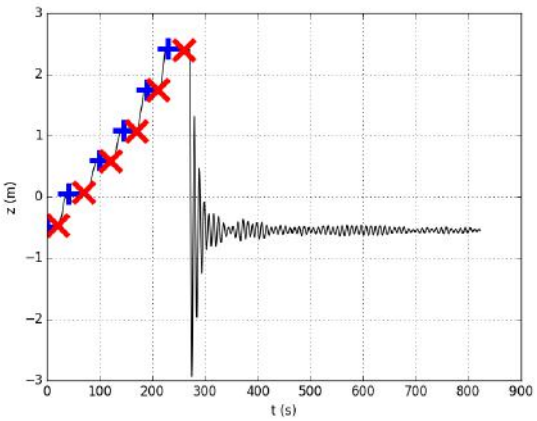

DB003

FIGURE 3-5 EXPERIMENTAL MOTIONS OF POINT O IN THE HEAVE DIRECTION DURING HEAVE PULL-OUT TESTS OF BUOY 3, OWC SPAR BUOY ARRAY, CONFIGURATION D

Results of the heave pull-out tests are presented in Figure 3-6. Differences were observed for tensions in load cells 3-2 between the experimental data and the modelled data. The tension decreased slightly in the experiment when it increased in the numerical model. The decreases in experimental values may be due to a different static equilibrium position of the buoys in the model and in the experiment. The tensions in load cells 3-5 are more similar between the model and the experiment.

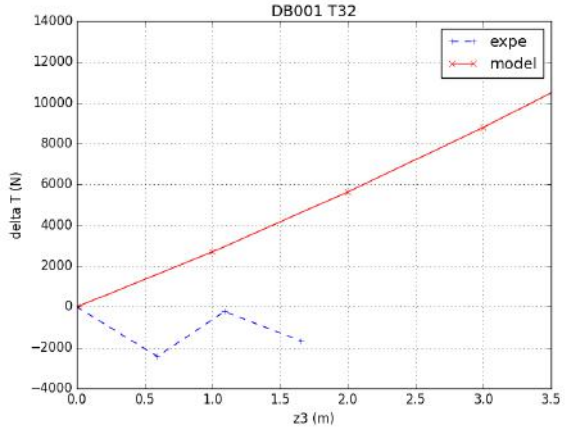

DB001 load cell 3-2

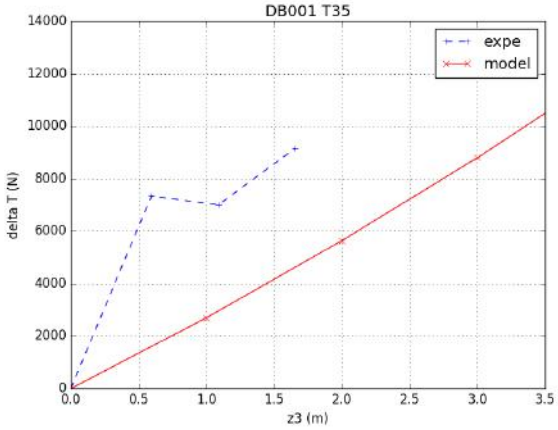

DB001 load cell 3-5

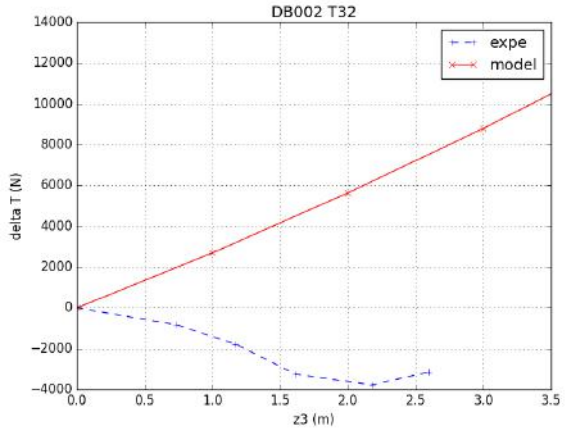

DB002 load cell 3-2

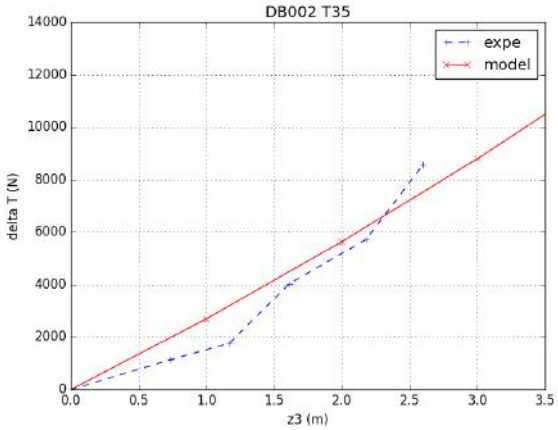

DB002 load cell 3-5

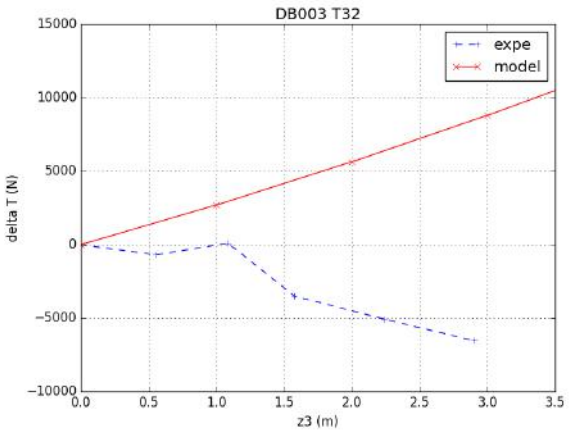

DB003 load cell 3-2

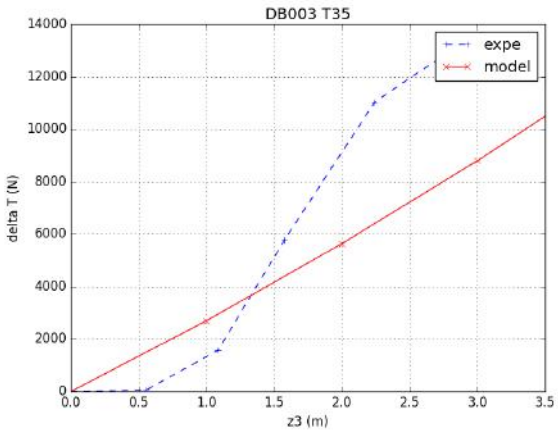

DB003 load cell 3-5

FIGURE 3-6 EXPERIMENTAL AND MODELLED VARIATIONS OF TENSIONS FOR DIFFERENT HEAVE POSITION DURING HEAVE PULL-OUT TEST OF BUOY 3, OWC SPAR BUOY ARRAY, CONFIGURATION D

3.6.2.3 Heave buoy 2 pull-out

Cases DB008, DB009 and DB0010 were used to compare the mooring stiffness when buoy 2 was lifted. The three tests were similar (same heave direction and same amplitude of heave). Motions in the pull-out direction are presented in Figure 3-7. The buoy was relatively still at each step of the pull-out test, however the buoy was not perfectly pulled along the Z axis.

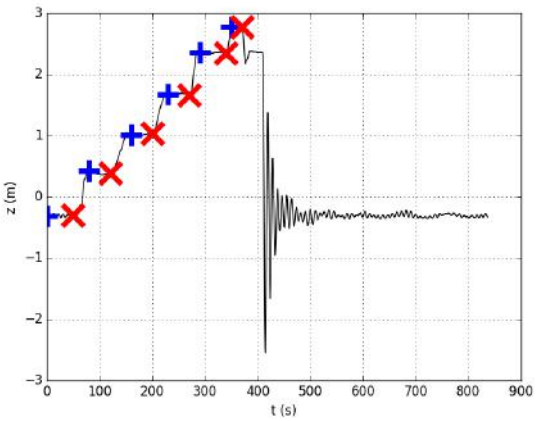

DB008

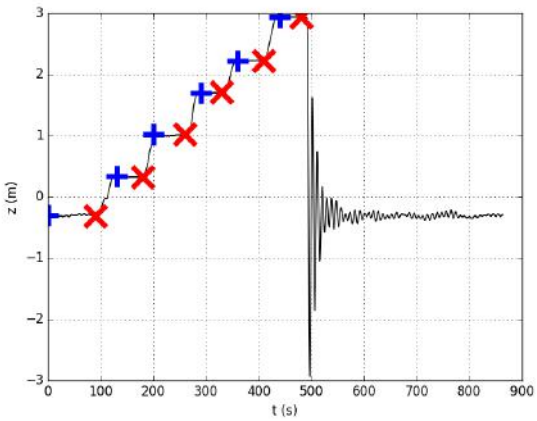

DB009

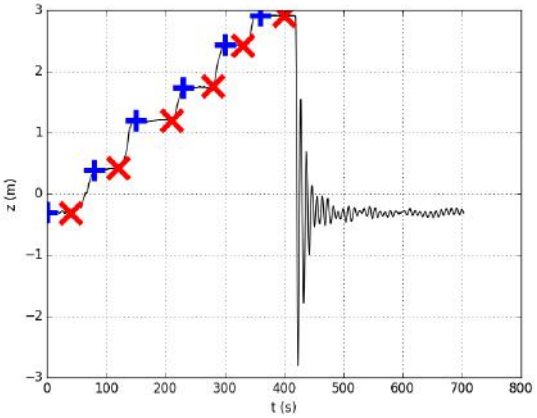

DB010

FIGURE 3-7 EXPERIMENTAL MOTIONS OF POINT O IN THE HEAVE DIRECTION DURING HEAVE PULL-OUT TESTS OF BUOY 2, OWC SPAR BUOY ARRAY, CONFIGURATION D

The loads resulting from the heave pull-out tests are presented in Figure 3-8. Differences are observed for tensions in load cells 2-3 between the experimental data and the modelled data. The tension slightly decreased in the experiment when it increased in the numerical model. The same behaviour was observed for tension 3-2 when buoy 3 was lifted. The tensions in load cells 2g were more similar between the model and the experiment. Very small differences were observed between the different experiments.

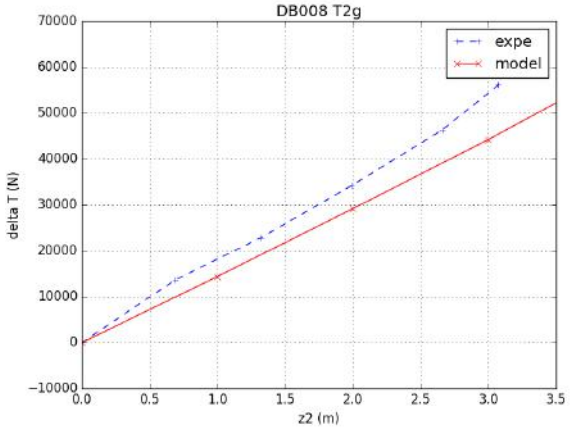

DB008 load cell 2g

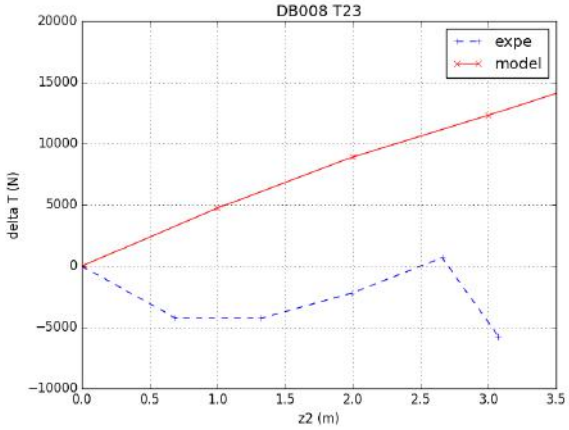

DB008 load cell 2-3

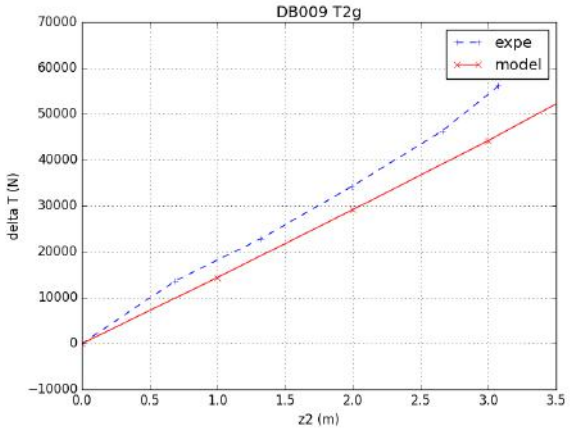

DB009 load cell 2g

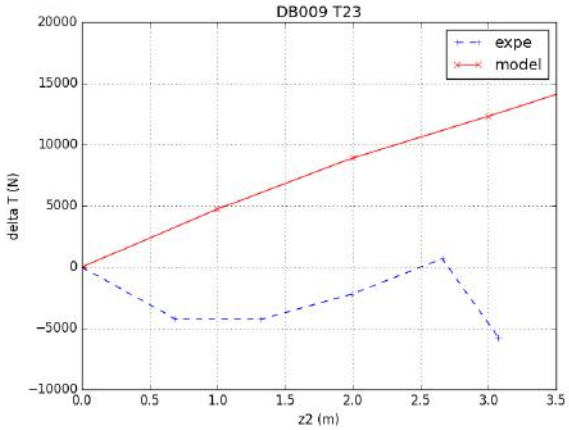

DB009 load cell 2-3

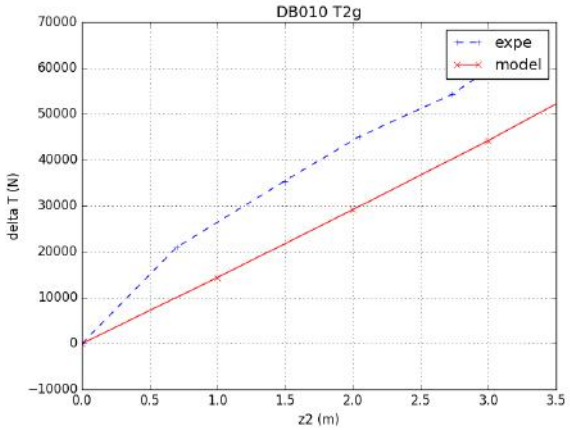

DB010 load cell 2g

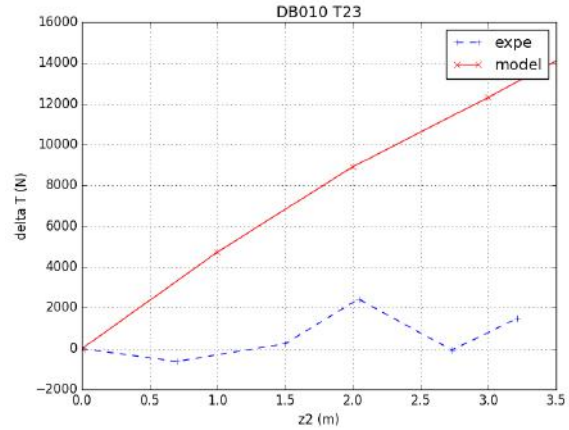

DB010 load cell 2-3

FIGURE 3-8 EXPERIMENTAL AND MODELLED VARIATIONS OF TENSIONS FOR DIFFERENT HEAVE POSITION DURING HEAVE PULL-OUT TEST OF BUOY 2, OWC SPAR BUOY ARRAY, CONFIGURATION D

3.6.2.4 Heave buoy pull-out summary

Results indicate that the numerical model predicted the tension in line 2g and 3-5 well. The tension in load cells 3-2 and 2-3 were not captured by the numerical model but this may be due to different equilibrium positions achieved by the experiment.

3.6.3 Regular wave tests

Experiments were conducted for similar waves as for the single spar buoy OWC. The experiment names, wave height and wave periods are summarised in Table 3-10 and Figure 3-9. Figure 3-9 indicates that experiments in regular waves were conducted far from the linear wave theory and wave breaking limits.

TABLE 3-10 SUMMARY OF THE REGULAR WAVE EXPERIMENT AND EXPERIMENT AND NUMERICAL MODEL STABILITY, OWC SPAR BUOY ARRAY, CONFIGURATION D

Simulation name	H (m)	T(s)	Unstable in experiment
DA032	2	7	
DA031	2	7,4	
DA030	2	7,9	
DA029	2	8,4	
DA028	2	8,7	
DA015	2	9,4	
DA022	2	9,4	
DA013	2	9,7	
DA012	2	9,9	
DA011	2	10	
DA021	2	10	
DA027	2	10	
DA034	2	10	
DA033	2	10,1	
DA010	2	10,2	
DA009	2	10,5	
DA020	2	10,5	
DA026	2	10,5	
DA008	2	11	
DA019	2	11	
DA025	2	11	
DA007	2	11,5	Y
DA018	2	11,5	Y
DA024	2	11,5	missing wave data
DA006	2	12	Y
DA023	2	12	Y
DA005	2	12,6	Y
DA004	2	14,1	
DA003	2	15,8	
DA002	2	18,1	
DA001	2	21,1	

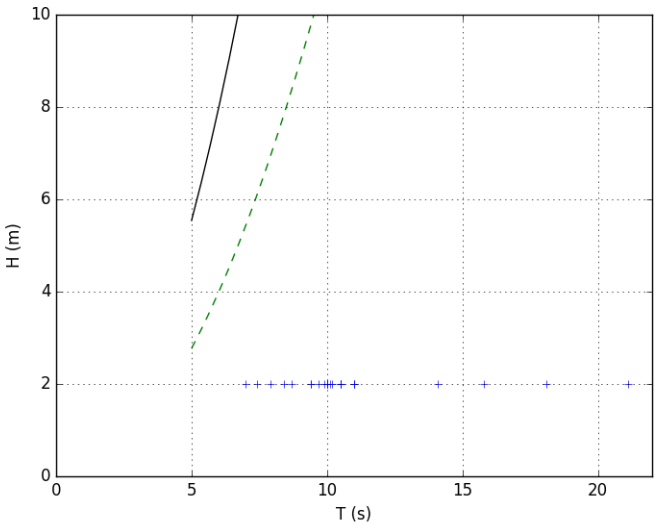

FIGURE 3-9 TESTED REGULAR WAVES (AIRY). GREEN DOTTED LINE: LIMIT OF LINEAR WAVES; BLACK LINE: WAVE BREAKING LIMIT. OWC SPAR BUOY ARRAY, CONFIGURATION D

However some experiments became unstable with increasing motions. This is for example the case for DA007, with *H* equal to 2 m and *T* equal to 11.5 s. Experimental motions of this device and tensions in the mooring lines are shown in Figure 3-10.

The peak observed in X4 and Z4 is a glitch in data probably caused by Qualisys which was not able to follow the device. This glitch has no physical meaning. It occurs on buoy 4 which was on the opposite side of the basin of the cameras, so device 4 may have been shadowed by device 5. An increasing pitch motion can be observed on all buoys, with increasing mooring line loads being observed at the same time. Surge motions are also modified and increase on buoy 3.

In the case of test DA007, the high pitch amplitudes observed for the central device do not seem to be related with parametric roll/pitch resonance, a common nonlinear effect found in these devices. Since the parametric roll/pitch resonance condition of having an incident wave period (11.5 s) near half the pitch/roll natural period (35.4 s) is not observed, it is likely that this nonlinear effect is triggered by the mooring system dynamics and the large heave amplitudes that are present in all devices. Due to the high nonlinearities found in these cases, the numerical model was not applied.

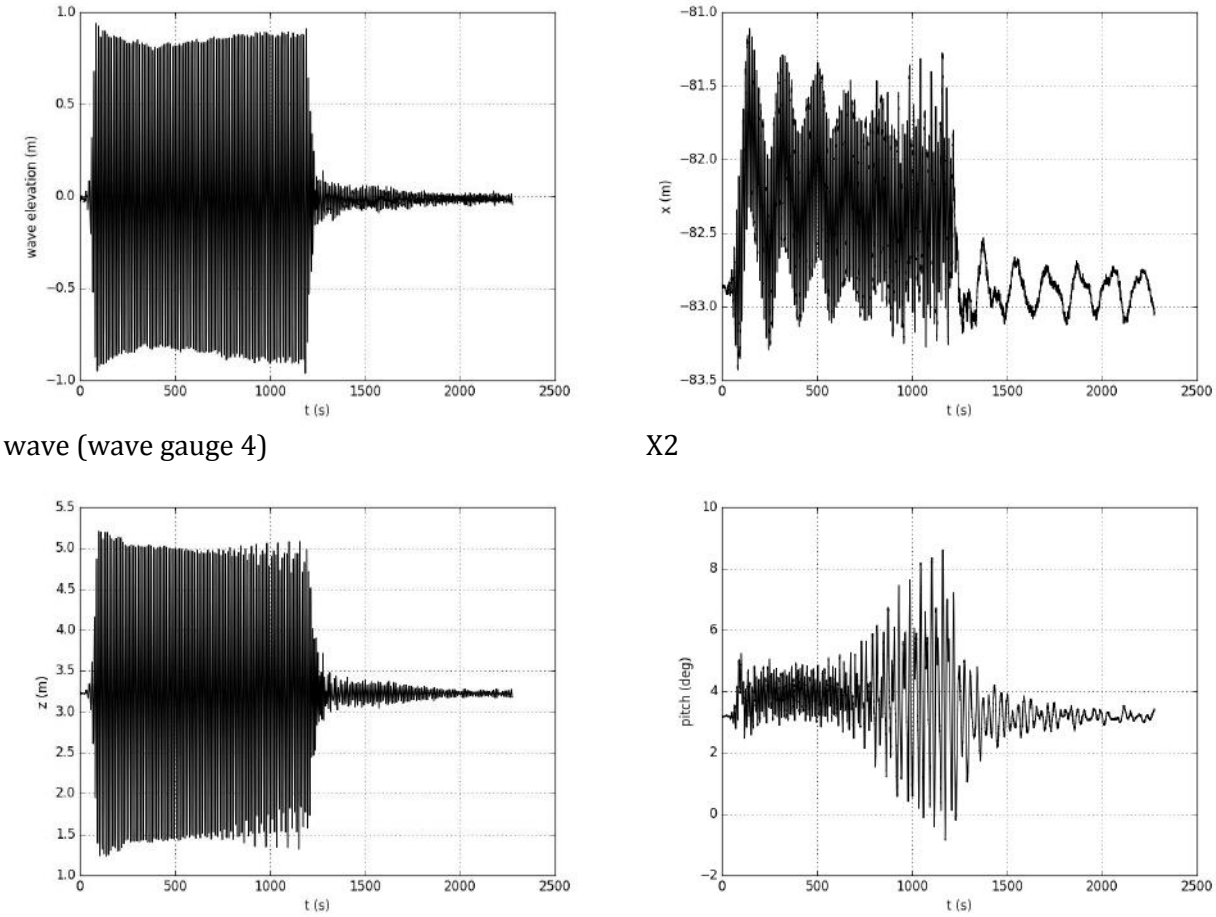

wave (wave gauge 4) X2

Z2 Pitch2

FIGURE 3-10 EXAMPLE OF EXPERIMENTAL TIME SERIES OF REGULAR WAVES FOR UNSTABLE CASE DA007 (*H* = 2 M AND *T* = 11.5 S). OWC SPAR BUOY ARRAY, CONFIGURATION D, BUOY 2

The surge RAOs are presented in Figure 3-11. It can be seen that the RAOs increased with period with experimental values up to 1.8 m/m. The experimental and modelled surge RAOs compared well for periods below 12 s. The numerical model underestimates the RAOs for periods over 12 s. A similar behaviour was observed for the single buoy (Figure 2-19). A similar behaviour was observed for all buoys below 12 s.

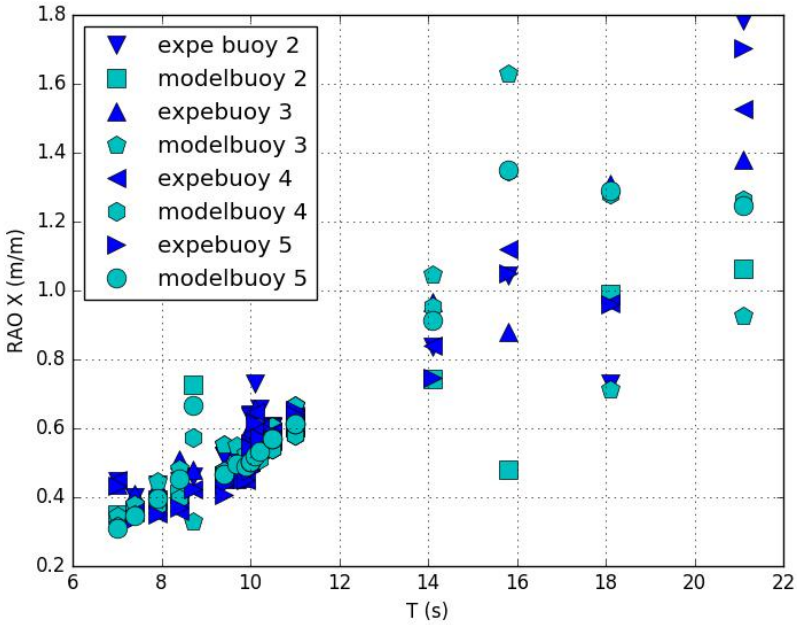

FIGURE 3-11 EXPERIMENTAL AND MODELLED DISPLACEMENT RAOS IN THE SURGE DOFS FOR BUOYS 2 TO 5. OWC SPAR BUOY ARRAY, CONFIGURATION D

The heave RAOs are shown in Figure 3-12, and increased for periods below 9 s with experimental values up to 3 m/m. The experimental and model behaviour was similar, however the modelled RAOs are generally smaller than the experimental RAOs, especially around the heave resonance. The heave motion is then likely to be underestimated by the numerical model. A similar behaviour was observed for the single buoy (Figure 2-19). A similar behaviour was observed for all buoys.

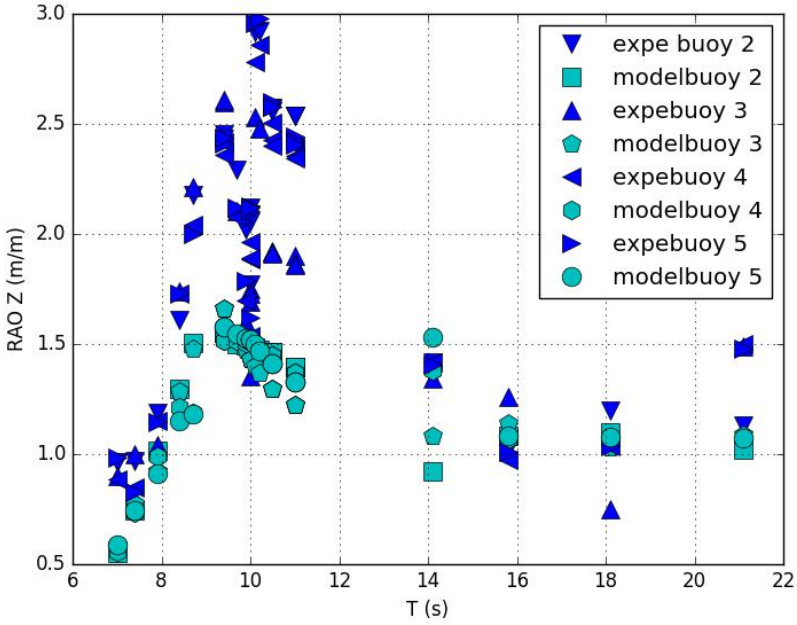

FIGURE 3-12 EXPERIMENTAL AND MODELLED DISPLACEMENT RAOS IN THE HEAVE DOFS FOR BUOYS 2 TO 5. OWC SPAR BUOY ARRAY, CONFIGURATION D

The pitch RAOs are presented in Figure 3-13. The RAOs were the highest for T = 16 s in the central buoy (buoy 3) in the experimental data. Pitch was similar for the single buoy for T below 12 s, but much lower for the single buoy than for the arrays above 12 s. This could be explained by the change in mooring configuration, with the line connecting the central device to the external device increasing the pitch motion.

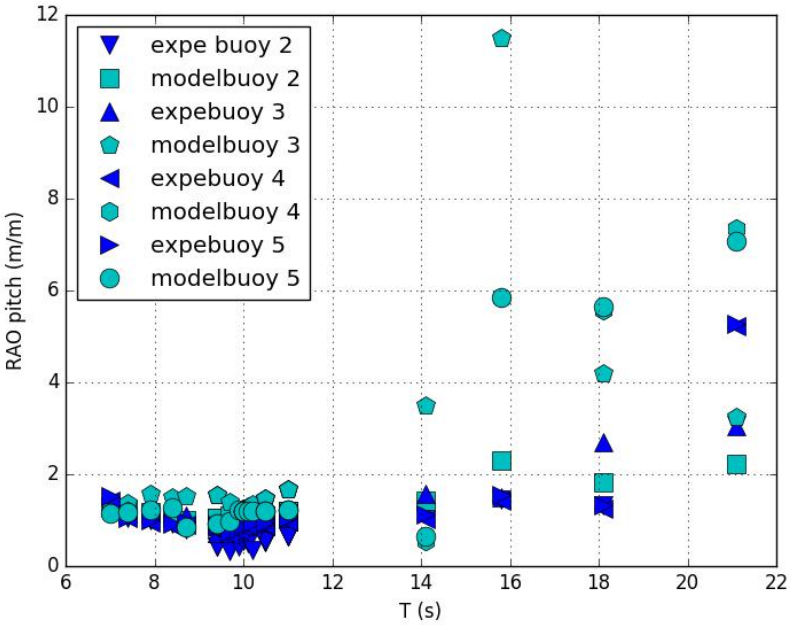

FIGURE 3-13 EXPERIMENTAL AND MODELLED DISPLACEMENT RAOS IN THE PITCH DOFS FOR BUOYS 2 TO 5. OWC SPAR BUOY ARRAY, CONFIGURATION D

The surge phase is plotted in Figure 3-14, results are for the central buoy (buoy 3) and are similar to those for the single device below 12 s. The surge phases of buoy 4 and 5 were similar, which is expected because these buoys are at the same distance from the wave paddles.

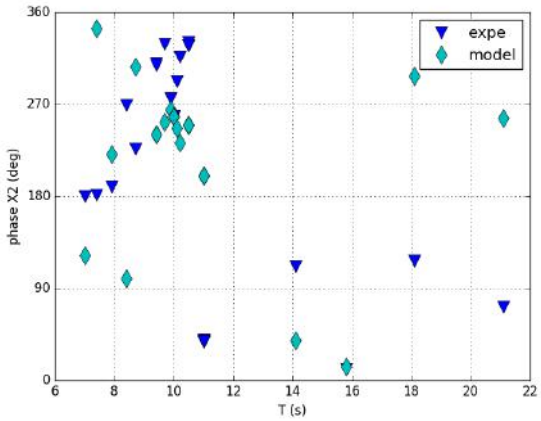

X2: surge buoy 2

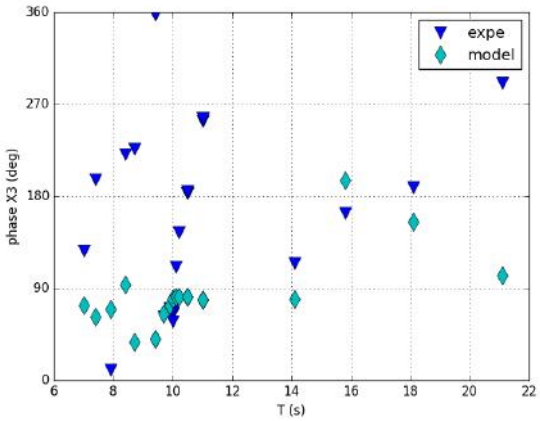

X3: surge buoy 3

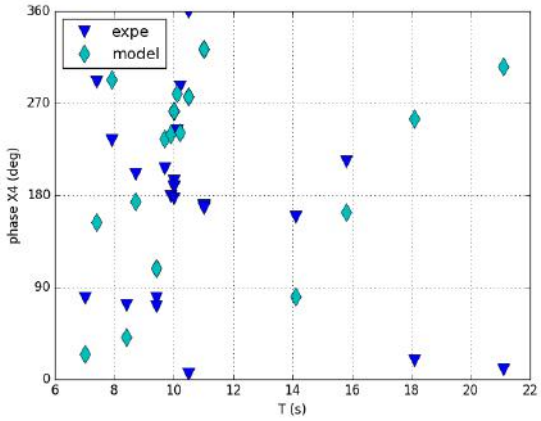

X4: surge buoy4

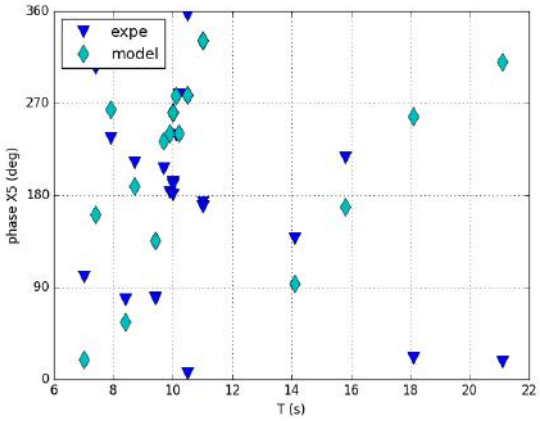

X5: surge buoy 5

FIGURE 3-14 EXPERIMENTAL AND MODELLED DISPLACEMENT PHASES IN THE SURGE DOFS FOR BUOYS 2 TO 5. OWC SPAR BUOY ARRAY, CONFIGURATION D

The heave phase variation, shown in Figure 3-15, was similar for the central buoy (buoy 3) and for the single device below 16 s. The heave phase of buoy 4 and 5 is similar, which is expected because these buoys are at the same distance from the wave paddles.

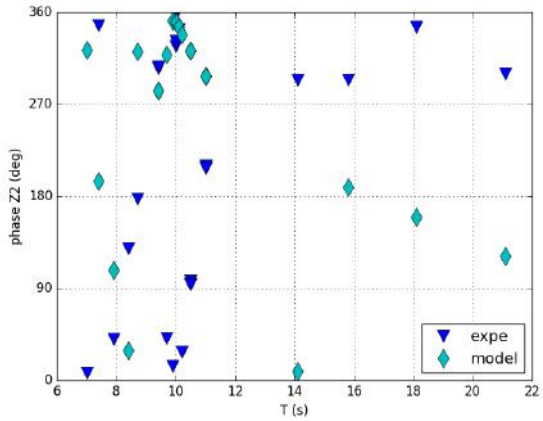

Z2: heave buoy 2

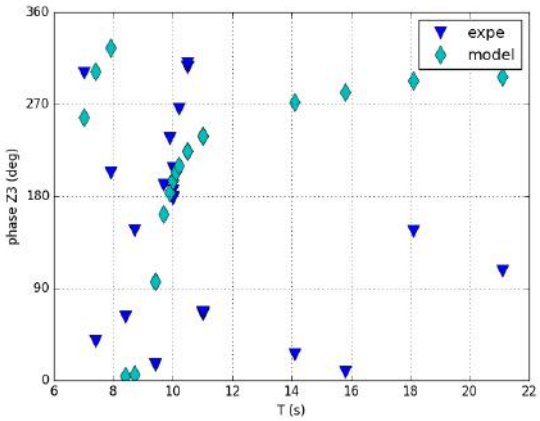

Z3: heave buoy 3

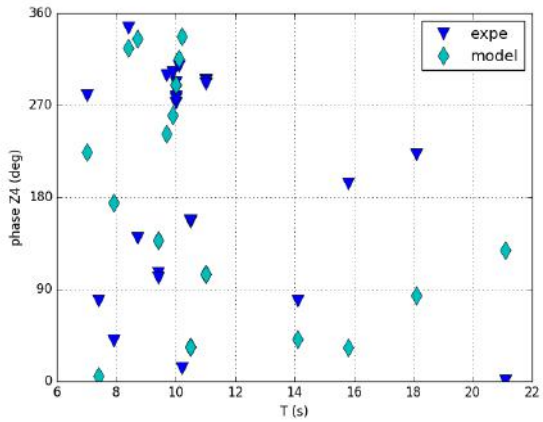

Z4: heave buoy 4

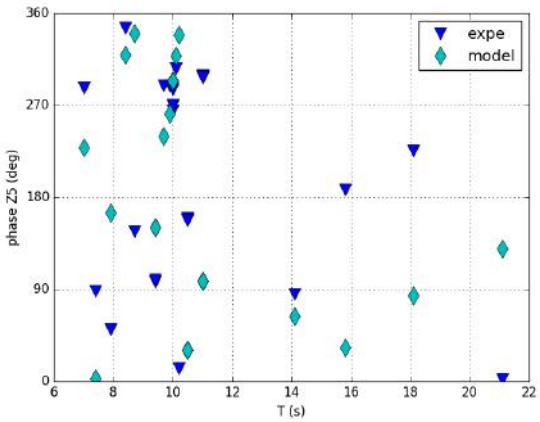

Z5: heave buoy 5

FIGURE 3-15 EXPERIMENTAL AND MODELLED DISPLACEMENT PHASES IN THE HEAVE DOFS FOR BUOYS 2 TO 5. OWC SPAR BUOY ARRAY, CONFIGURATION D

Figure 3-16 shows that the pitch phase was different between the central buoy (buoy 3) and the single device. This can be explained by the change of mooring system. The pitch phase of buoy 4 and 5 was similar, which is expected because these buoys are at the same distance from the wave paddles.

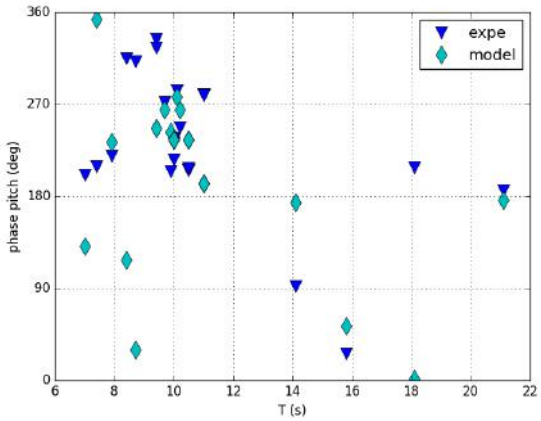

pitch buoy 2

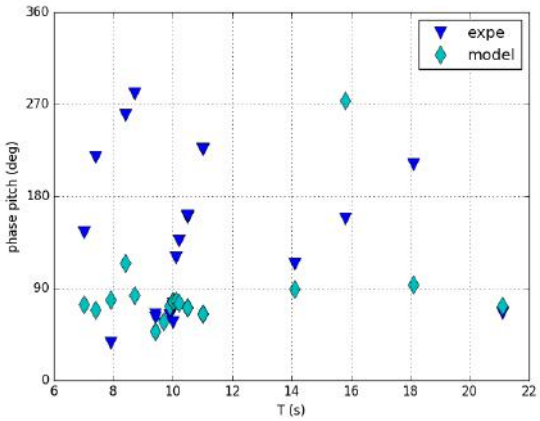

pitch buoy 3

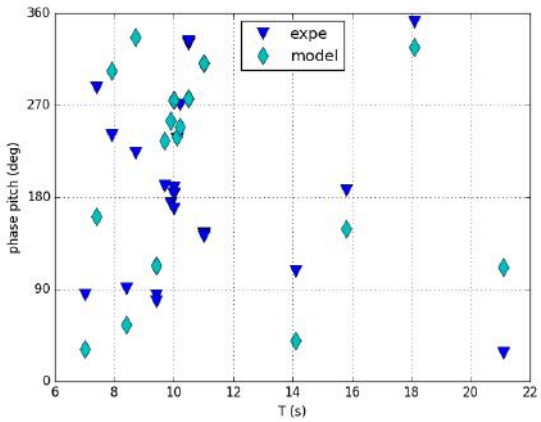

pitch buoy 4

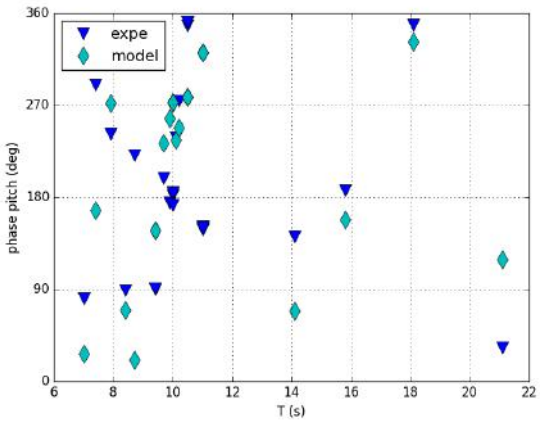

pitch buoy 5

FIGURE 3-16 EXPERIMENTAL AND MODELLED DISPLACEMENT PHASES IN THE PITCH DOFS FOR BUOYS 2 TO 5. OWC SPAR BUOY ARRAY, CONFIGURATION D

The mean drift in the X direction was similar for all four buoys, as shown in Figure 3-17 and was similar to the mean drift of the single device. However, the buoys in the arrays showed an increase in mean drift for *T* above 14 s or 16 s. The mean drift of the central buoy is smaller (<6 m) than the mean drift of the other buoys (12–-14 m) which can be explained by the reaction force of the internal mooring lines.

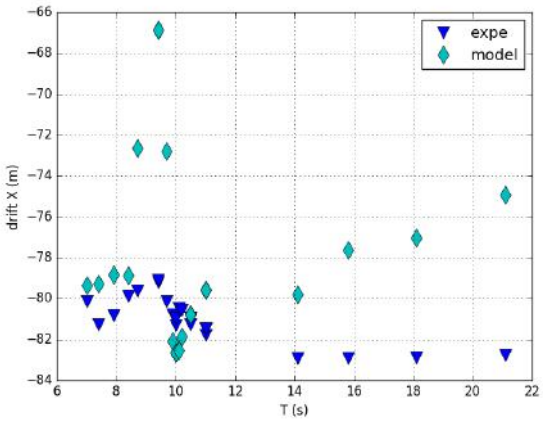

drift buoy 2

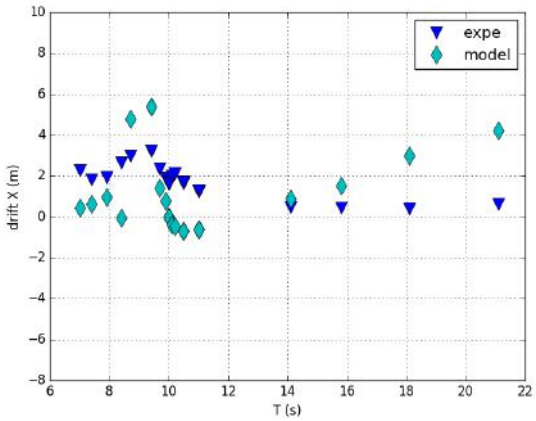

drift buoy 3

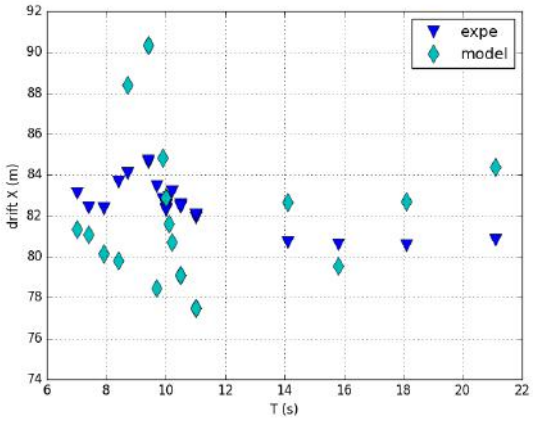

drift buoy 4

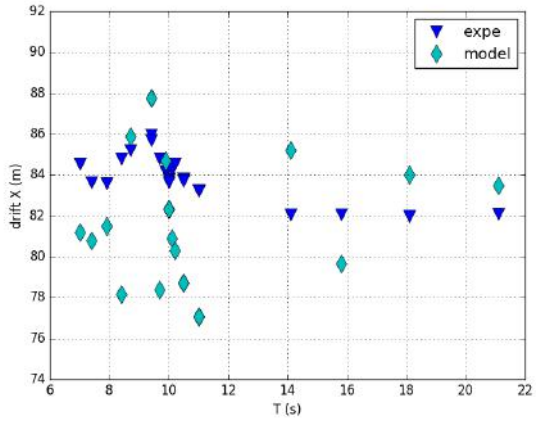

drift buoy 5

FIGURE 3-17 EXPERIMENTAL AND MODEL DRIFT (MEAN X POSITION) IN THE SURGE DIRECTION. OWC SPAR BUOY ARRAY, CONFIGURATION D

The experimental and modelled mooring load RAOs (Figure 3-18) were similar in the two front external mooring lines 1g and 2g. The mooring load RAOs did not differ strongly between the numerical model and the experiment except for values below 8 s where the model overestimated the tension. The behaviour was different from the behaviour of the single device mooring lines. This could be expected because the mooring system of the array differs from the single device mooring system. The RAOs of the bottom external mooring line 4g are slightly different from those for the front lines 1g and 2g, with for example a decrease in loads below 8 s.

The behaviour of the four internal lines 2-3, 3-2, 3-5 and 4-3 is similar. Loads decreased for periods below 10 s then increased. The model predicts the tension well for periods below 14 s but generally overestimated the tensions above 14 s.

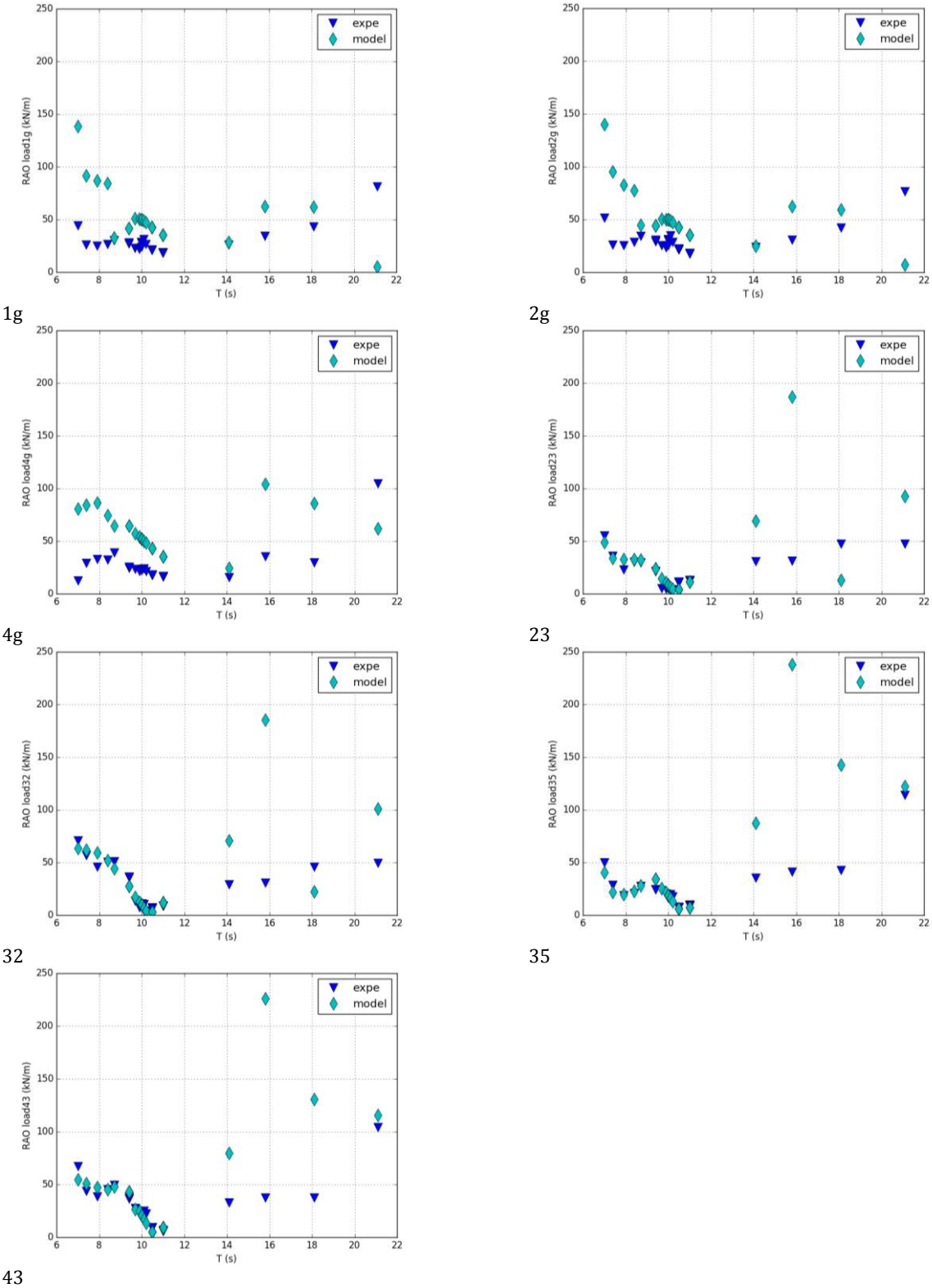

FIGURE 3-18 EXPERIMENTAL AND MODELLED MOORING LINE RAOS IN SELECTED MOORING LINES. OWC SPAR BUOY ARRAY, CONFIGURATION D

Figure 3-19 shows the line load phases. Similarly to the line load RAOs, the experimental and modelled mooring line load phases were similar in the two front external mooring lines 1g and 2g. A lag of approximately 90° was observed between the experimental and modelled data below 12 s. The

behaviour was different from the behaviour of the single device mooring lines, which can be expected with the different mooring arrangements. The behaviour of the four internal lines 2-3, 3-2, 3-5 and 4-3 was similar. The phases increased steeply between 8 s and 12 s and this behaviour was also observed for the single device mooring lines. The model fairly estimates the phases.

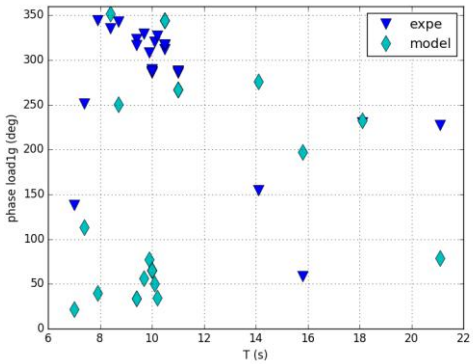

1g

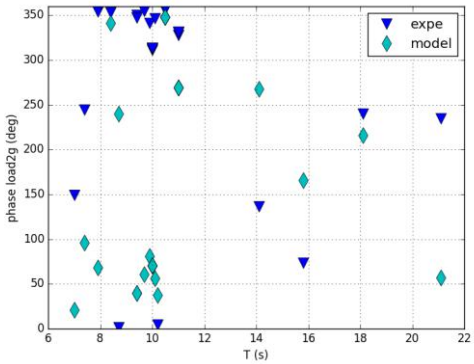

2g

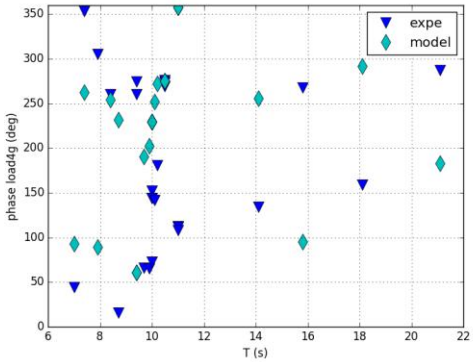

4g

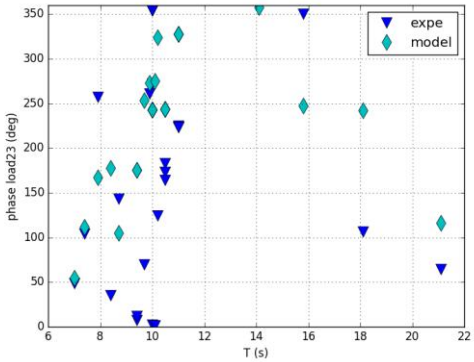

23

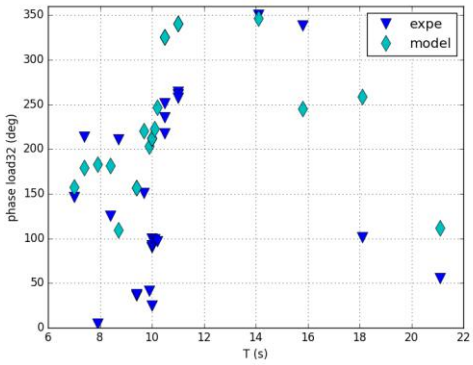

32

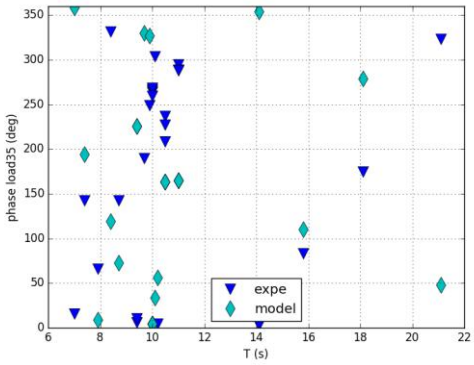

35

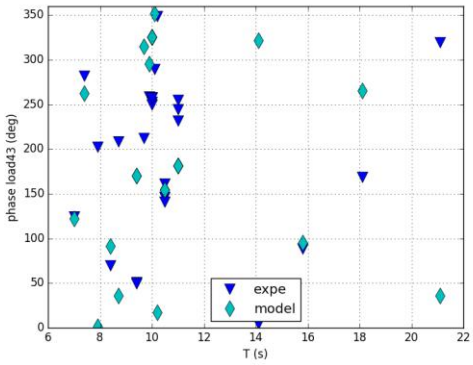

43

FIGURE 3-19 EXPERIMENTAL AND MODELLED MOORING LINE PHASES IN SELECTED MOORING LINES. OWC SPAR BUOY ARRAY, CONFIGURATION D

The times series for motions and loads under small amplitude, average wave period waves (H = 2 m, T = 10 s) are given in Figure 3-20. The results show a nearly linear behaviour in motions and mooring loads. A drift was observed between experimental and model mooring loads which can be either caused by a different pre-tension of mooring lines (for example caused by the use of different weights and floats in the experiment and the model), or by an inaccurate calibration of the load cells. The experimental results occur always before the model results with a constant lag between data.

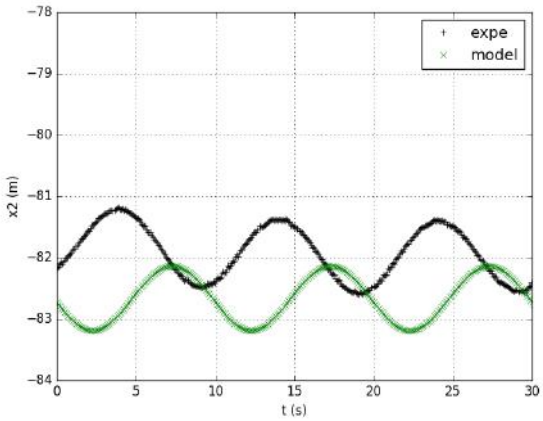

X2: surge buoy 2

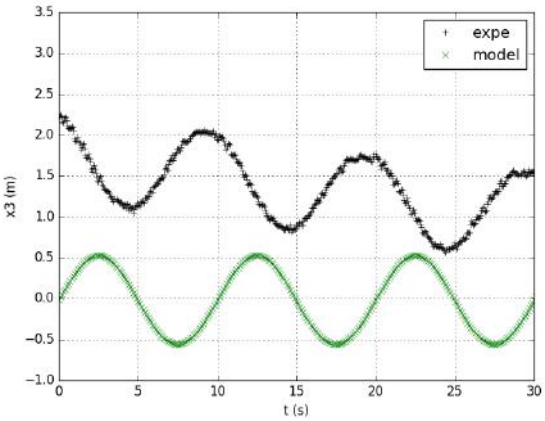

X3: surge buoy 3

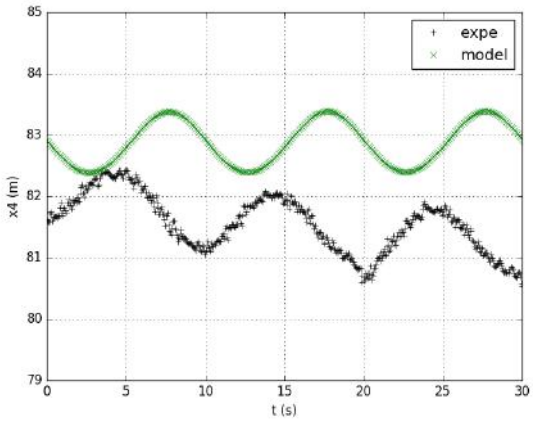

X4: surge buoy 4

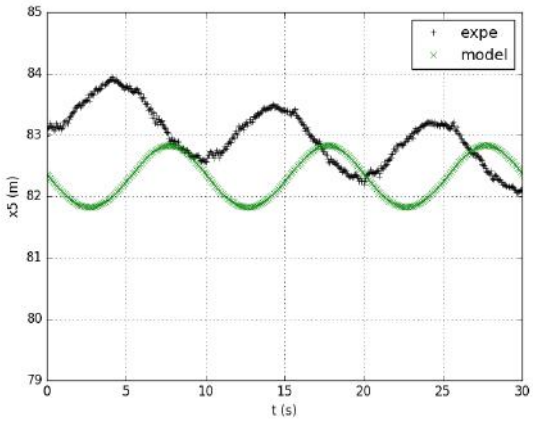

X5: surge buoy 5

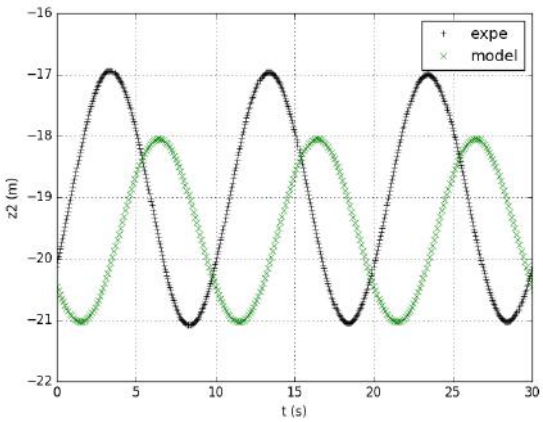

Z2: heave buoy 2

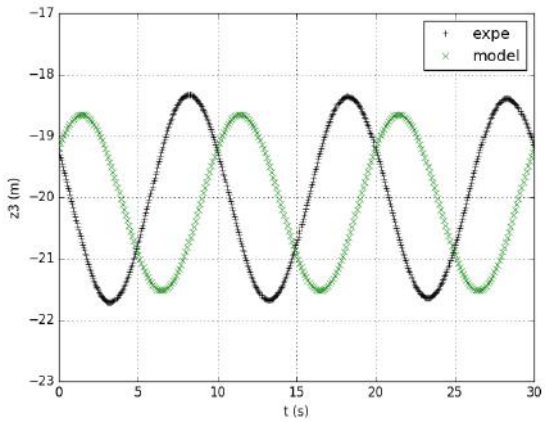

Z3: heave buoy 3

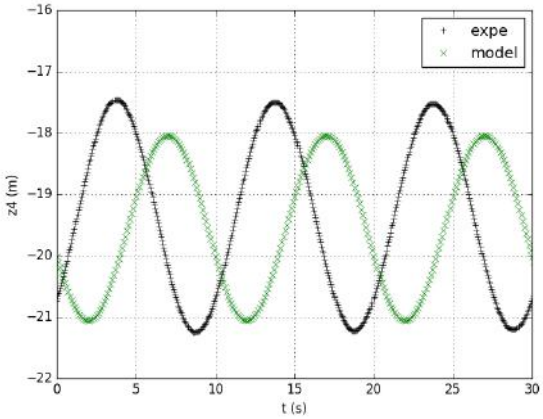

Z4: heave buoy 4

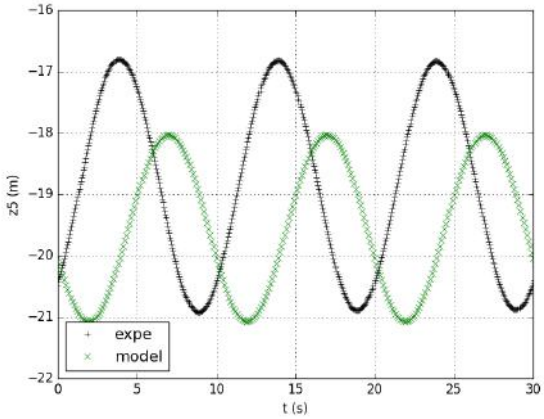

Z5: heave buoy 5

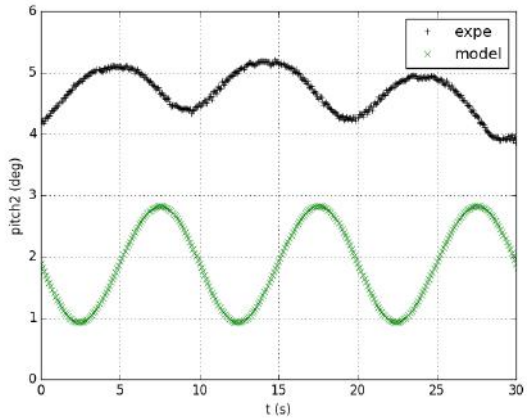

Pitch buoy 2

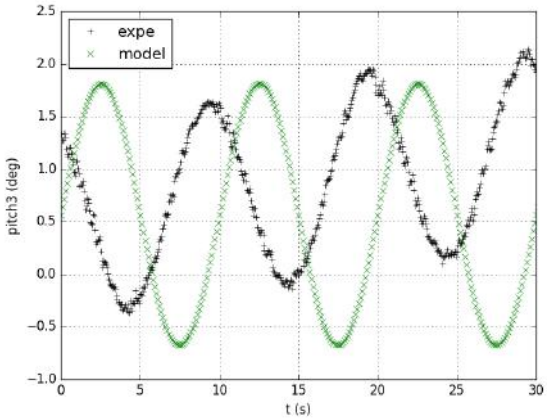

Pitch buoy 3

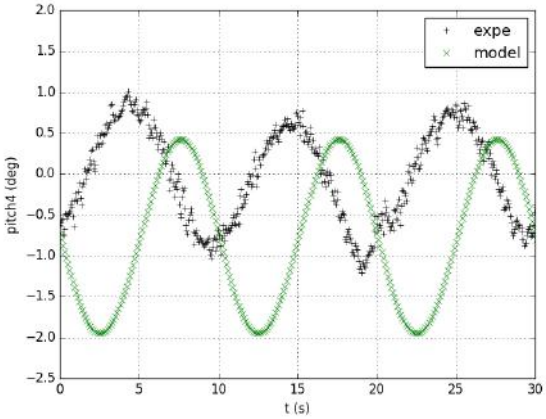

Pitch buoy 4

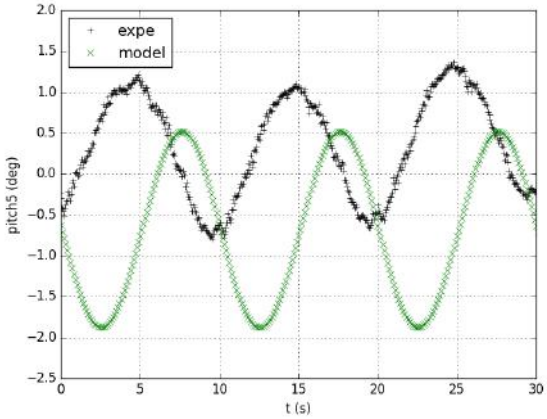

Pitch buoy 5

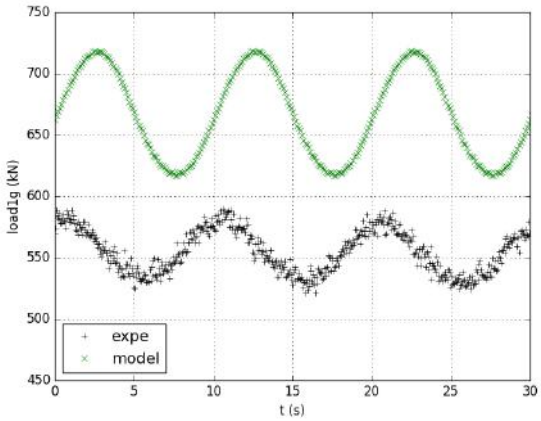

Load 1g

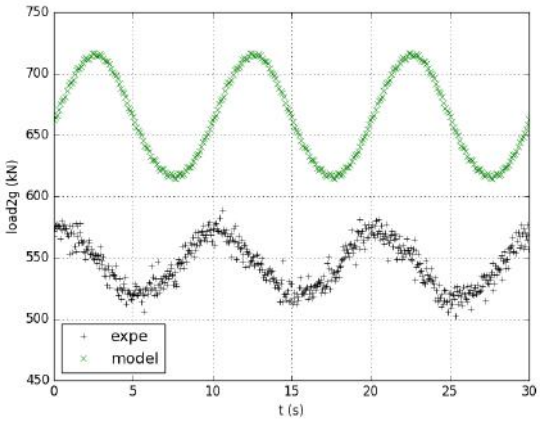

Load 2g

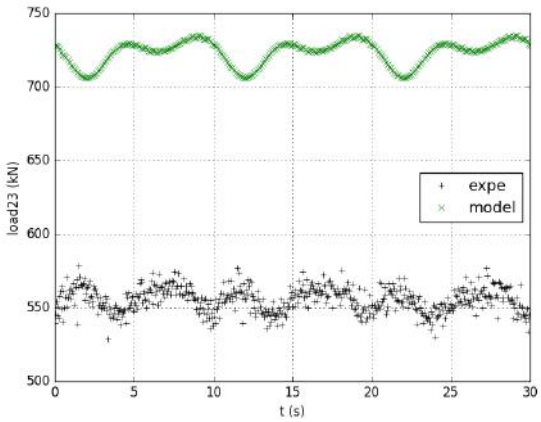

Load 23

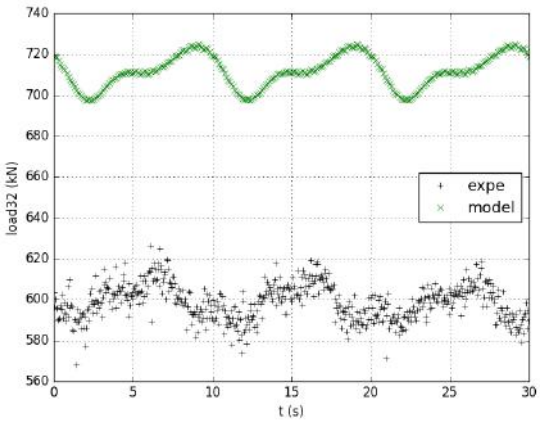

Load 32

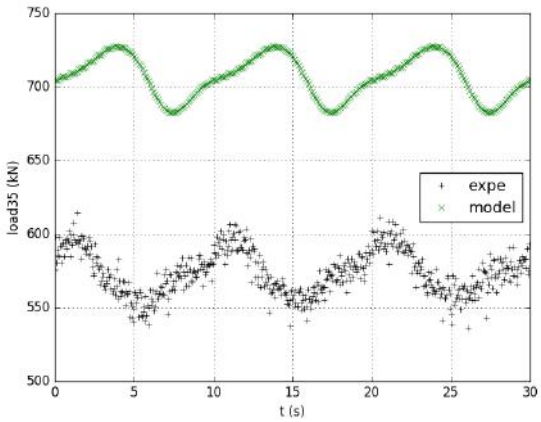

Load 35

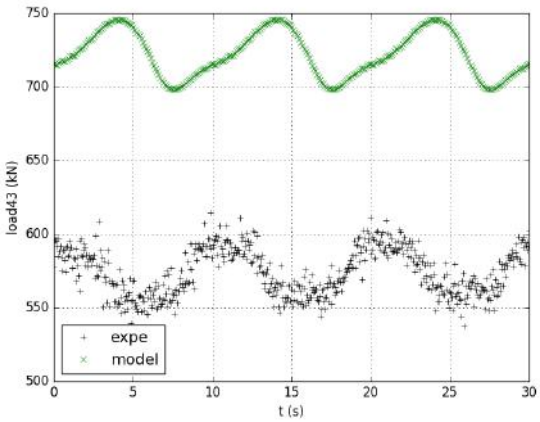

Load 43

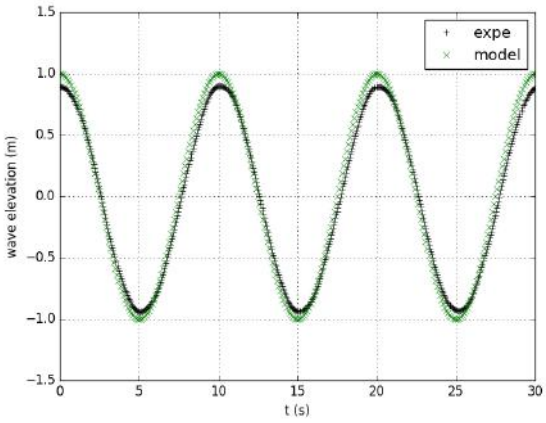

wave

FIGURE 3-20 EXAMPLE OF TIME SERIES OF REGULAR WAVES FOR CASE DA011 (H = 2 M AND T = 10 S). OWC SPAR BUOY ARRAY, CONFIGURATION D

3.6.4 Irregular wave tests

The irregular wave tests were conducted for approximately 10 minutes (model scale). The name of the tests, significant wave height, peak period, and equivalent simulation with empty basin are summarised in Table 3-11. All irregular wave tests were conducted with the PTO. Empty tank wave data at point (0;0;0) were used as input in the numerical model. Simulation DA038 was chosen for comparison with the numerical model because empty tank data are available for this simulation.

Parametric roll/pitch resonance does not seem to occur on the selected simulations. This can be assumed because of the extrema of pitch motions which are relatively small and have been summarised in Table 3-11.

TABLE 3-11 SUMMARY OF THE IRREGULAR WAVE EXPERIMENT (NOT INCLUDING SURVIVAL CASES). OWC SPAR BUOY ARRAY, CONFIGURATION D.

Simulation name	Hs (m)	Tp(s)	Equivalent simulation with empty basin
DA035	2.3	7.6	None
DA037	2.3	7.6	None
DA038	2.3	9.9	A034
DA039	2.3	12.2	A037

In addition, the pitch motion, shown in Figure 3-21 for a selected simulation, does not seem to grow. The assumption of small pitch motion for the linear theory is thus respected. In addition, the wave

amplitude was small compared to the body dimensions and to the wavelength. Finally, viscous effects on the floater are taken into account by additional damping which was calibrated on the single device.

These simulations should then be within numerical model capabilities.

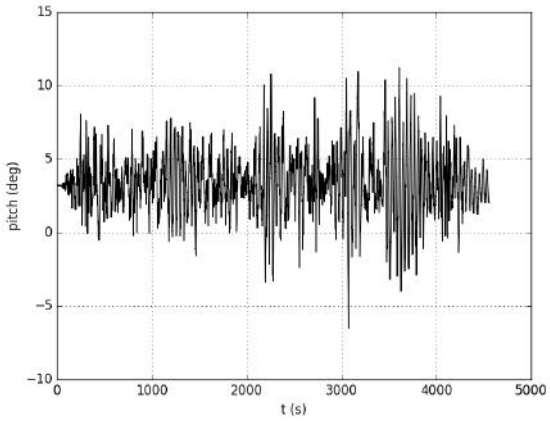

pitch buoy 2

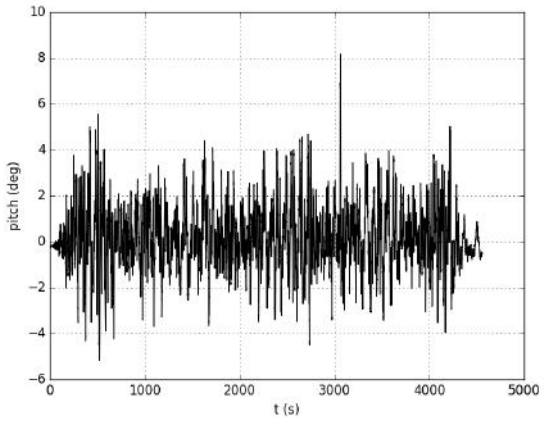

pitch buoy 3

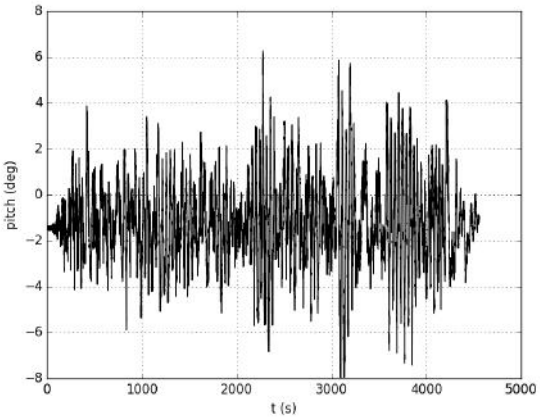

pitch buoy 4

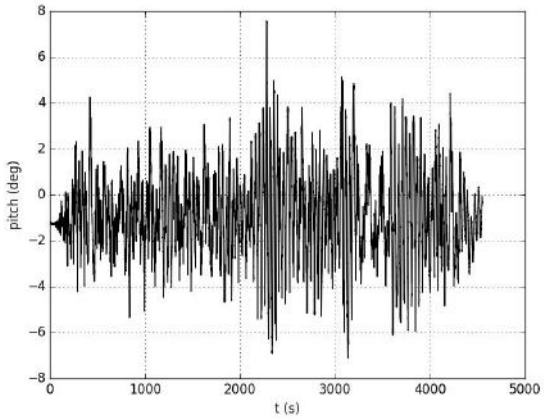

pitch buoy 5

FIGURE 3-21 TIME SERIES OF PITCH EXPERIMENTAL DATA FOR IRREGULAR WAVES FOR CASE DA038 (*HS* = 2.9 M AND *T* = 9.9 S). OWC SPAR BUOY ARRAY, CONFIGURATION D

Experimental and numerical time series of motion and mooring loads for an example moderate sea state are compared in Figure 3-22. Results indicate a fair modelling of motion and mooring loads. The mean X motion was different between the model and experiment: a slow drift motion, which was also observed for the single device can clearly be observed on all devices. The wave frequency motion looks similar. The Z motion was well replicated for all buoys, with a smaller amplitude for modelled data than for experimental data. Again, this was also observed for the single device. The pitch motions were not well replicated by the numerical model. This may be a consequence of the coupling between surge and pitch, with inaccuracies in surge. A shift was also observed in tensions and is likely to be caused by the inaccuracies in surge.

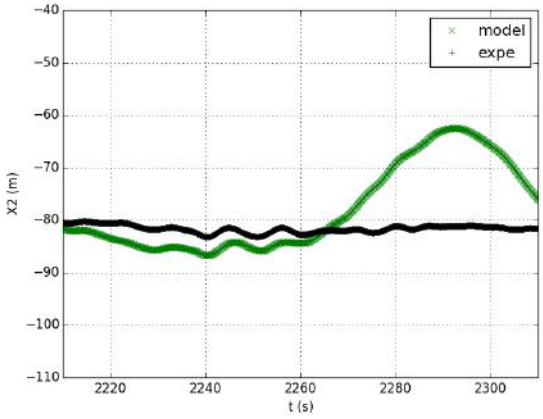

X2: surge buoy 2

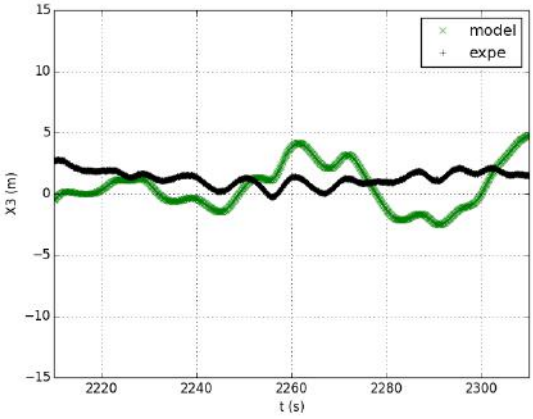

X3: surge buoy 3

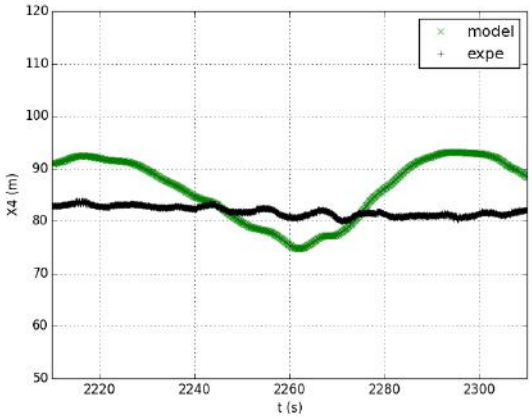

X4: surge buoy 4

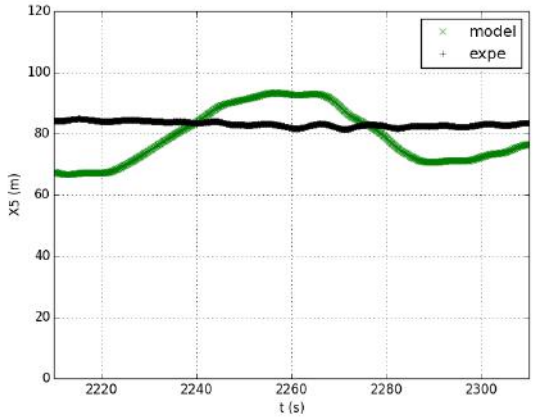

X5: surge buoy 5

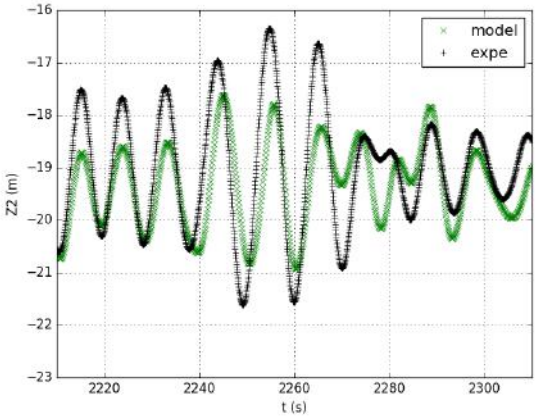

Z2: heave buoy 2

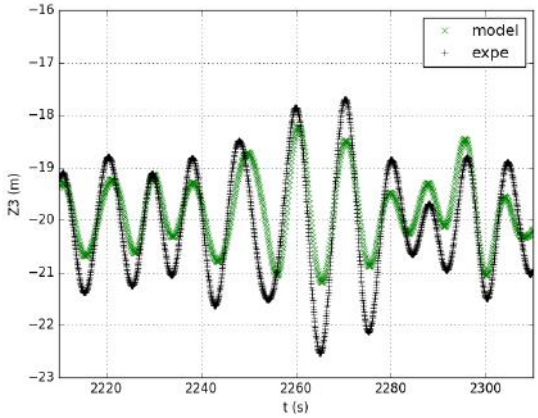

Z3: heave buoy 3

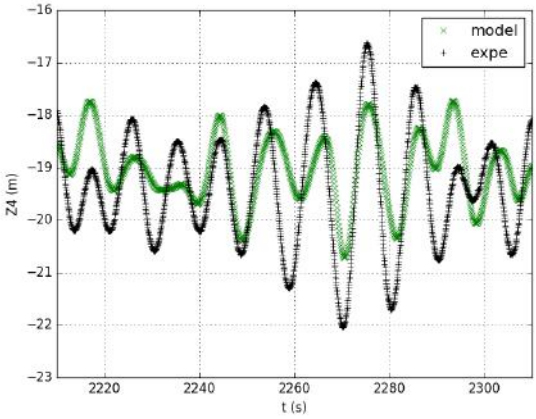

Z4: heave buoy 4

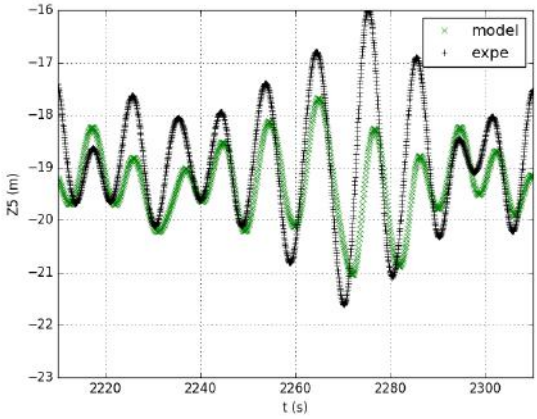

Z5: heave buoy 5

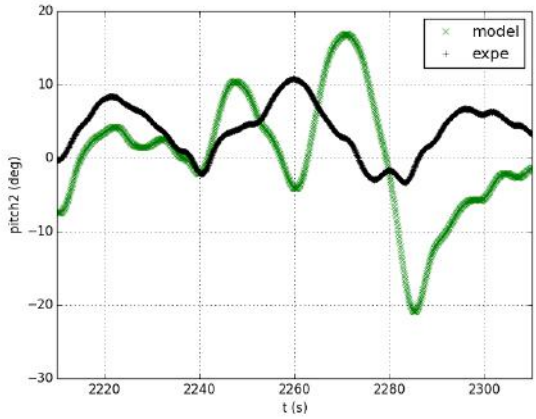

pitch buoy 2

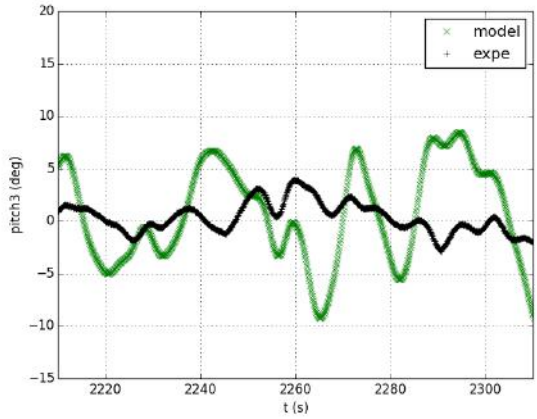

pitch buoy 3

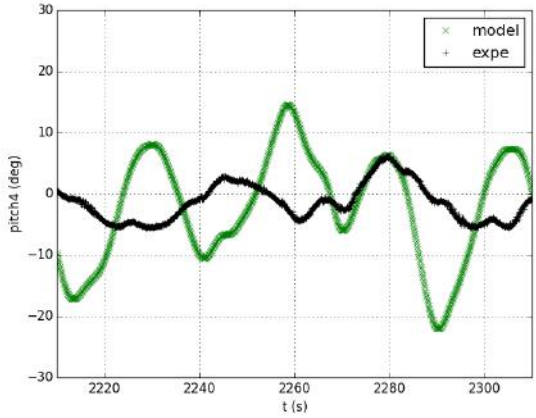

pitch buoy 4

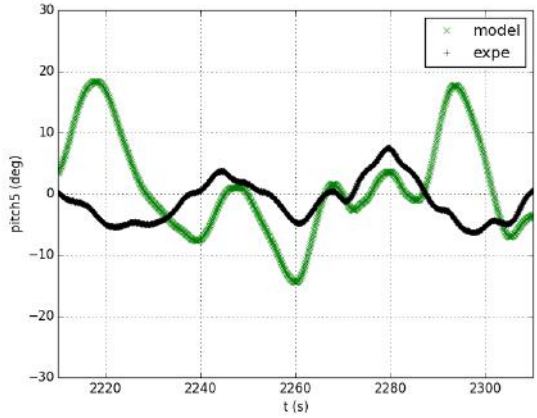

pitch buoy 5

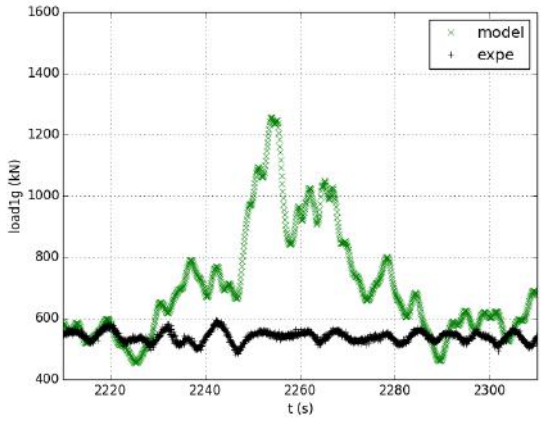

Load 1g

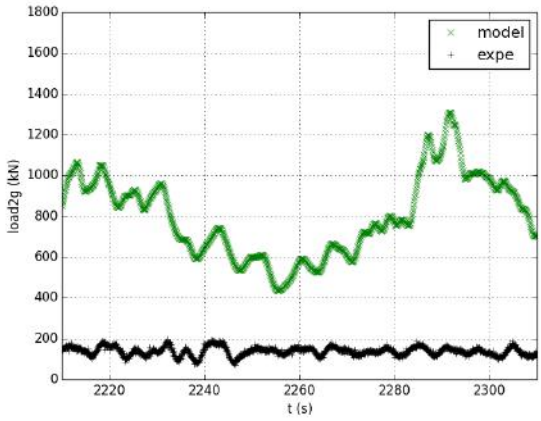

Load 2g

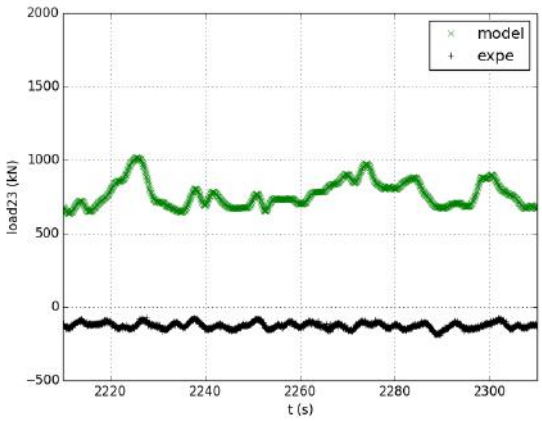

Load 23

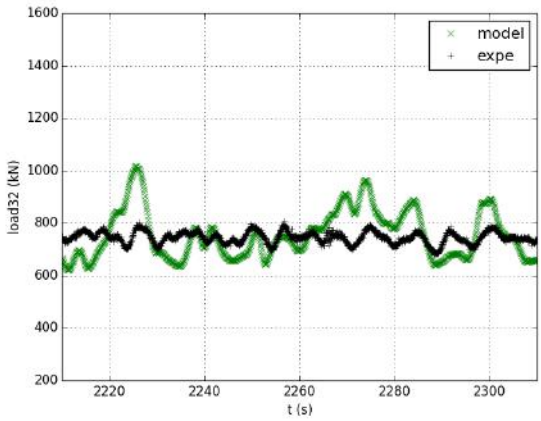

Load 32

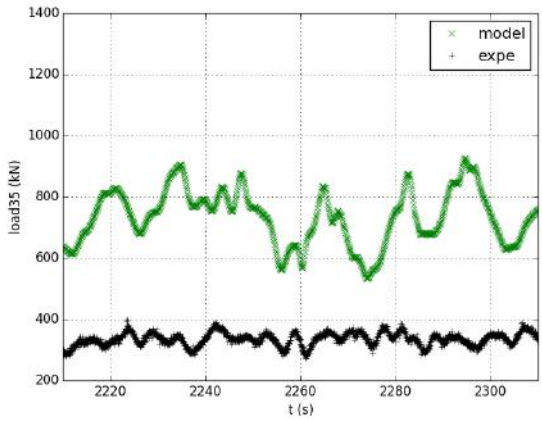

Load 35

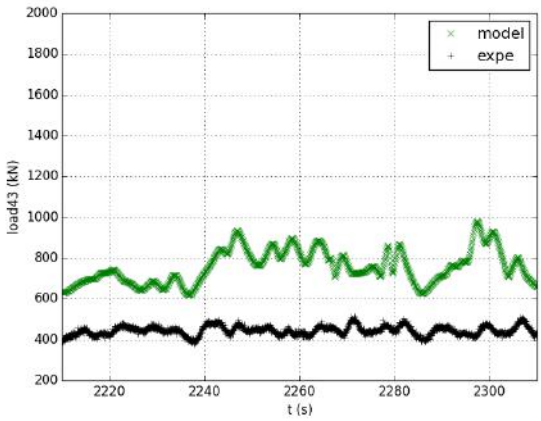

Load 43

FIGURE 3-22 EXAMPLE OF TIME SERIES OF EXPERIMENTAL AND MODELLED DATA FOR IRREGULAR WAVES FOR CASE DA038 (H_S = 2.9 M AND T = 9.9 S). OWC SPAR BUOY ARRAY, CONFIGURATION D

For comparisons of amplitudes and phases of the loads, data are plotted with their mean removed in Figure 3-23. Differences are observed between buoy 4 and 5, mainly in modelled data, which may be due to yaw leading to non-symmetric effects. Once their means were removed, a low frequency variation in the mooring loads was highlighted on modelled data which did not occur on experimental data. Wave frequency variations are similar in experiment and model.

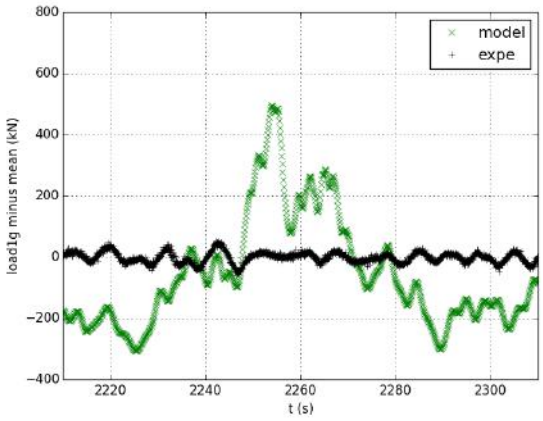

Load 1g

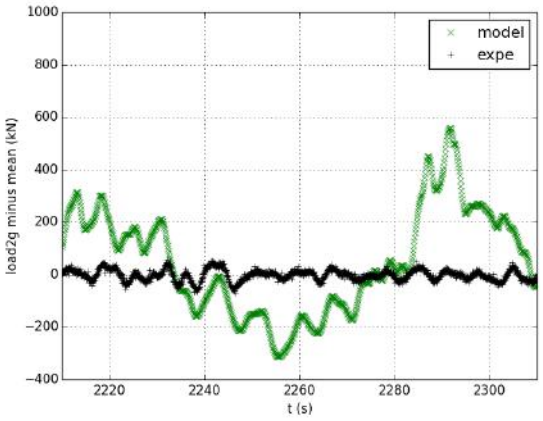

Load 2g

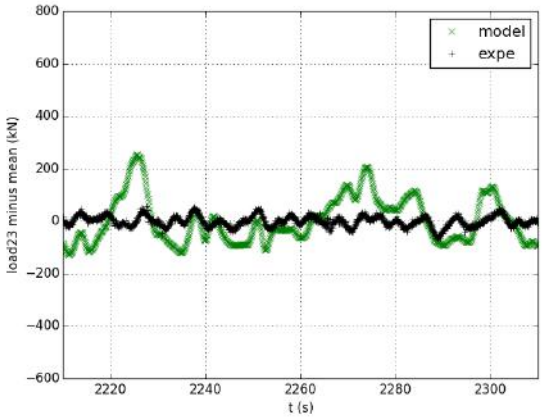

Load 23

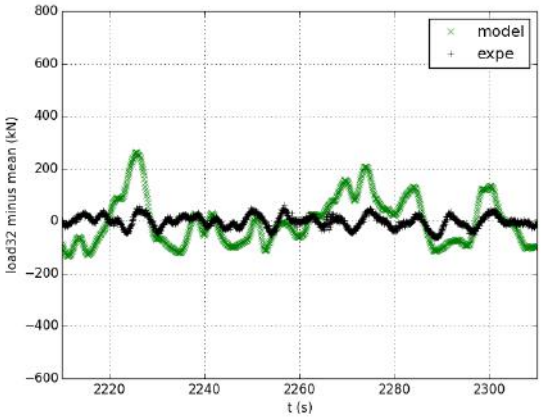

Load 32

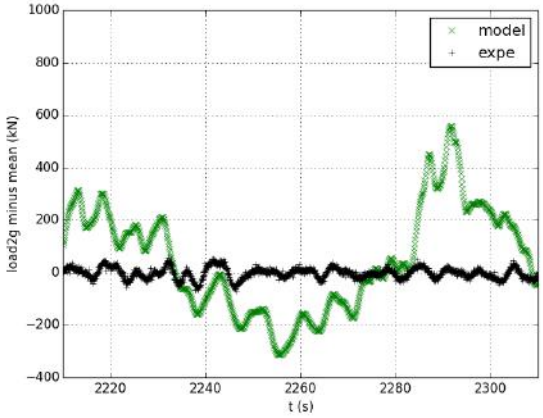

Load 35

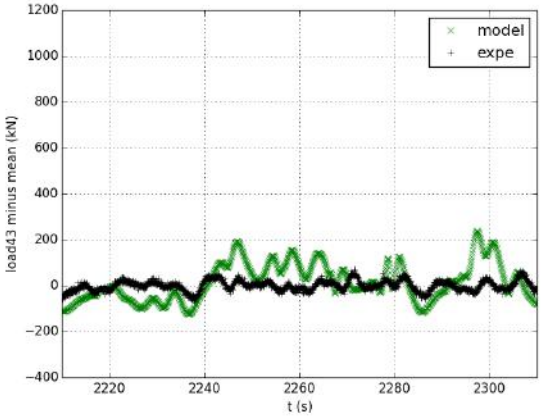

Load 43

FIGURE 3-23 EXAMPLE OF TIME SERIES OF EXPERIMENTAL AND MODELLED DATA FOR IRREGULAR WAVES FOR CASE DA038 (H_S = 2.9 M AND T = 9.9 S). MEAN VALUES HAVE BEEN REMOVED FOR COMPARISON OF AMPLITUDES AND PHASES. OWC SPAR BUOY ARRAY, CONFIGURATION D

In addition, calculations have been conducted without second order loads. Results are presented for surge motion in Figure 3-24 and for mooring loads in Figure 3-25. Results show a better agreement but still with a low frequency motion being modelled. There was no damping in the model on low frequency motions which may explain why low frequency motions can be so high in the model. These second order

loads may be common second order loads, which are nonlinear loads generated by the diffraction analysis.

The QTF data in a multibody group are correct for small surge motions. Once the buoys are far from their initial positions, the QTFs may not be representative anymore.

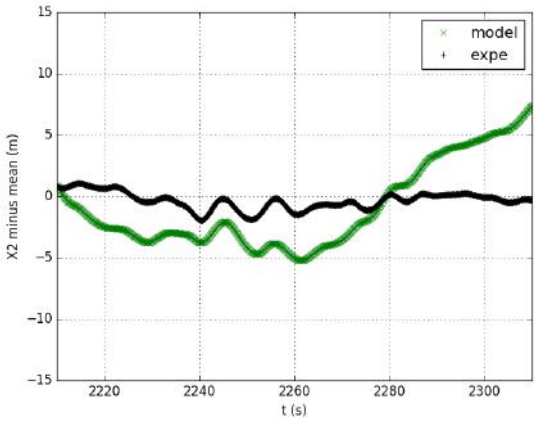

X2: surge buoy 2

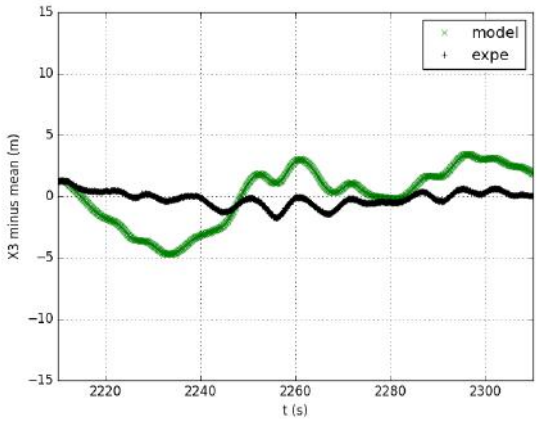

X3: surge buoy 3

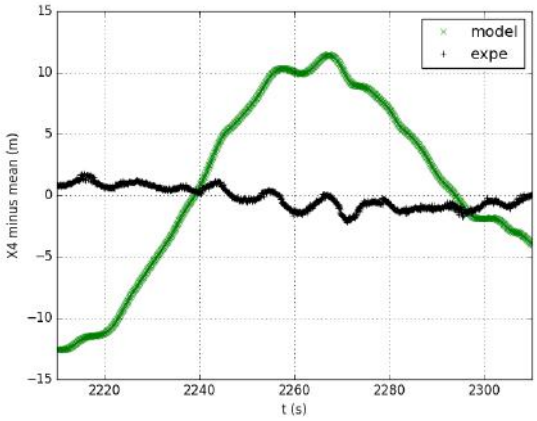

X4: surge buoy 4

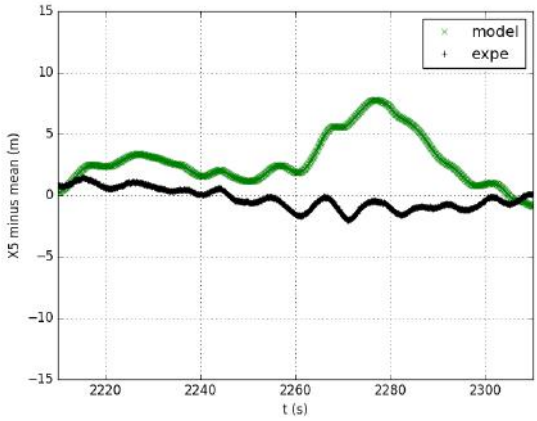

X5: surge buoy 5

FIGURE 3-24 EXAMPLE OF TIME SERIES OF EXPERIMENTAL AND MODELLED SURGE MOTION FOR IRREGULAR WAVES FOR CASE DA038 (H_S = 2.9 M AND T = 9.9 S). QTFS HAVE NOT BEEN INCLUDED IN THE CALCULATION. MEAN VALUES HAVE BEEN REMOVED FOR COMPARISON OF AMPLITUDES AND PHASES. OWC SPAR BUOY ARRAY, CONFIGURATION D

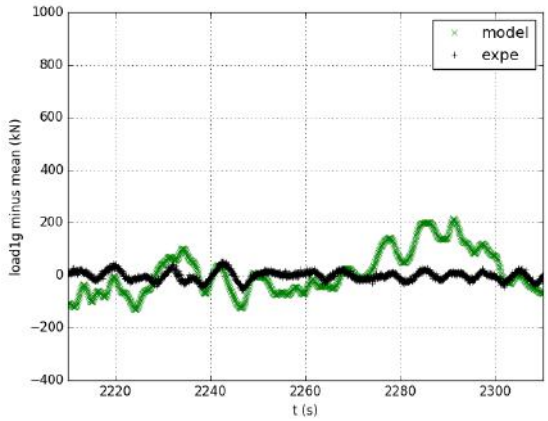

Load 1g

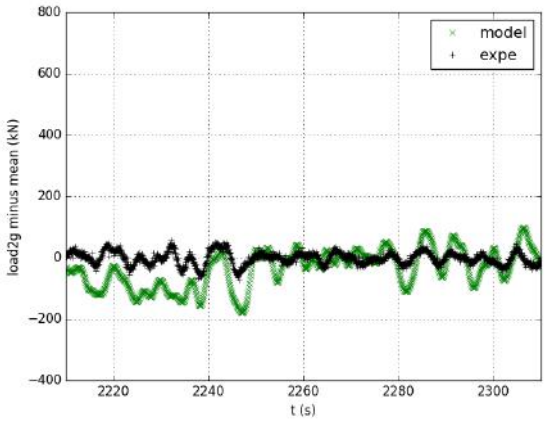

Load 2g

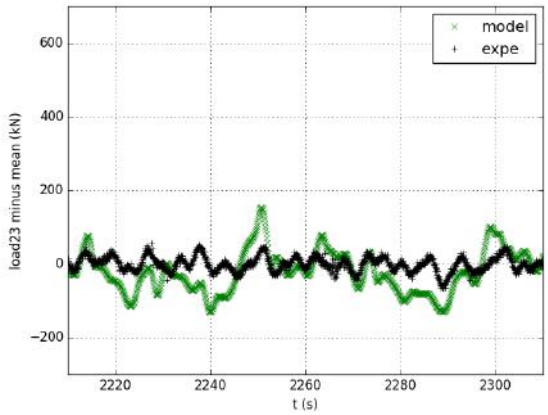

Load 23

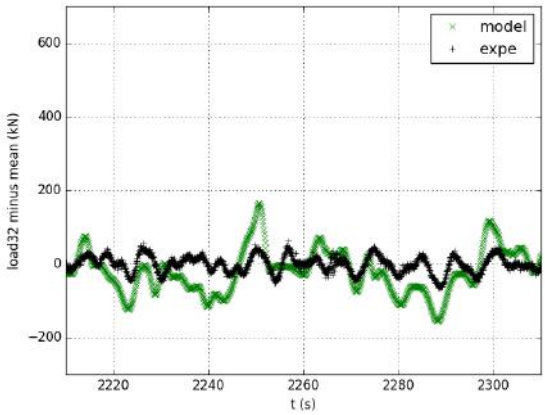

Load 32

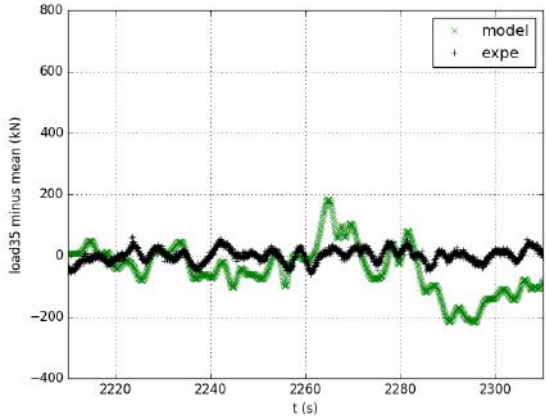

Load 35

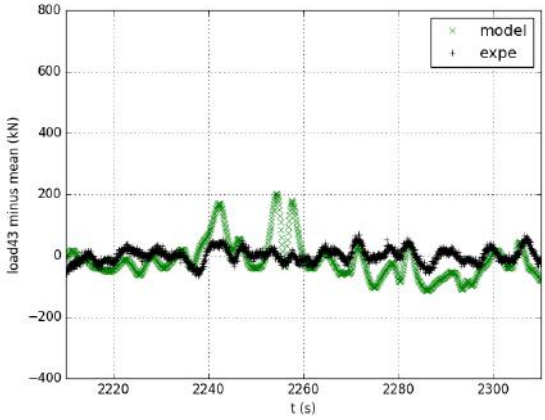

Load 43

FIGURE 3-25 EXAMPLE OF TIME SERIES OF EXPERIMENTAL AND MODELLED DATA FOR IRREGULAR WAVES FOR CASE DA038 (H_s = 2.9 M AND T = 9.9 S). QTFS HAVE NOT BEEN INCLUDED IN THE CALCULATION. MEAN VALUES HAVE BEEN REMOVED FOR COMPARISON OF AMPLITUDES AND PHASES. OWC SPAR BUOY ARRAY, CONFIGURATION D

Statistical results for this example are presented in Table 3-12. Experimental data are compared with numerical model with low frequency loads. Some statistical values of experimental positions could not be estimated because of a jump in values caused by an incorrect tracking by the Qualisys system. Results

indicated that the mean positions were estimated well by the model with less than 3% relative difference for surge and heave except for X3 (surge buoy 3) mean position. Relative differences were large for the mean pitch position because the mean angle was small (below 4°). However, absolute differences between mean pitch positions were small.

TABLE 3-12 COMPARISON OF STATISTICAL VALUES FOR CASE DA038 (H_s = 2.9 M AND T = 9.9 S): EXPERIMENTAL VALUE / MODEL VALUES WITHOUT QTF. FOR TENSIONS, MIN AND MAX ARE ASSESSED AROUND THEIR MEAN. OWC SPAR BUOY ARRAY, CONFIGURATION D. GREEN IS FOR RELATIVE DIFFERENCE BELOW 10 %, ORANGE BETWEEN 10 AND 100%, RED OVER 100%

m, deg or kN	Mean	Max	Min	Std
X2	-81.3/-79.7	-75.6/-56.1	-85.2/-101.2	1.1/6.6/
X3	1.5/0.3	5.9/10.3	-1.1/-10.1	0.8/3.3/
X4	82.1/81.3	87.7/109.2	78.2/64.2	1.2/6.6
X5	83.4/80	88.6/106.8	/	1.3/8.3
Z2	-19.1/-19.4	-15.6/-16.2	-22.3/-21.5	1/0.7
Z3	-20.1/-20	-17.1/-17.4	-23.0/-21.9	0.9/0.6
Z4	-19.4/-19.4	-16.4/-16.3	-22.4/-21.5	0.9/0.7
Z5	-18.9/-19.4	/	-21.9/-21.8	1/0.6
Pitch2	3.4/0.9	11.2/26.5	-6.5/-24.4/	2.1/6.5
Pitch3	0.2/0.2	8.2/14.3	-5.2/-17.9	1.5/4.6
Pitch4	-1.1/-0.6	6.3/23.2	-8/-30.6	1.9/6.1
Pitch5	-0.9/-0.4	7.6/28.9	-7.1/-25.7	1.9/6.3
Load 1g	129/721	113/897	-73/-278/	23/115
Load 2g	141/710	120/643	-102/-277	26/116
Load 23	-124/744	116/634	-96/-237	23/106
Load 32	598/733	140/634	-92/-257	26/110
Load 35	334/727	117/752	-89/-283	22/126
Load 43	445/739	128/795	-93/-273	25/107

Maximum and minimum values are well estimated for heave motions (less than 4% relative difference), and fairly well estimated for surge motion (less than 19% difference except for buoy 3). However, minimum and maximum values were not captured well by the numerical model for pitch motion. Maximum experimental pitch was equal to 11° which is relatively small and seems to indicate that parametric roll/pitch did not occur in this run.

Standard deviations of motions and loads were poorly evaluated by the numerical model except for heave motions, where the standard deviation was underestimated by approximately 3% by the numerical model.

The values for tension did not show a good agreement between experimental and modelled data. Experimental data may be shifted by an inaccurate calibration. That is why extrema values were compared once the mean was removed. Results indicated a large over-prediction by the numerical model (by 4 to 7 times). Model results were on the conservative side. The numerical model was not able to estimate accurately mooring line tensions. This is likely to be caused by the inaccurate modelling of

second order motion in surge. This inaccurate modelling is likely to be caused by inaccuracies in the physical mooring line length or clump weight, which are sensitive parameters in the numerical model as shown in 2.3.6 and 2.3.7.

To conclude, the numerical model seems to estimate the motion of the single buoy and the load in the mooring lines for the single device fairly well. However, the numerical model can only replicate simulations with moderate sea states, because of the instability in the numerical model of the buoy and the occurring of parametric roll/pitch in some sea states in the experiment.

For the flexible array configuration D, the numerical model replicates the heave motion well, but with too much damping in the numerical model. The surge motion is fairly well replicated. However, the pitch motion and mooring line loads are not estimated well. This is likely to be due to inaccuracies in second order load modelling and the lack of damping on these second order motions.

4 RIGID ARRAY: 5 DEVICES

In addition to the flexible moored array, a compact rigid array was conceived by IST. The model was manufactured at UoP for physical model testing as described in D6.3 [6] and D6.5 [7]. A numerical model of the five-device array with heave plate was created and is presented in this section.

4.1 Rigid array models

The design of the rigid array model base unit had the same geometry for each of the different configurations. The geometry and dimensions of the rigid array, and corresponding isolated device, are depicted in D6.3 [6]

Each single unit can be described was a floating column with inner OWCs. The five-device array has the same configuration as the flexible array, and includes a damping plate. More details about the construction of the device are given in D6.3 [6]. The most relevant dimensions are given in Table 4-1.

TABLE 4-1 PHYSICAL PROPERTIES OF THE FULL-SCALE RIGID ARRAY, IDEALISED 1:40 SCALE AND CONSTRUCTED MODELS.

	Isolated device with heave plate			Array with ballast plate		
Parameter	**Idealised 1:40 scale**	**CAD model**	**Physical model**	**Idealised 1:40 scale**	**CAD model**	**Physical model**
L [mm]	1450	1451	1457	1075(1)	1075	**1080** (mean value)
D [mm]	1200	1206(2)	1180(3)	837	840(2)	853 – 880(3)
Mass, M [kg]	44.7	42.3	43.6	231	232	**237** (05/10/2017) **243** (20/10/2017)(4)
I_{xx} [kg m^2]	2.81	2.79	n.d.	45	39.3	n.d.
CoB to MWL [mm](5)	565	568	n.d.	547	n.d.	n.d.
CoM to MWL [mm](6)	657	657	635	699	689	n.d.
Base of model to CoM [mm](7)	168	168	170	126	135	n.d.
Plate width [mm]	375	375	374.5	1061	1061	1060
Top of plate to fairleads [mm]	168	/	168(8)	168	/	168(8)

NOTES ON VALUES
Values in bold fall within of the range of values specified for that parameter
(1) L for array taken to base of devices since ballast plate dimensions were not achievable given materials being used
(2) CAD draught estimated using the enclosed volume of the model and the model mass
(3) Physical model draught values changed over time owing to water ingress, so are given for guidance only
(4) Extra mass was a result of trim weights and extra foam used to get desired draught despite water ingress
(5) MWL is in reference to the value of draught given in that column
(6) CoM values are taken from the base of the device not including any ballast plates
(7) Discrepancy in CAD model may be due to deviation in properties of fasteners
(8) Fairleads were rung nuts screwed onto an embedded thread centred on a point 168 mm from the base of the device

The design draught of the model was 825 mm measured from the top of the heave plate. The models took on water between the construction layers and so effectively the mass of the device increased over the testing period. On the first day, the draught was approximately 825 mm and it reached a maximum at the end of the experimental period of 872 mm. The Qualisys files should be consulted for the draught on any given day.

4.2 Moorings

Mooring lines were simple catenary (chains) anchored to the basin floor and attached to load cells on the fairleads. Fairleads were built into the surfaces of the corner devices in the array. The full-scale and 1:40-scale values of the mooring lines are given in Table 4-2.

TABLE 4-2 MOORING PROPERTIES FOR THE FULL-SCALE AND 1:40 SCALE CONDITIONS. RIGID ARRAY

	Full scale	1:40 scale idealised	1:40 scale measured
Number of lines	4	4	4
Anchor radius [m]	240	6	6
Length of chain [m]	232.35	5.81	5.81
Chain diameter [mm]	148	3.7	4
Chain wet weight per unit length [N/m]	4108.5	2.57	2.51

Based on measured values of mass per unit length and values of material and water density taken to be 2700 kg/m³ and 1000 kg/m³ respectively.

4.3 Experimental set-up

4.3.1 Layout

The devices were moored in each configuration so that the centre of the array was coincident with the centre of the UoP Ocean Basin. Table 4-3 gives the line lengths and anchor positions. The body axes of the array as defined in Qualisys are defined in Figure 4-1. The device was then moved with an angle of 45° but this position is not studied in this document.

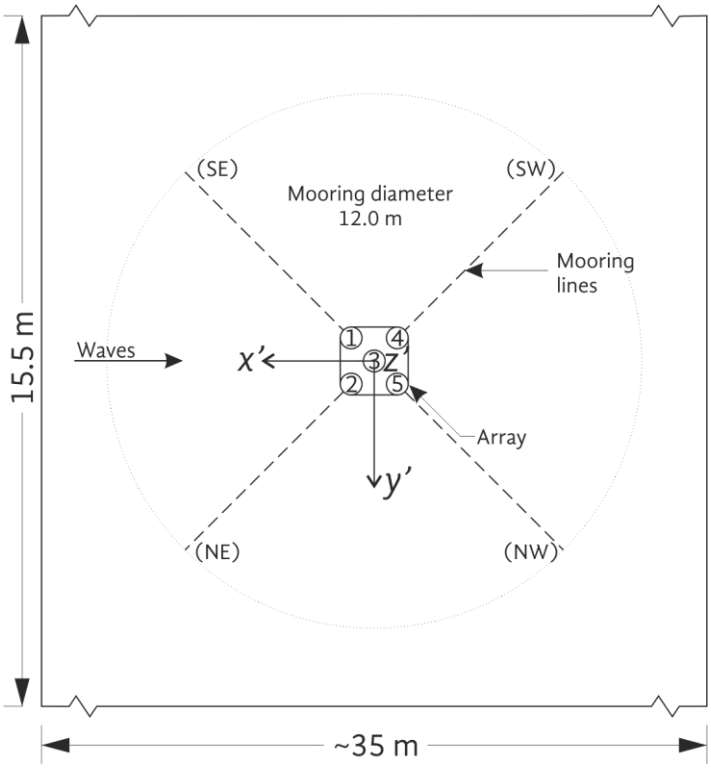

FIGURE 4-1 BASIN SET-UP FOR THE RIGID ARRAY SHOWING THE DEVICE BODY AXES (X', Y', Z'). X' AXIS IS OPPOSITE TO THE SURGE DIRECTION, Y' OPPOSITE TO THE SWAY DIRECTION. Z AXIS UPWARDS IS THE HEAVE DIRECTION

In addition to measuring the length, which was dependent on chain tension, the mass of the mooring lines was taken to ensure consistency between the lines. This is given in Table 4-3 along with the anchor positions of each line.

TABLE 4-3 POSITIONS OF THE ANCHORS WITH RESPECT TO THE BODY AXES OF THE RIGID ARRAY

Device	Line #	Length [m]	Chain mass [kg]	Anchor position	
				X' [m]	*Y'* [m]
4	SW	5.812	1.699	-6.000	-6.000
5	NW	5.806	1.694	-6.000	6.000
1	SE	5.804	1.695	6.000	-6.000
2	NE	5.806	1.693	6.000	6.000

Wave gauges were positioned around the basin in similar positions to those for the OWC spar buoy experiments, as shown in Figure 4-2 with the values given in the Appendix.

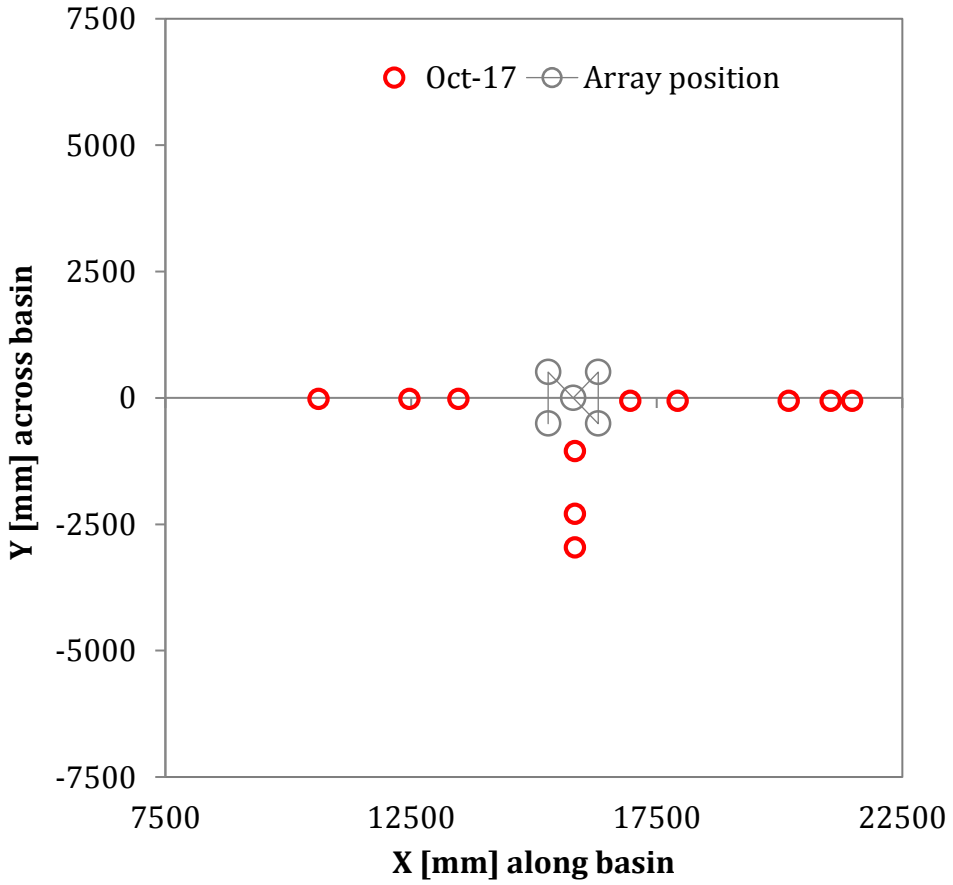

FIGURE 4-2 POSITIONS OF WAVE GAUGES RELATIVE TO THE ARRAY FOR THE RIGID ARRAY EXPERIMENTS

4.3.2 Input wave conditions

Waves were the same as for the OWC spar buoy experiments but with a run time of the survivability waves extended to 31m18s (201m7s full scale).

4.3.3 Data acquisition

Similar processes for data acquisition were used for the rigid array experiments as for the OWC spar buoy experiments, although there were a few notable differences:

- Only 3 cameras were available for filming
- Data acquisition fully synchronised with the wave makers so all recordings finished 30 s after the run
- Wave gauges inside the OWCs (manual calibration)

The wave gauge layout was chosen to be simpler than for the flexible array. The following layout was decided:

- 3 gauges in front of the array (on centreline);
- 5 behind (on centre line);
- 3 out to the side in line with the central device (to examine possible radiation/reflection from the walls).

Load cells were positioned between each mooring line and fairlead, with designations given in Table 4-4. Still water load readings are directly influenced by the draught of the model since this affects the amount of chain lifted and hence the still water reading. Since the draught changed between days, the still water reading should be taken from specific still water reading files or from the beginning of each experiment file.

TABLE 4-4 LOAD CELL DESIGNATIONS FOR THE RIGID ARRAY EXPERIMENTS

Line number	Load cell number	No load reading [N]
SW	698 315	-0.092
NW	698 317	+0.412
SE	698 312	-0.069
NE	698 313	-0.674

4.4 Description of the numerical model

The numerical model was based on linear wave theory and small amplitude motions. The hydrodynamic databases, including radiation and diffraction coefficients, were computed using WAMIT. The response amplitude operators (RAOs) of the floating structure are also computed in WAMIT.

4.4.1 Hydrodynamic databases

The full-scale array presented in D6.3 [6] was considered. For the case under consideration the columns were separated 21 m in the radial direction from the vertical axis of the central column to the vertical axis of each of the 'peripheral' columns (Configuration D). For the hydrodynamic databases

computation, the geometry was discretized into several 'low-order' plane panels. The array had a square plate at the bottom with a side dimension of 43.668 m. The plate was approximated as a thin surface with an offset of 1 m from the plane formed by the bottom of the columns. The system simulated here considers three degrees of freedom (DoF) for the physical structure, named, surge, heave and pitch, modes 1, 3, and 5, respectively, identified in the attached WAMIT output files.

For the simulations, the incident wave angle was set to zero degrees, so the waves travel in the *X*-axis direction. Due to the symmetry of the problem, the 3 DoFs are sufficient to describe the whole system. Furthermore, the device has five freely moving oscillating water columns (OWCs), where the pressure in the inner free surface is equal to the atmosphere. No oscillation modes were used to define the inner free surface motions. In total, the system was analysed with 3 DoFs, as presented in Table 4-5.

TABLE 4-5 CORRESPONDENCE OF OSCILLATING MODES IN WAMIT FOR THE RIGID ARRAY

Mode description	WAMIT mode
Surge of rigid structure	1
Heave of rigid structure	3
Pitch of rigid structure	5

The WAMIT computations were carried out for a full-scale device. The hydrodynamic coefficients are presented in their dimensionless form, using a characteristic length (ULEN) of 12 m, a water density (RHO) of 1025 kg/m^3 and an acceleration due to gravity (GRAV) of 9.80665 m/s^2. For the dimensional form of WAMIT output quantities, please refer to the expressions presented in sections 4.2, 4.3 and 4.4 of the WAMIT manual for versions 6.4, 6.4PC, 6.3S, 6.3S-PC. The outputs are displayed in output files with the extension '.1', for the case of the radiation coefficients, and files '.2' and '.3' for the case of the diffraction coefficients.

4.4.2 Calculation of the response amplitude operators

The displacement response amplitude operators (RAOs) were computed using WAMIT (output file .4). As stated before, the OWC free surfaces were subject to uniform atmospheric pressure. The turbine damping effect was neglected. The stiffness of the mooring lines was considered through the use of an external stiffness matrix (in the .FRC file). The inertia of the system was defined through an external inertia matrix. A summary of the values used for the construction of the external inertia, damping and stiffness matrices is presented in Table 4-6.

TABLE 4-6 PARAMETERS USED FOR THE CALCULATION OF THE RESPONSE AMPLITUDE OPERATORS OF THE RIGID ARRAY (WAMIT)

Parameter	Value
Mass of device [kg]	18.989×10^{6}
Displaced water volume [m^3]	18.526×10^{3}
Moment of inertia at *X*-axis in the output coord. system [kg m^2]	19321.52×10^{6}
Moment of inertia at *Z*-axis in the output coord. system [kg m^2]	6406.86×10^{6}
Centre of gravity *Z*-coordinate [m]	-27.95
Centre of buoyancy *Z*-coordinate [m]	-24.33
Stiffness of mooring system in surge [N/m]	74.68×10^{3}
Stiffness of mooring system in yaw [N m/rad]	42.83×10^{6}
Hydrostatic stiffness of structure in heave [N/m]	686.837×10^{3}
Hydrostatic stiffness of structure in pitch/roll [N m/rad]	801.976×10^{6}
Hydrostatic stiffness of each OWC in heave [N/m]	530.838×10^{3}

The plot of the RAOs as a function of the wave period is shown in Figure 4-3. The stiffness coefficients of the mooring system in surge and yaw were determined though a quasi-static inelastic catenary chain model. The physical characteristics of the device were determined based on the original drawing.

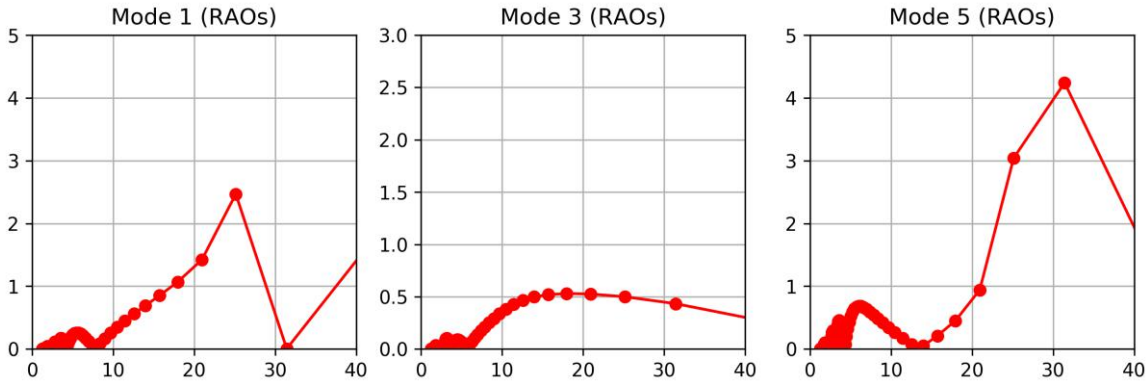

FIGURE 4-3 RESPONSE AMPLITUDE OPERATORS OF THE RIGID ARRAY COMPUTED IN WAMIT AS A FUNCTION OF THE FULL-SCALE WAVE PERIOD [S]. MODE 5 (PITCH) IS PRESENTED IN DEG/M, WHERE THE REFERENCE IS THE INCIDENT WAVE HEIGHT.

The computation of the hydrostatic coefficients in WAMIT was made through the numerical integration of the geometry discretised volumes. However, some approximations were done in this model, namely:

- damping plate modelled as a zero-thickness plate
- tubes connecting the structure not considered

OrcaFlex model is shown in Figure 4-4.

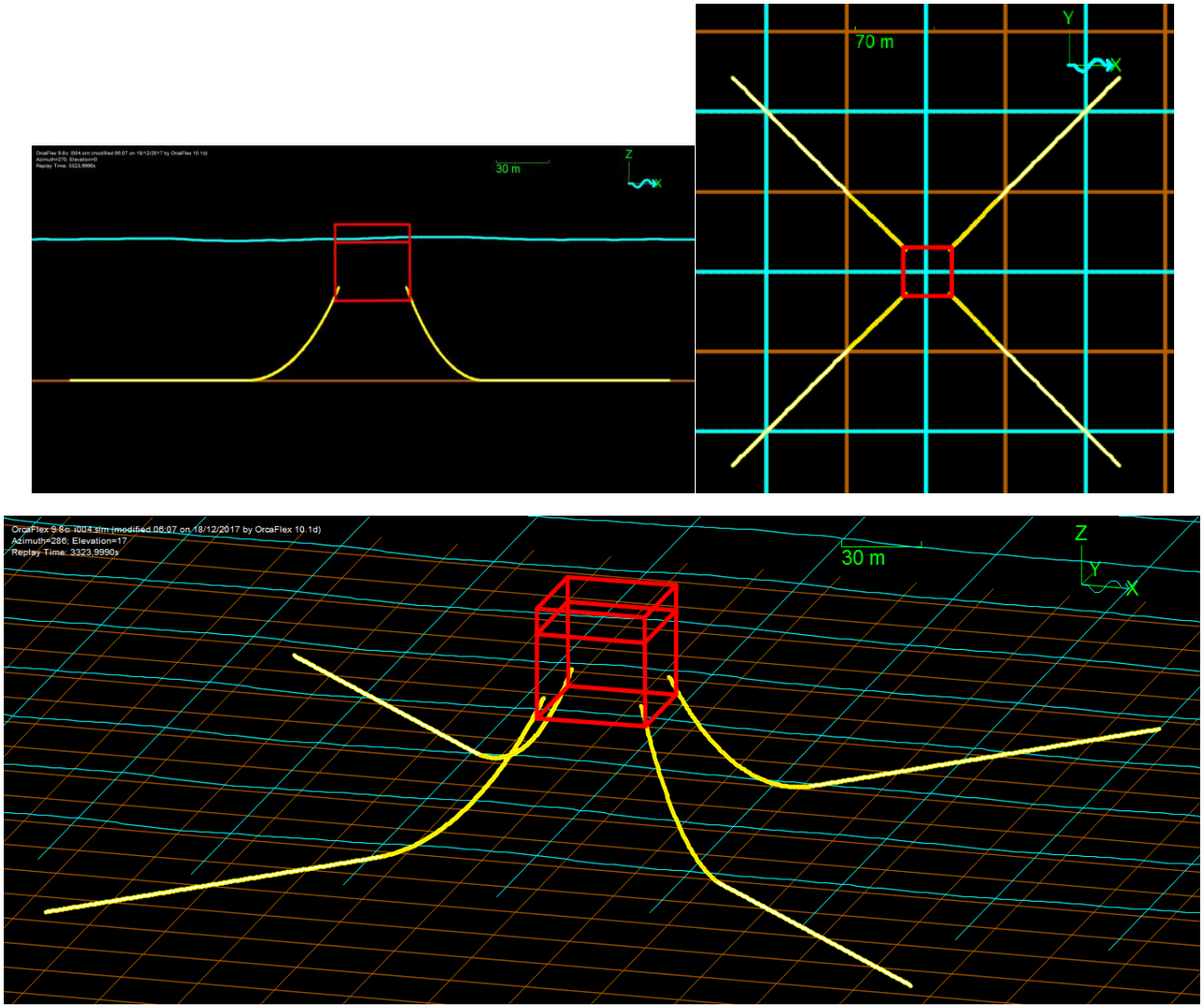

FIGURE 4-4 ORCAFLEX MODEL OF THE RIGID ARRAY WITH 5 DEVICES

4.5 Results

All results are given at full scale. For simplicity, the ideal system was modelled, with the target values for masses or lengths for example. However, the measured line length was used for more accuracy. All tests were conducted with the PTO and with the mooring system.

4.5.1 Water ingress

Water ingress was observed. Trim weights were removed and foam was added to counter this. This resulted in differences every day in the position of the target CoM. In addition, the global origin was set on the first day of experiments at the still water line but any variation in the water depth (water behind the paddles, evaporation, automatic refilling of the tank… etc) will change this.

Variability in the results, besides observational error, can be attributed to water ingress into the model. This caused a change in the density of the model and resulted in a change in the draught. Physical modelling experiments were conducted over a two-week period and the total draught change during this period was 27 mm. With the data obtained, it was not possible to quantify the influence of the

change of draught but typically, when the model was lower in the water, the heave amplitudes lower. Figure 4 6 shows the de-trended motion in the Z-direction of the array in regular waves. The periods of the motions, and indeed their location in the time series, were nearly identical in the repeated experiments. This was apparent even at the end of a time series in which all variables were measured for an additional 30 s after the wave paddles were stopped.

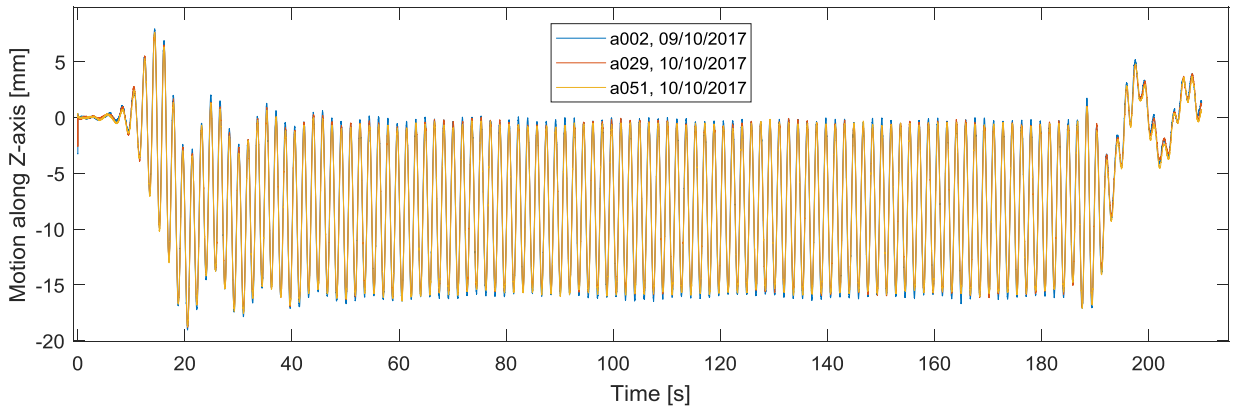

FIGURE 4-5 DE-TRENDED HEAVE MOTION OF THE ARRAY IN SMALL REGULAR WAVES: H = 0.05 M (2 M FULL-SCALE), T = 1.74 S (11.0 S FULL-SCALE)

4.5.2 Statics tests

Qualisys data were not available for a still case, so the values at the beginning of a regular wave test for the short waves were used instead.

The name of the simulation used for this analysis are summarised in Table 4-7. The 20 first seconds (model scale) were used for this analysis.

TABLE 4-7 SUMMARY OF THE STATICS TESTS EXPERIMENT FOR THE RIGID ARRAY

Simulation name	H (m)	T (s)
A019	1	6.32

4.5.2.1 Position of the buoy in the other DOFs

Statics positions were observed in the other DOFs

Statics values for angles were below 1°. Measured static X and Y positions are in the order of 2 m and 1 m respectively, which was acceptable compared to the dimensions of the buoy.

TABLE 4-8 EXPERIMENTAL AND MODELLED VALUES FOR THE RIGID ARRAY FOR THE STATICS VALUES OF X AND Y (IN M) AND HEEL AND TRIM ANGLES (IN DEG)

		Experimental (Qualisys)	Numerical model
With mooring	**X**	1.8	0.1
	Y	0.7	0.0
	Heel	0.8	0.0
	Trim	0.5	0.0
	Heading	0.5	0.0

4.5.2.2 Mooring line tensions

The experimental and modelled mooring line tensions are compared in Table 4-9. The sensor dry offsets were provided and were used for this comparison (Table 4-4).

Good agreement was found between the experimental and the numerical values with less than 18% difference except for line NE. At equilibrium, the mooring loads should be similar in the 4 lines. Differences can be caused by the slightly off-centred buoy position –see Table 4-8) or by inaccuracies in the load cell calibration.

TABLE 4-9 EXPERIMENTAL AND MODELLED STATICS VALUES FOR THE RIGID ARRAY FOR THE MOORING LINE TENSION (IN N)

Line	Experimental	Numerical model	Relative difference
NE	3.41E+05	4.06E+05	-19%
SE	4.00E+05	4.06E+05	-1%
SW	3.89E+05	4.06E+05	-4%
NW	4.40E+05	4.06E+05	8%

4.5.2.3 Summary

A good agreement was found for the statics position and mooring line tension. The most noticeable point is that water ingress was observed.

4.5.3 Pull-out tests

Pull-out tests were not conducted.

4.5.4 Decay tests

Decay tests were not conducted.

4.5.5 Regular wave tests

Experiments were conducted for two wave heights *H*: 2 m and 4 m and a wide range of periods, between 6 s and 22 s. In addition, several additional experiments were run for *T* equal to 11.00 s and *H* varying between 1 m and 8 m. Experimental results show limited differences between results with different wave heights, therefore only the results with H equal to 2 m are used in this section. The experiment names, wave height and wave periods are summarised in Table 4-10 and Figure 4-6.

The rigid array was designed to have a surge, heave and pitch natural periods above the common wave periods. The OWCs have a natural period of 14.6 s.

TABLE 4-10 SUMMARY OF THE REGULAR WAVE EXPERIMENT AND NUMERICAL MODEL STABILITY OF THE RIGID ARRAY WITH H = 2 M

Simulation name	H (m)	T(s)
a019	2	6.3
a013	2	6.7
a022	2	7.0
a015	2	7.4
a017, a036, a050	2	7.9
a012, a032, a047	2	8.4
a014, a034, a058	2	8.7
a005, a025, a056	2	9.0
a010, a030, a059	2	9.4
a011, a038, a055	2	9.7
a008, a023, a048	2	9.9
a020, a031, a049	2	10.0
a016, a028, a046	2	10.2
a018, a024, a057	2	10.5
a033, a042, a052	2	10.7
a039, a040, a060	2	10.9
a002, a029	2	11.0
a035, a043, a053	2	11.1
a037, a041, a044	2	11.3
a009, a026, a054	2	11.5
a006, a027, a045	2	12.0
a004	2	12.6
a003	2	14.1
a021	2	15.8
a007	2	18.1
a001	2	21.1

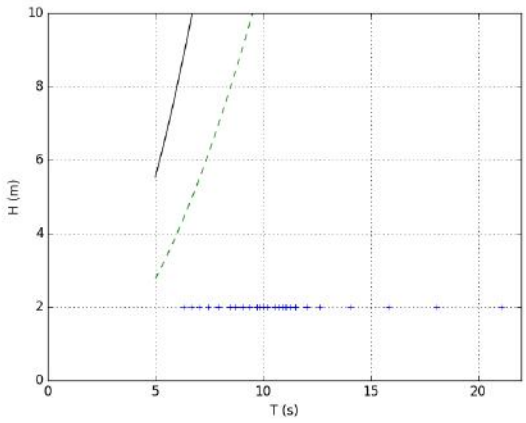

FIGURE 4-6 TESTED REGULAR WAVES (AIRY) FOR THE RIGID ARRAY WITH H = 2 M. GREEN DOTTED LINE: LIMIT OF LINEAR WAVES; BLACK LINE: WAVE BREAKING LIMIT

The RAOs for the surge, heave and pitch are shown in Figure 4-7 (H = 2 m).

The surge RAOs generally increased with period with experimental values up to 1.5 m/m. The experimental and modelled surge RAOS compared well. The numerical model underestimated the RAOs for periods between 11 s and 15 s.

The heave RAOs increased for periods below 12 s with experimental values up to 0.85 m/m. The experimental and model behaviour was similar however the modelled RAOs were higher than the experimental RAOs for periods below 11 s and smaller for periods over 11 s. The PTOs were not modelled which may explain the difference in behaviour between the experiment and numerical model.

The experimental pitch RAO increased for periods below 11 s, then decreased for periods below 16 s and increased again. Experimental values remained small with a maximum at 1.4°/m. The model RAOs did not compare very well but remained small with a maximum at 0.3°/m.

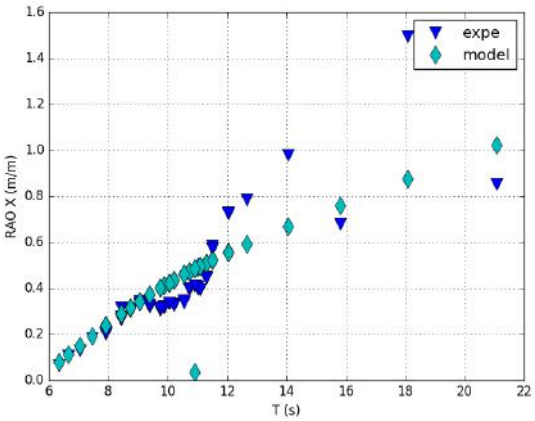

X: surge

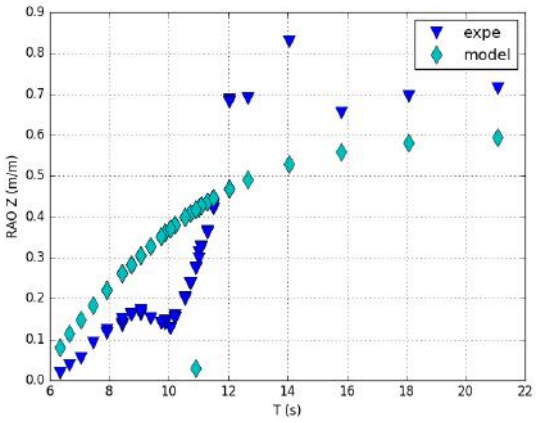

Z: heave

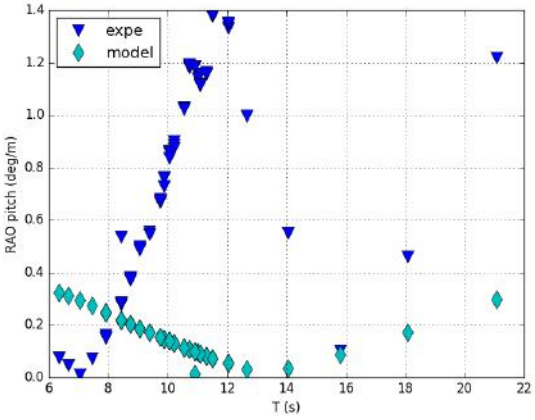

pitch

FIGURE 4-7 EXPERIMENTAL AND MODELLED DISPLACEMENT RAOS OF THE RIGID ARRAY IN THE 3 MAIN DOFS, *H* = 2 M

The displacements phases for surge, heave and pitch are shown in Figure 4-8 (H = 2 m)

The surge phase varied in the experiment but was more stable in the numerical model. A 90° to 180° lag was observed between the experimental and the numerical model values.

The experimental heave phase varied between 10 s and 13 s. The experimental and model behaviour was generally similar. The PTOs were not modelled which may explain the difference in behaviour between the experiment and numerical model.

The pitch phase was stable in the numerical model for periods below 12 s and for periods over 16 s. It increased in the experiment for periods below 11 s.

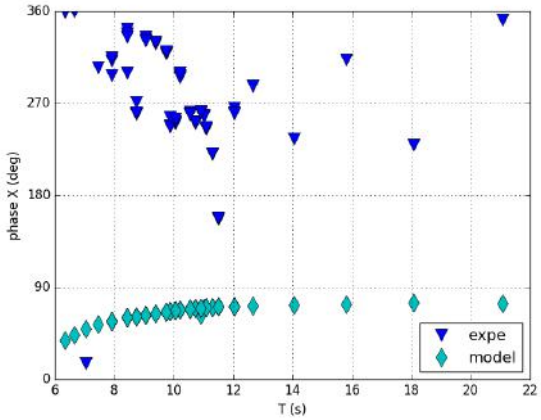

X: surge

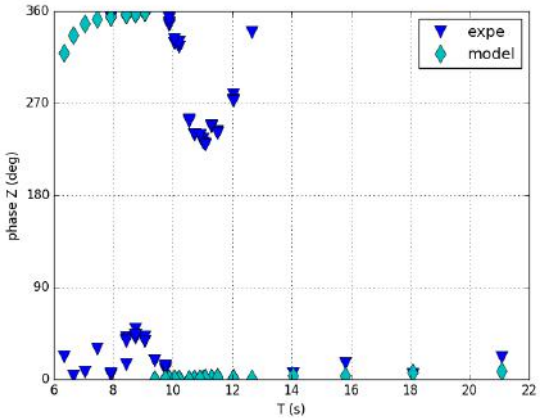

Z: heave

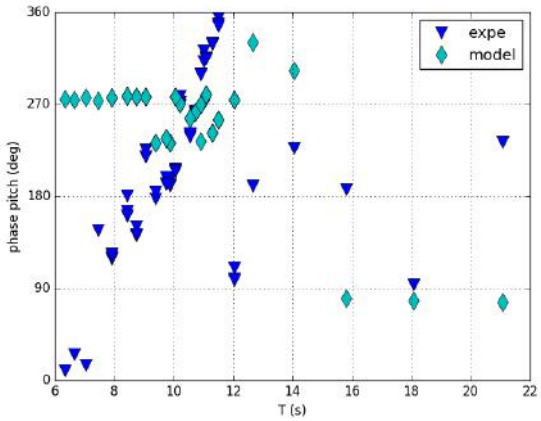

pitch

FIGURE 4-8 EXPERIMENTAL AND MODELLED DISPLACEMENT PHASES OF THE RIGID ARRAY IN THE THREE MAIN DOFS, *H* = 2 M

The mean drift shown in Figure 4-9 varied between 0.5 m and 2 m for the experimental values and between 0 m and 0.25 m for the modelled values. The modelled values did not include second order loads (QTFs) which explains why these values are lower. In addition, the statics position was different (Table 4-8).

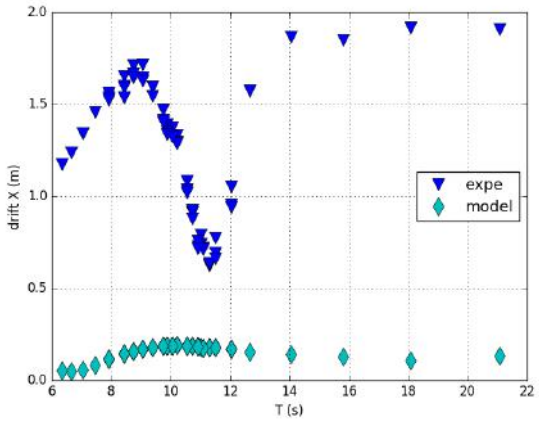

FIGURE 4-9 EXPERIMENTAL AND MODEL DRIFT OF THE RIGID ARRAY IN THE SURGE DIRECTION, H = 2 M

The experimental and modelled mooring load RAOs are given in Figure 4-10 for H = 2 m. The results are similar in the front lines and in the back lines and do not differ strongly between the numerical model and the experiment. The RAOs are stable for periods below 12 s and increased for higher periods.

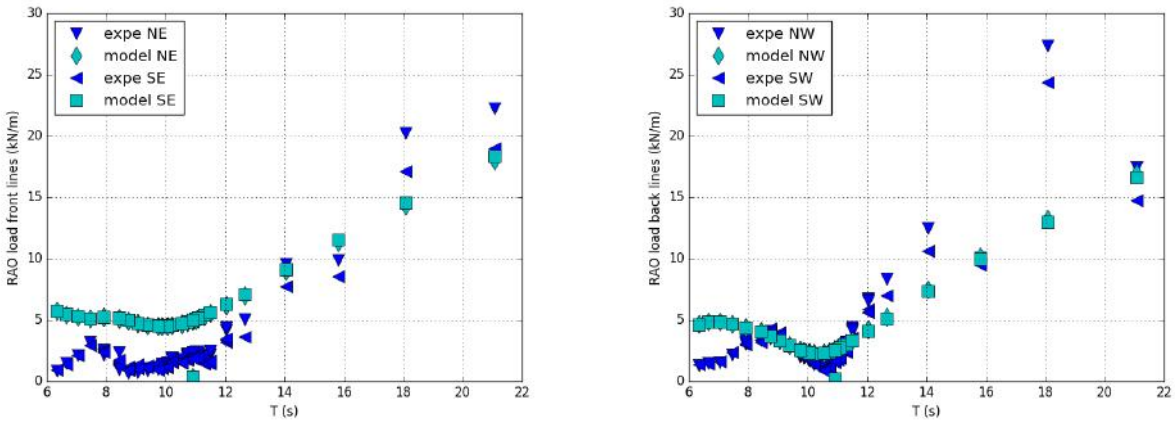

NE and SE (front) SW and NW (back)

FIGURE 4-10 EXPERIMENTAL AND MODELLED MOORING LINE RAOS OF THE RIGID ARRAY, H = 2 M

The experimental and modelled mooring line load phases are given in Figure 4-11 for H = 2 m. As with the RAOs, the phases were similar in the front lines in the back lines and did not differ strongly between the numerical model and the experiment. The phases were stable for periods below 8 s or over 14 s and varied strongly in between.

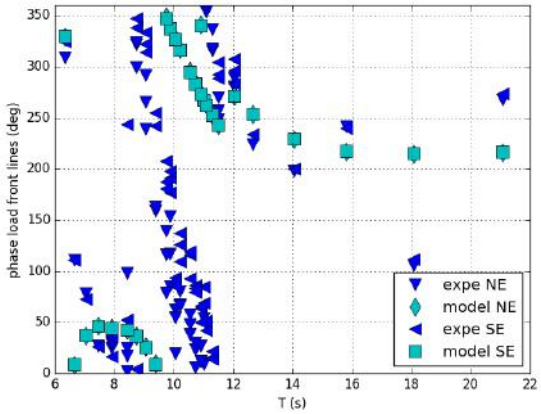

NE and SE (front)

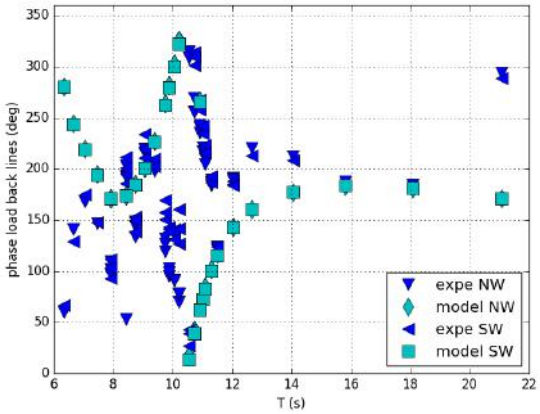

SW and NW (back)

FIGURE 4-11 EXPERIMENTAL AND MODELLED MOORING LINE PHASES OF THE RIGID ARRAY, H = 2 M

The time series describing the waves, motions and loads for H = 2 m and T = 6.3 s are given in Figure 4-12. The time series showed a linear behaviour (sinusoids are observed). Mean drift is observed for the experimental surge motion and is not observed in the model which does not include second order loads. Load measurements were noisy because the variation in load was small (20 kN peak to peak). Surge and pitch occurred together, slightly before the wave. Experimental heave was very small (<0.1 m).

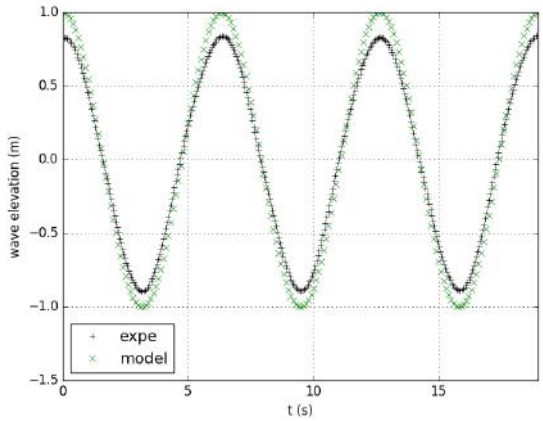

Waves

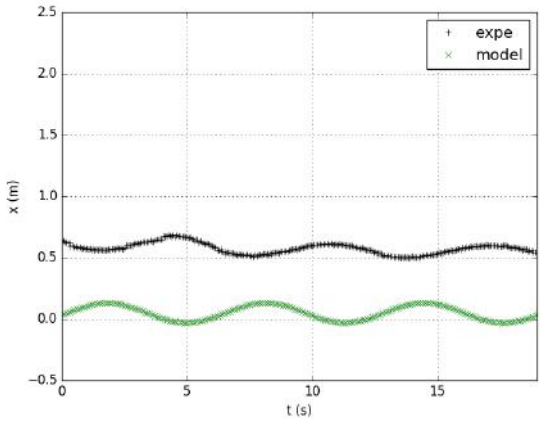

X: Surge

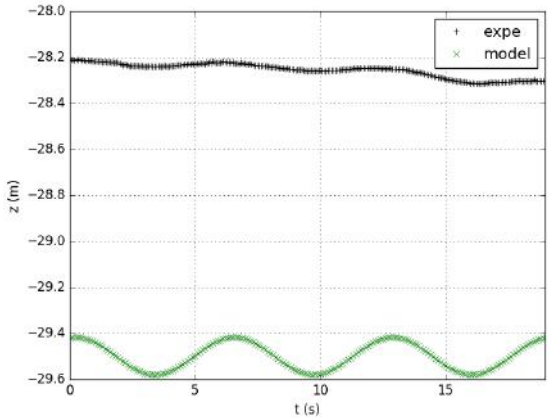

Z: Heave

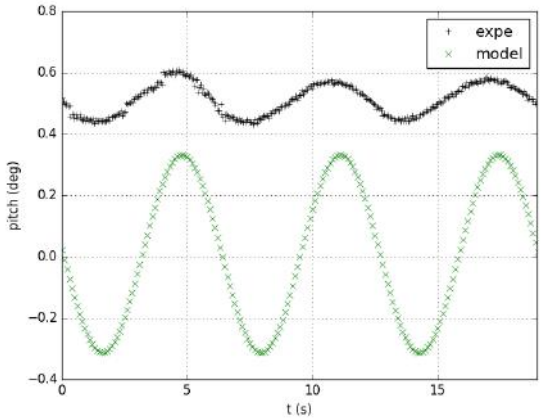

Pitch

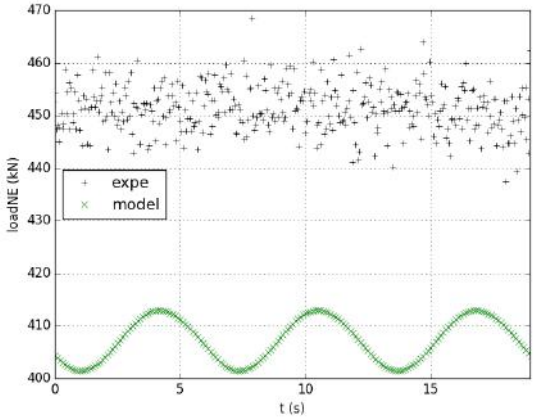

NE (front)

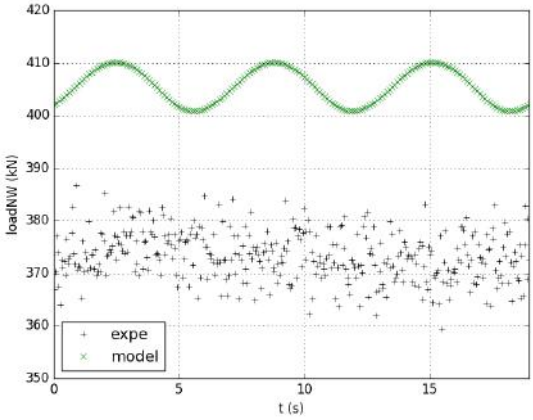

NW (back)

FIGURE 4-12 EXAMPLE OF TIME SERIES OF REGULAR WAVES OF THE RIGID ARRAY FOR CASE A019 (*H* = 2 M AND *T* = 6.3 S)

The time series describing the waves, motions and loads for H = 2 m and T = 14.1 s are given in Figure 4-13. The results show a linear behaviour. Surge and pitch occurred together, slightly before the wave and heave at the same time than the wave. Load measurements were noisy but a sinusoidal behaviour could be observed. The phase was different between the experimental and numerical mooring loads.

This can be explained by a difference in mean drift between experimental and numerical data leading to a difference in surge phase.

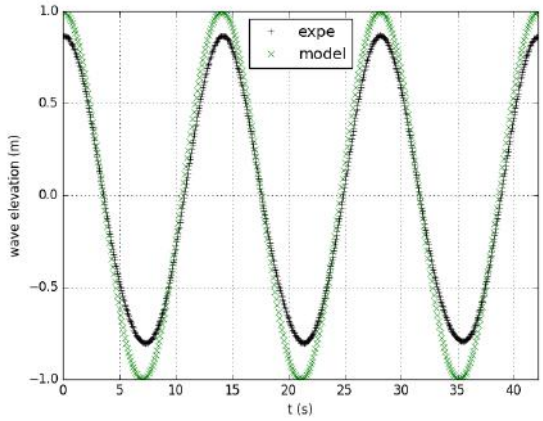

Waves

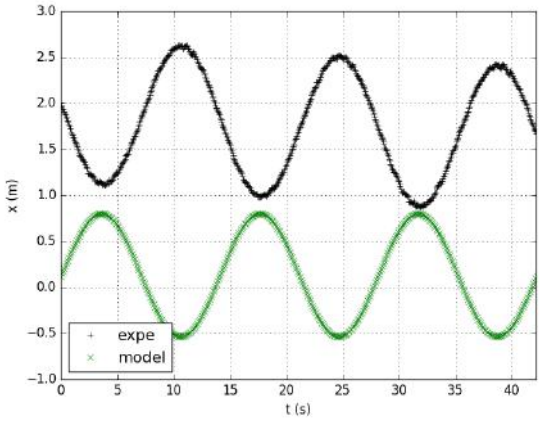

X: Surge

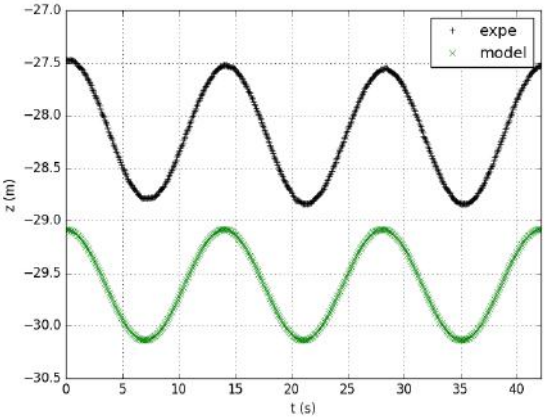

Z: Heave

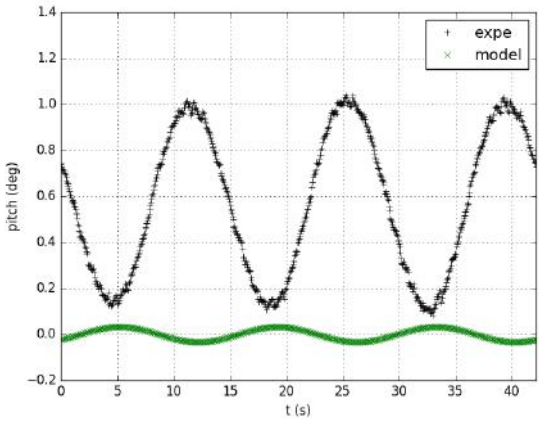

Pitch

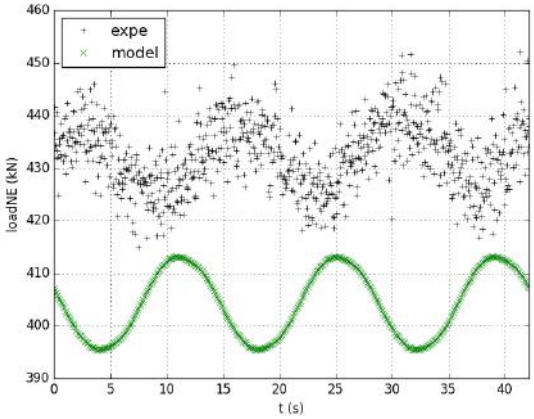

NE (front)

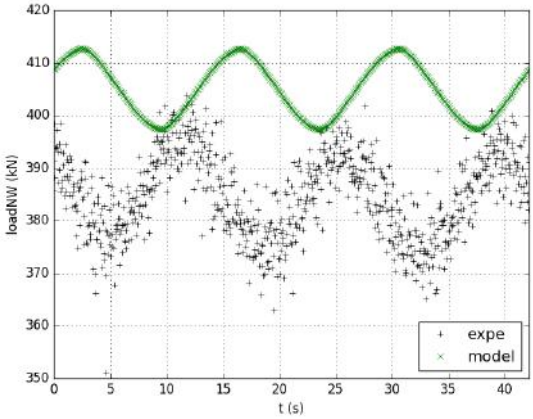

NW (back)

FIGURE 4-13EXAMPLE OF TIME SERIES OF REGULAR WAVES OF THE RIGID ARRAY FOR CASE A003 (*H* = 2 M AND *T* = 14.1 S)

The time series describing the waves, motions and loads for H = 2 m and T = 21.1 s are given in Figure 4-14. The results show a linear behaviour. The phase was different between the experimental and numerical mooring loads. This can be explained by a difference in mean drift between experimental and numerical data leading to a difference in surge phase.

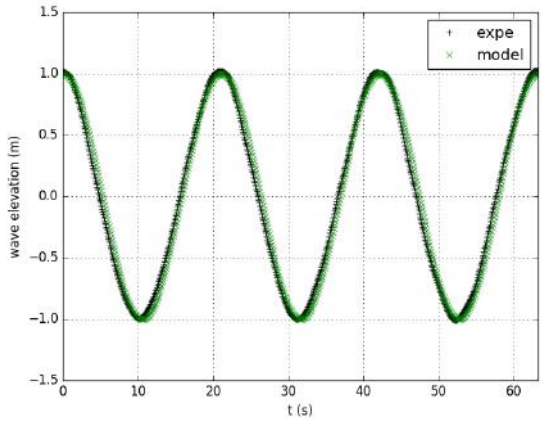

Waves

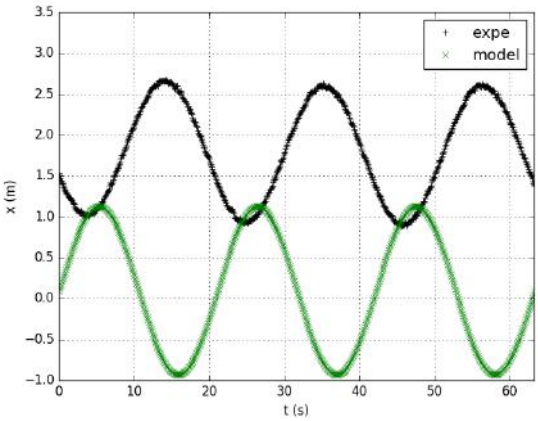

X: Surge

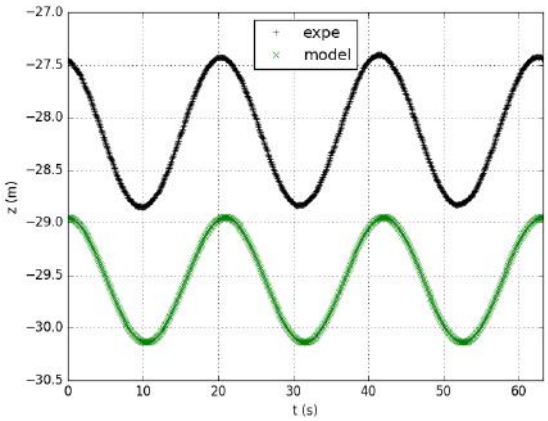

Z: Heave

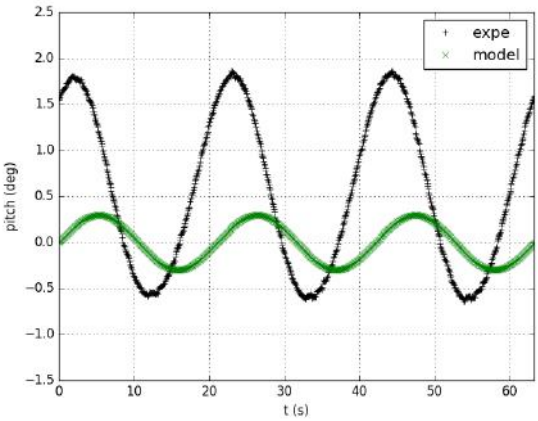

Pitch

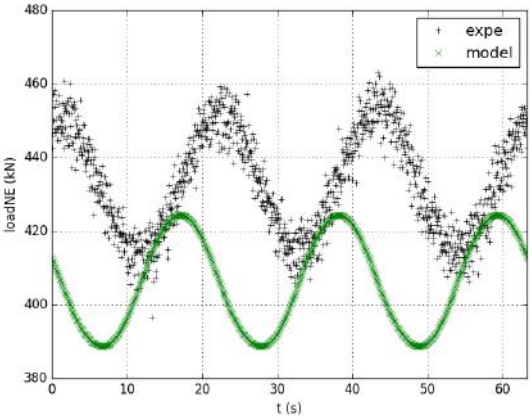

NE (front)

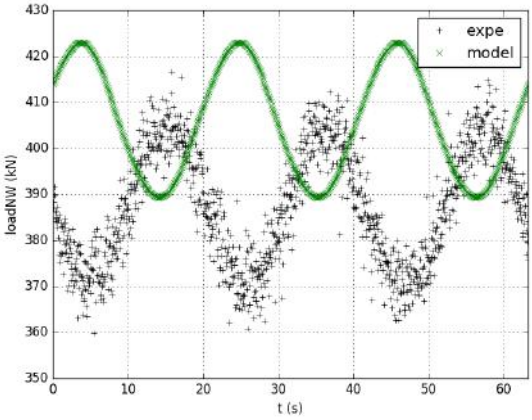

NW (back)

FIGURE 4-14 EXAMPLE OF TIME SERIES OF REGULAR WAVES OF THE RIGID ARRAY FOR CASE A001 (H = 2 M AND T = 21.1 S)

4.5.6 Irregular wave tests

The experiment names, significant wave height, peak periods and case (operational or survival) are summarised in Table 4-11. Irregular wave tests were conducted for approximately 10 minutes, which corresponds to 1 h full scale.

TABLE 4-11 SUMMARY OF THE IRREGULAR WAVE EXPERIMENT OF THE RIGID ARRAY

Simulation name	Hs (m)	Tp (s)	Case	Equivalent simulation with empty basin
i001	2.24	7.59	Operational	A019
i002	2.24	9.93	Operational	A020
i004	2.24	14.55	Operational	A036
i005	2.24	12.21	Operational	A037

Experimental and numerical time series of motion and mooring loads in moderate sea conditions were compared. For comparisons of amplitudes and phases, data are plotted with their mean removed (Figure 4-15). Results indicate a fair modelling of motion and mooring loads.

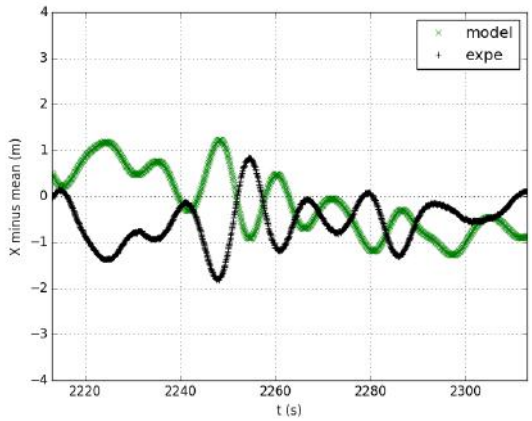

X: Surge

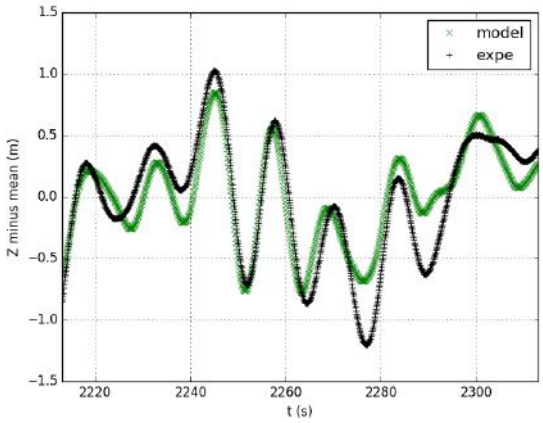

Z: Heave

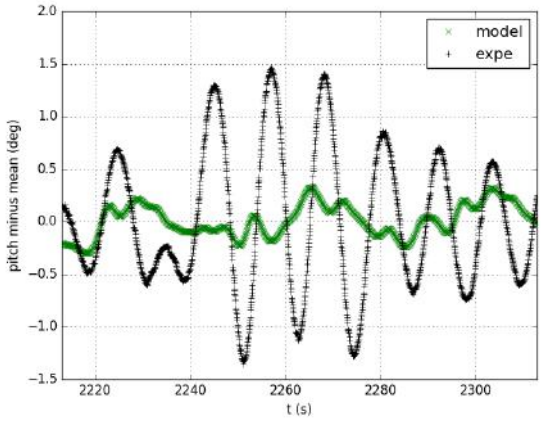

Pitch

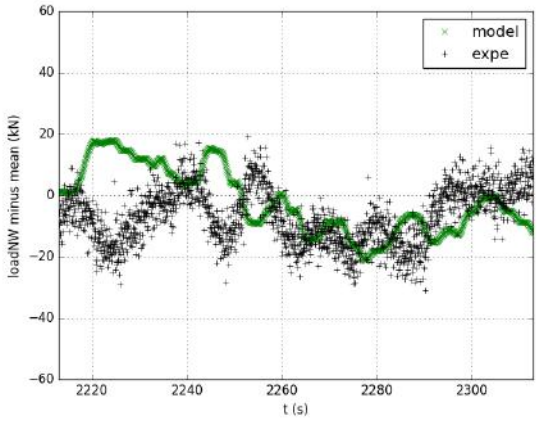

NW

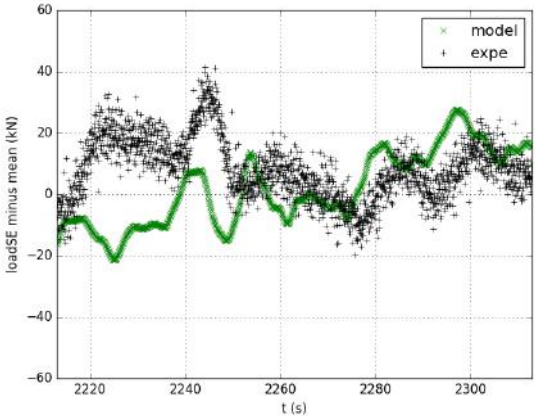

SE

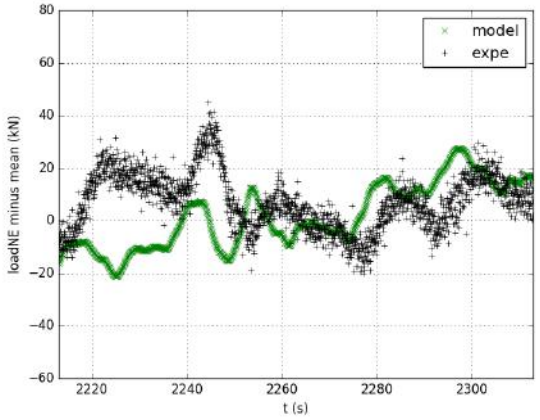

NE

FIGURE 4-15 EXAMPLE OF TIME SERIES OF EXPERIMENTAL AND MODELLED DATA OF THE RIGID ARRAY FOR IRREGULAR WAVES FOR CASE I004 (H_S = 2.24 M AND T_P = 14.55 S). MEAN VALUES HAVE BEEN REMOVED FOR COMPARISONS OF AMPLITUDES AND PHASES

Surge motions are in the same range of amplitudes in the model and in the experiment, however the model had a low frequency surge motion which did not occur during the experiment, and the phase is different between the wave frequency motions. Heave motions are well represented. Pitch motions are very small with amplitudes below 0.5° for the experiment and below 2° for the model. This motion is not well modelled but it does not matter with such low amplitude.

A good correlation is found for mooring load, however the model adds some low frequency variations to the mooring loads. Mooring load is similar in all lines, because the surge motion amplitude is small and mooring loads seem mainly driven by heave motion.

Experimental and modelled power spectral densities (PSDs) are compared (Figure 4-16). Peaks occur at the same frequency for surge and mooring loads (for a period close to 200 s).

For the surge PSD, a narrow peak occurred at a frequency corresponding to a period around 200 s. This is not surprising for a large structure with a catenary mooring system.

For the heave PSD, a narrow peak occurred at a frequency corresponding to a period around 63 s and a second more spread peak at a frequency corresponding to a period around 15 s.

For the pitch PSD, a peak occurred at a frequency corresponding to a period around 12 s.

The mooring loads PSDs look very similar to the surge PSD, meaning that the mooring loads are driven by the surge motion of the floating structure.

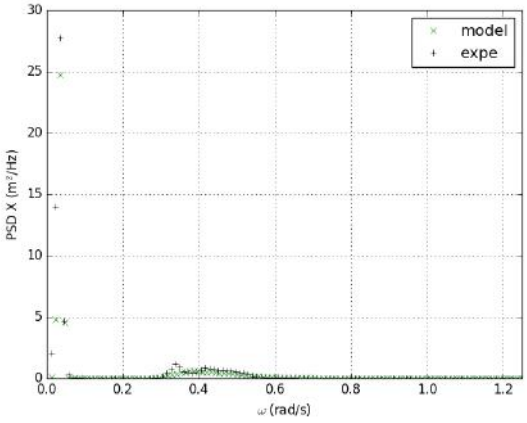

X: Surge

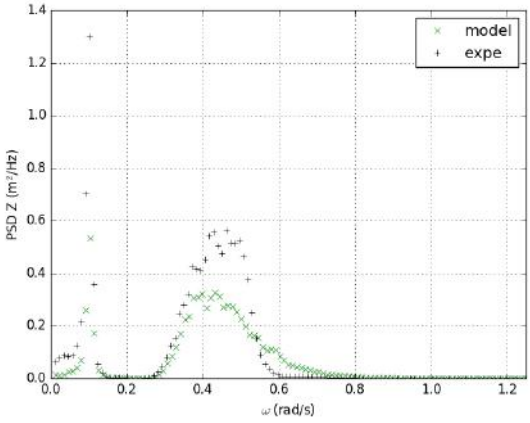

Z: Heave

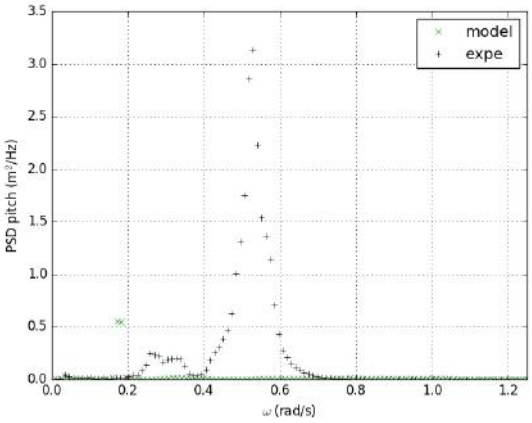

Pitch

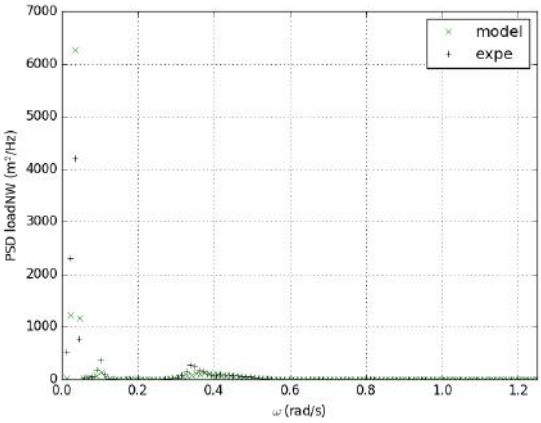

NW (back)

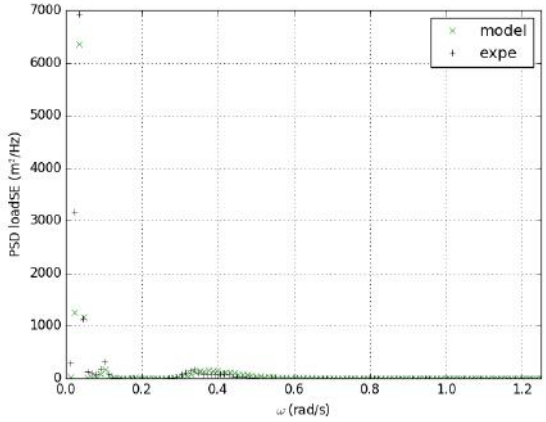

SE (front)

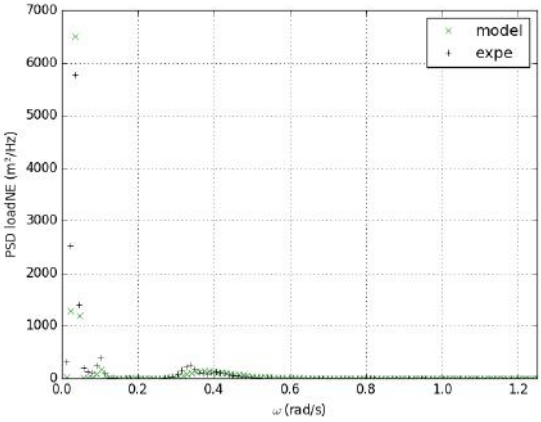

NE (front)

FIGURE 4-16 EXAMPLE OF PSD OF THE RIGID ARRAY OF EXPERIMENTAL AND MODELLED DATA FOR IRREGULAR WAVES FOR CASE I004 (H_S = 2.24 M AND T_P = 14.55 S)

Statistical results for this example are given in Table 4-12.

Results indicate that the difference in mean X position during irregular tests is of the same order of magnitude as during statics tests (Table 4-8). The variations around the mean position were slightly higher in the model, but the standard deviation was similar.

As observed in the statics equilibrium, the mean Z position is similar, however, this position varied during tests because of water ingress. Similarly to the surge position, the variations around the mean position were slightly higher in the model, but the standard deviation was similar.

Surge values were small, below 2°.

Mean mooring loads were well estimated. Variations behave similarly to the surge variations: the variations around the mean loads were slightly higher in the model, but the standard deviations were similar.

TABLE 4-12 COMPARISON OF STATISTICAL VALUES OF THE RIGID ARRAY FOR CASE I004 (H_S = 2.24 M AND T_P = 14.55 S): EXPERIMENTAL VALUE / MODEL VALUES. GREEN IS FOR RELATIVE DIFFERENCE BELOW 10 %, ORANGE BETWEEN 10% AND 100%, RED OVER 100%

m, deg or kN	Mean	Min-mean	Max-mean	Std
X	0,1/1,2	-1,9/-3,1	2,1/3,1	0,7/0,8
Z	-29,6/-29,1	-1/-1,4	0,8/1,1	0,3/0,4
Pitch	0/0,4	-0,5/-1,4	0,5/1,9	0,1/0,5
Load NE	405/400	-30/-51	32/63	12/13
Load SE	409/428	-31/-48	32/60	12/13
Load SW	405/382	-27/-67	30/61	12/13
Load NW	409/374	-27/-53	30/56	11/12

To conclude, the numerical model seems to estimate fairly the motion of the rigid array and the load in the mooring lines.

5 CONCLUSIONS

For the flexible device (loosely connected),

- The single device model generally shows a good agreement with experiments. First order surge and pitch motions and heave motions are predicted well. Mooring loads are also predicted well.

  Inaccuracies are observed in surge and pitch caused by a slow drift motion which appears in the numerical model, and which is likely to be caused by inaccuracies in the experimental setup. A sensitivity analysis showed that this type of mooring is highly sensitive to the lengths or masses of the mooring system components.

  In addition, the heave motion is slightly overdamped. For example, the highest values of the heave displacement Response Amplitude Operators (RAOs) are equal to 1.6m/m for the model while they are equal to 2.4 m/m for the experiment.

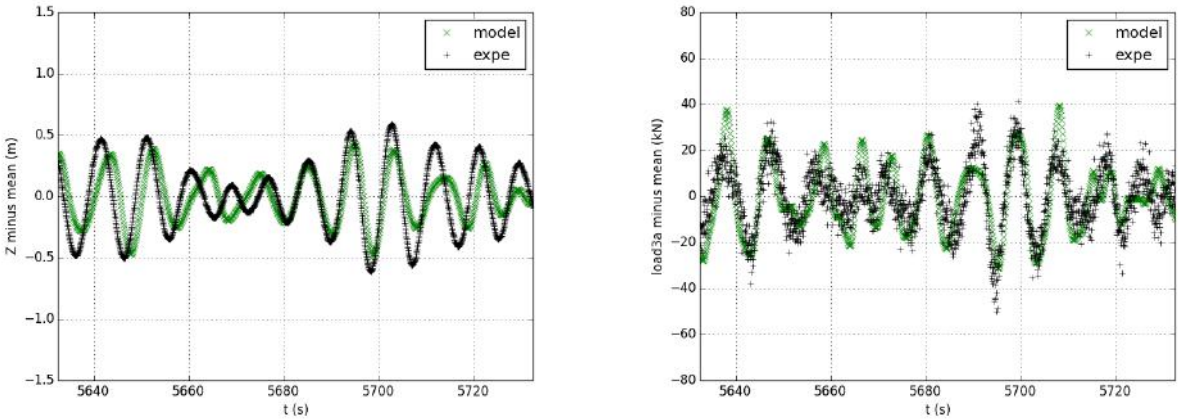

Z: Heave 3a

EXAMPLE OF TIME SERIES OF EXPERIMENTAL AND MODELLED DATA OF THE ISOLATED OWC SPAR BUOY FOR IRREGULAR WAVES FOR CASE C001 (H_S = 1.24 M AND T_P = 7.59 S). MEAN VALUES HAVE BEEN REMOVED FOR COMPARISONS OF AMPLITUDES AND PHASES

An improved heave damping could be estimated in a future model for example with sensitivity analysis. In addition, the OWC could be modelled. The model could also be built with the measured lengths and masses instead of target lengths and masses.

- The array Configuration D has been chosen for numerical modelling. This array used 5 devices similar to the single device previously considered. The devices are connected with few mooring lines: one external mooring line for each external buoy of the array, and one line connecting each external device to the internal device.

  The array Configuration D is more complex to model than the single device. First order motions and loads are modelled well with results similar as for the single device. The heave motions of the devices are replicated well in regular and irregular waves, but overdamped. This was also observed in the single device results. In irregular waves, a slow drift motion appears in the

modelled data which makes the modelling of pitch and surge, and consequently of mooring line load inaccurate.

The differences in slow drift motion may be due to the quadratic transfer function (QTFs) which are valid for the initial position at which they have been calculated, especially for a multibody model, to the lack of damping of second order motion, but also and similarly to the single device to inaccuracies in experimental layout.

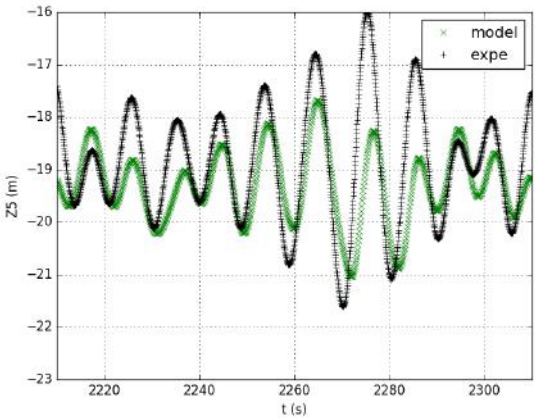

Z3: heave buoy 3

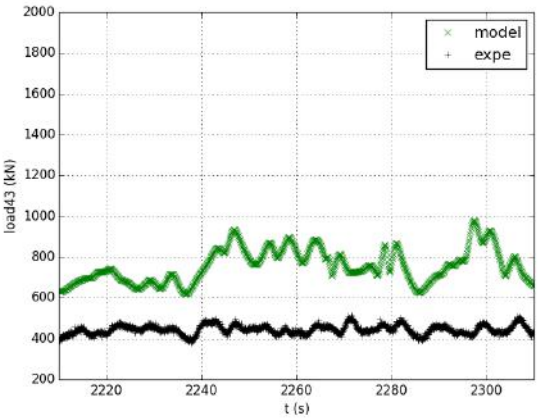

Load 43

EXAMPLE OF TIME SERIES OF EXPERIMENTAL AND MODELLED DATA FOR IRREGULAR WAVES FOR CASE DA038 (H_s = 2.9 M AND T = 9.9 S). OWC SPAR BUOY ARRAY, CONFIGURATION D

Similarly to the single device, in a future model, an improved heave damping could be estimated and the OWCs could be modelled. The model could also be built with the measured lengths and masses instead of target lengths and masses.

For the rigid device (compact aggregates),

- The numerical model was with low complexity, with standard catenary mooring lines, and limited motion amplitudes. The numerical model estimates fairly the motion of the rigid array and the load in the mooring lines in the experiments. The heave motion is predicted well.

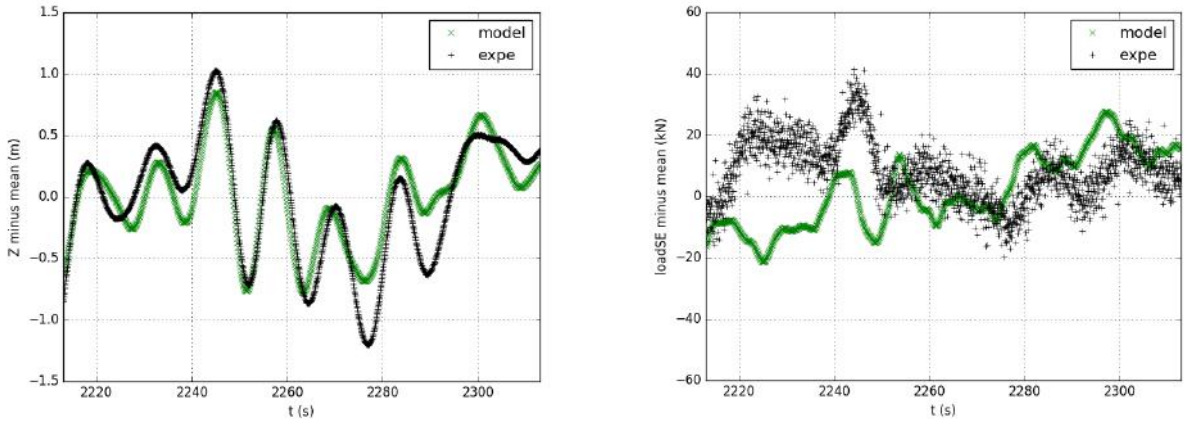

Z: Heave Load SE

EXAMPLE OF TIME SERIES OF EXPERIMENTAL AND MODELLED DATA OF THE RIGID ARRAY FOR IRREGULAR WAVES FOR CASE I004 (H_S = 2.24 M AND T_P = 14.55 S). MEAN VALUES HAVE BEEN REMOVED FOR COMPARISONS OF AMPLITUDES AND PHASES

The Power-Take off (PTO) and heave plates were not taken into account in the numerical model which may explain some differences between experimental and modelled results.

They could be added in a future model. Decay tests would be required to calibrate the damping generated by the heave plates.

All models generally show a good agreement with experiments and can be used to predict first order motions and mooring loads. These results can be used to predict a full size system with some adjustments [1] :

- The stiffness of the air spring is not scaled correctly.
- Viscosity does not scale appropriately and is likely to be overestimated during tank test.
- Friction does not scale appropriately.

In addition, there might be inaccuracies in sea trials in anchor position. Inaccuracies in line length and clump weight are also likely in sea trials. They have already been observed in tank tests. Their influence on results has been assessed with sensitivity analysis with the numerical model.
Due to the large size of the array, it would be complicated to conduct tank tests at a higher scale. Further scaled tests at a larger scale could be conducted in the sea, in sheltered locations.

These models could also be used in future developments of the devices.
The hydrodynamic databases do not need to be modified if the distance between devices is the same and if the hull of the devices is the same. For the flexible devices, all mooring configurations and other mooring configurations could be investigated, and for the rigid device the mooring configuration could be modified.
Otherwise, new hydrodynamic databases will need to be calculated. The methodology developed in this study can be used again, and the limitations of the numerical model are likely to be similar.

Some preliminary comments, based on the validated experimental work, of the benefits or influences of having shared mooring between devices of the array can be made below. These points will be discussed in more details in D6.5 [7].

- The flexible array is more complex to model than the related single device.

Large pitch motions are observed in the case of the array. This is likely to be detrimental to the power production and to increase mooring loads.

- The rigid array is less complex to model than the flexible array. This numerical model could be used for optimisation, for example on the mooring system.
  In addition, the rigid array is a large device which does not move much, and probably less than the related single device. This means that using an array is likely to be a benefit for power production.

6 BIBLIOGRAPHY

[1] Tank Testing of Wave Energy Conversion Systems, Marine Renewable Energy Guides, EMEC, 2009

[2] OrcaFlex user manual https://www.orcina.com/SoftwareProducts/OrcaFlex/Documentation/Help/

[3] WAMIT user manual https://www.wamit.com/manual.htm

[4] Faltinsen, O.M. (1990) *Sea Loads on Ships and Offshore Structures*, Cambridge University Press edn., Cambridge, UK

[5] IST, OWC_Spar_buoy_WETFEET12x36_15mm_toPU_2016-06-03.pdf, in WETFEET project. 2016, Instituto Superior Técnico. p. 2.

[6] D6.3 - Report on the 1:40 physical models, in WETFEET project. 2017

[7] D6.5 - Design guidance on the use of shared moorings in compact arrays, in WETFEET project. 2017

7 APPENDIX

7.1 Single OWC spar buoy: decay tests

7.1.1 Sway

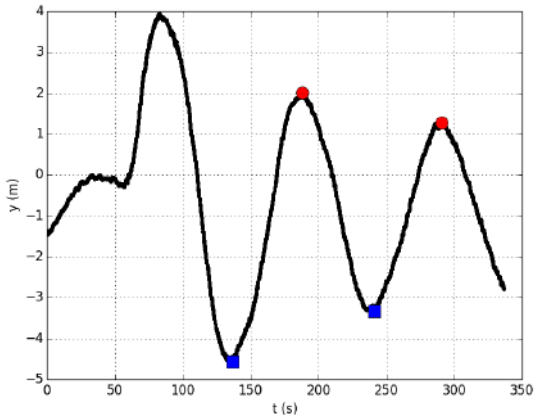

G014

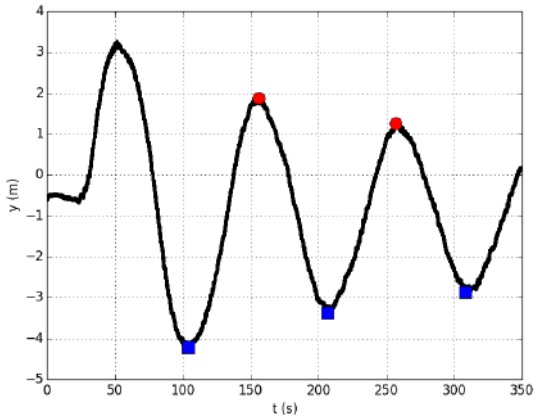

G015

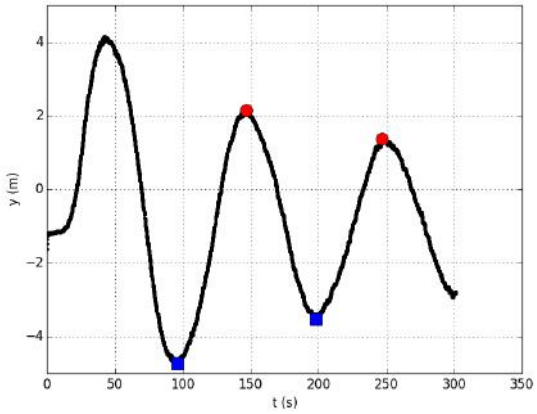

G016

FIGURE 7-1 SWAY DECAY TESTS OF THE ISOLATED SPAR BUOY. EXPERIMENTAL MOTIONS IN SWAY AND PEAKS (RED DOTS) AND TROUGHS (BLUE DOTS) USED FOR DAMPING COEFFICIENTS CALIBRATION AND NATURAL PERIOD ESTIMATION

7.1.2 Heave

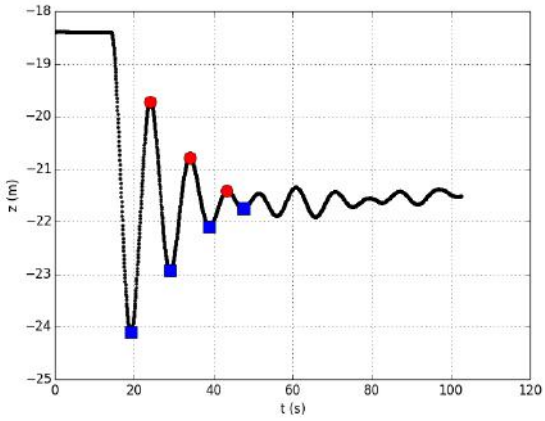

G001

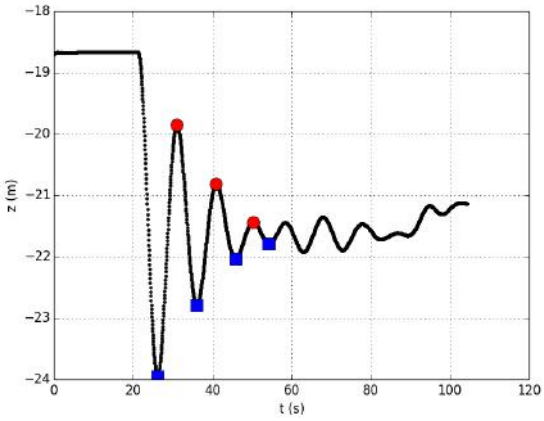

G002

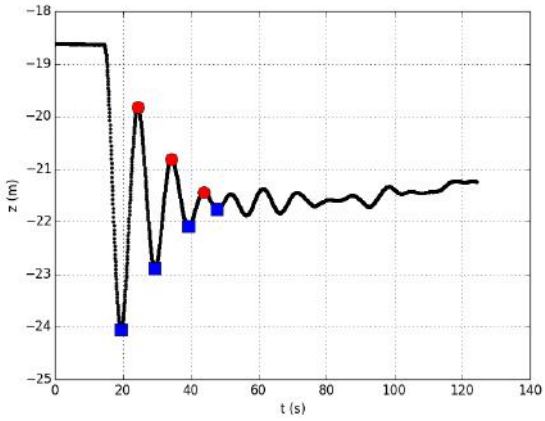

G003

FIGURE 7-2 HEAVE DECAY TESTS OF THE ISOLATED SPAR BUOY. EXPERIMENTAL MOTIONS IN HEAVE AND PEAKS (RED DOTS) AND TROUGHS (BLUE DOTS) USED FOR DAMPING COEFFICIENTS CALIBRATION AND NATURAL PERIOD ESTIMATION

7.1.3 Roll

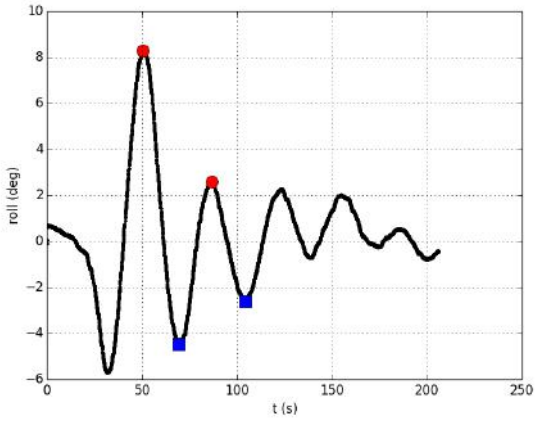

G010

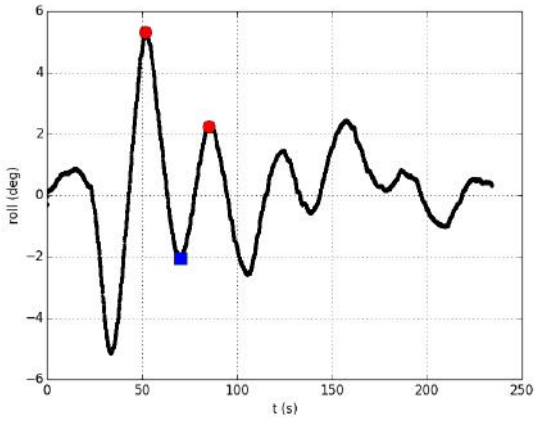

G011

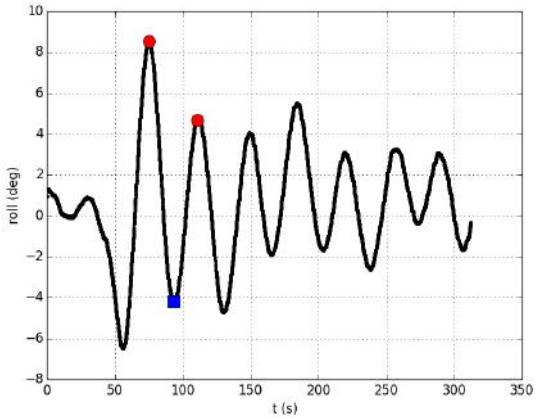

G012

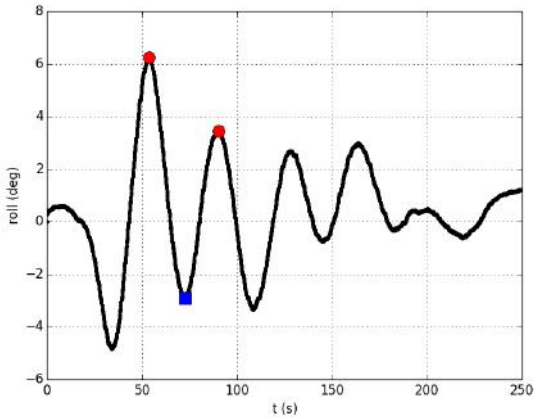

G013

FIGURE 7-3 ROLL DECAY TESTS OF THE ISOLATED SPAR BUOY. EXPERIMENTAL MOTIONS IN ROLL AND PEAKS (RED DOTS) AND TROUGHS (BLUE DOTS) USED FOR DAMPING COEFFICIENTS CALIBRATION AND NATURAL PERIOD ESTIMATION

7.1.4 Pitch

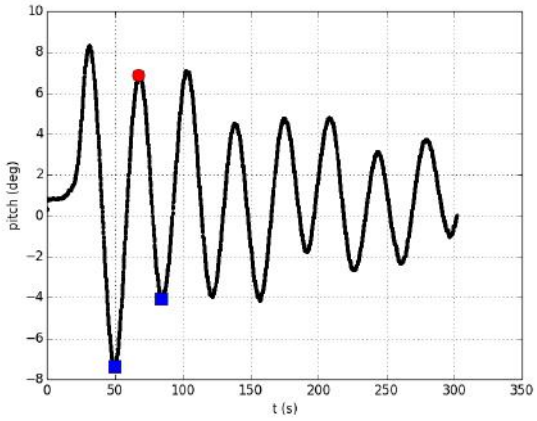

G004

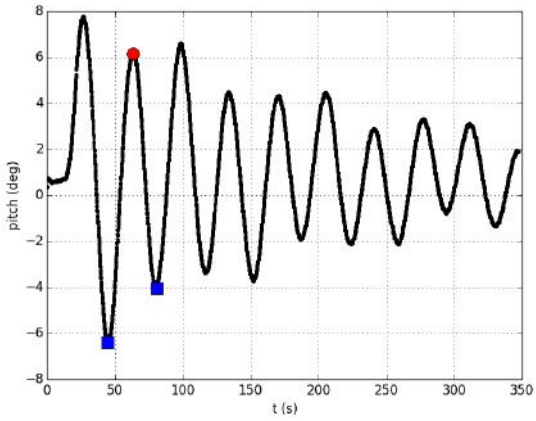

G005

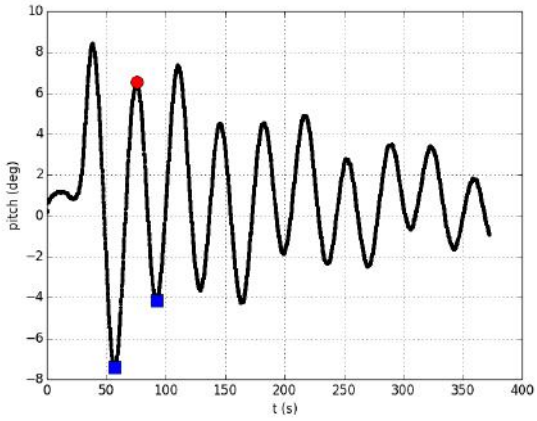

G006

FIGURE 7-4 PITCH DECAY TESTS OF THE ISOLATED SPAR BUOY. EXPERIMENTAL MOTIONS IN ROLL AND PEAKS (RED DOTS) AND TROUGHS (BLUE DOTS) USED FOR DAMPING COEFFICIENTS CALIBRATION AND NATURAL PERIOD ESTIMATION

7.2 Wave gauge layouts

Measurements are given in millimetres with respect to the centre of the basin. In general:

- Layout 1 used for preliminary testing and some of isolated spar buoy tests
- Layout 2 used for the empty basin tests
- Layout 3 used for some isolated spar buoy tests and spar buoy arrays

In between experimental testing sessions, all gauges were removed and all support structure was removed so there was some small difference between the placement of the gauges during each testing session.

TABLE 7-1 WAVE GAUGE LAYOUTS

	spar buoy tests						Rigid tests	
	Nov-2016 (Layout 1)		Dec-2016 (Layout 2)		Jan-2017 (Layout 3)		Oct-2017	
Gauge #	***X***	***Y***	***X***	***Y***	***X***	***Y***	***X***	***Y***
1	-4230	0	-4230	0	-4730	0	-5185	-25
2	-1860	-1410	-1410	1410	-2750	2000	-3330	-25
3	-1410	0	-1410	0	-1430	0	-2335	-25
4	-750	0	-1410	-1410	-2750	-2000	-1055	35
5	0	2820	-750	0	-750	0	35	-2295
6	960	1410	0	2820	0	2820	35	-2960
7	1410	0	0	0	1250	2000	1165	-65
8	2820	0	960	1410	1906	0		
9			--	--	3318	0		
10			1410	1410				
11			0	-1410				
12			1410	-1410				
13			0	-2820				

7.3 Files produced and example headers and columns

TABLE 7-2 FILES PRODUCED AND EXAMPLE HEADERS AND COLUMNS

Waves example header									
#EDL	Date	d.m.yyyy	Local Time	hh:mm:ss	Run name				
Rate (Hz)	Main array								
128	element_1	element_2	element_3	element_4	element_5	element_9	element_10	element_11	element_12
Times	Gauge m	Gauge m	Gauge m	Gauge m	Gauge m	Gauge m	Gauge m	Gauge m	Gauge m
Pressure and load example header									
LabVIEW Measurement									
Delimiter	Tab								
Project Type	External								
Project Title									
Run name	B068								
Description									
DAQmx Task(s)	161101_WETFEET								
Channels	4								
Sample rate (Hz)	1667								
Date	dd/mm/yyyy								
Time	hh:mm:ss								
X_value	Pressure_1	Force_1_698315	Force_2_698317		Force_3_698314				
Seconds	Volts	Newtons	Newtons		Newtons				

Motions and rotations example header																		
NO_OF_FRAMES	23433																	
NO_OF_CAMERAS	6																	
NO_OF_BODIES	1																	
FREQUENCY	128																	
NO_OF_ANALOG	0																	
ANALOG_FREQUENCY	0																	
DESCRIPTION	--																	
TIME_STAMP	yyyy-mm-dd, hh:mm:ss	54270 6.3																
DATA_INCLUDED	6D																	
BODY_NAMES	TMX_0																	
Frame	Time	TMX_0 X	Y	Z	Yaw	Pitch	Roll	Residual	Rot[0]	Rot[1]	Rot[2]	Rot[3]	Rot[4]	Rot[5]	Rot[6]	Rot[7]	Rot[8]	

7.4 Load cells linearity

TABLE 7-3 LOAD CELLS LINEARITY

Sensor number	Non-linear error (% rated output)
698 315	+0.029
698 314	-0.026
698 316	0.451
698 317	-0.068
546 533	-0.050
698 313	+0.008
546 534	-0.064
546 532	-0.052
698 312	-0.012
546 535	-0.030